

e-mosty

ISSUE 01/2022

PELJEŠAC BRIDGE, CROATIA

MCKINLEY STREET BRIDGE, USA



PELJEŠAC
BRIDGE

LIST OF CONTENTS

PELJEŠAC BRIDGE, CROATIA - DESIGN AND CONSTRUCTION	page 08
<i>Marjan Pipenbaher, Pipenbaher Consulting Engineers, Slovenska Bistrica; Ponting Bridges, Maribor, Slovenia</i>	
SPHERICAL BEARINGS FOR THE PELJEŠAC BRIDGE IN CROATIA	page 35
<i>Luca Paroli, MAURER</i>	
AUTOMATIC CLIMBING FORMWORK XCLIMB 60 FOR PIERS AND PYLONS OF THE PELJEŠAC BRIDGE, CROATIA	page 41
<i>František Madleňák, Global Expertise Center Infrastructure, DOKA</i>	
MCKINLEY STREET STEEL TIED ARCH BRIDGE, CITY OF CORONA, CALIFORNIA, USA	page 44
<i>José C Calisto da Silva, Engineering Manager, Director Complex Analyses; Mahsa Farzad, Staff Engineer; Austin Emrich, Assistant Engineer; Ben Chan, Assistant Engineer, Biggs Cardosa Associates</i>	

Photo on the Front Cover: Pelješac Bridge, Croatia Credit: Pipenbaher Consulting Engineers
Photo on the Back Cover: McKinley Street Bridge (Rendering), USA Credit: Biggs Cardosa Associates

International, interactive magazine about bridges
e-mosty ("e-bridges"). Peer-reviewed.

It is published at www.e-mosty.cz. Open Access.

Released quarterly:

20 March, 20 June, 20 September and 20 December

Number: 01/2022, March. **Year:** VIII.

Chief Editor: Magdaléna Sobotková
Contact: info@professional-english.cz

Editorial Board

The Publisher: PROF-ENG, s. r. o. (Ltd.)
Velká Hraštice 112, 262 03 Czech Republic
VAT Id. Number: CZ02577933

E-MOSTY ISSN 2336-8179

©All rights reserved. Please respect copyright. When referring to any information contained herein, please use the title of the magazine „e-mosty“, volume, author and page. In case of any doubts please contact us. Thank you.

Dear Readers

This Issue is dedicated to two Bridge Projects: **Pelješac Bridge in Croatia**, and **McKinley Street Bridge in the USA**.

In the first article of this issue, **Marjan Pipenbaher** provides information about the Design and Construction of the Pelješac Bridge in Croatia. The 2,404 m long bridge is designed as a multi-span cable-stayed bridge with a semi-integral hybrid structure with five 285 m long central spans.

The next article also dedicated to this outstanding structure was prepared by **Luca Paroli of Maurer**. He brings some technical details and information about spherical bearings and expansion joints.

František Madleňák of Doka prepared an article about Automatic climbing formwork Xclimb 60 which was used for the construction of the piers and pylons of the Bridge. In his article, you can find the description of the equipment and information on how it works.

The second part of this issue is dedicated to **McKinley Street Steel Tied Arch Bridge in the USA** which is a bridge currently being constructed in the City of Corona. **Biggs Cardosa Associates** provides detailed information about the design and construction of this Arch Bridge. The authors of this article also focus on some innovative aspects of the bridge design.

On the following pages, you will also find information about our new magazine **e-BRIM** and our partnership offer.

I would like to **thank all authors and companies for their cooperation**, and also **Ken Wheeler, Juan C. Gray and David Collings** for reviewing this issue.

I would also very much like to thank our **partners for their continuous support**.

June Edition of e-mosty is going to be dedicated to the **1915 Çanakkale Suspension Bridge**. We would like to celebrate this masterpiece and share information about it so for this special edition, we welcome your articles, cooperation and assistance. I also welcome advice and tips on who and what we shall include in this special edition. Please contact me by email, WhatsApp or LinkedIn. Thank you.

On this occasion, we would also like to congratulate the people and companies involved in this spectacular project on the recent opening of the Bridge to traffic.

Magdaléna Sobotková

Chief Editor



e-mosty



SUBSCRIBE

The magazine **e-mosty** (“e-bridges”) is an international, interactive, peer-reviewed magazine about bridges.

It is published at www.e-mosty.cz and can be read free of charge (open access) with the possibility to subscribe.

It is published quarterly: 20 March, 20 June, 20 September and 20 December.

The magazines stay **available online** on our website as pdf.

The magazine **brings original articles about bridges and bridge engineers** from around the world.

Its electronic form enables the publishing of high-quality photos, videos, drawings, links, etc.

We aim to include **all important and technical information** and show the grace and beauty of the structures.

We are happy to provide media support for important bridge conferences, educational activities, charitable projects, books, etc.

Our **Editorial Board** comprises bridge engineers and experts mainly from the UK, US and Australia.

The readers are mainly bridge engineers, designers, constructors and managers of construction companies, university lecturers and students, or people who just love bridges.



e-BrIM

In August 2021 we established a new magazine, **e-BrIM**, which focuses on Bridge Information Modelling.

We would like to follow the concept of the e-mostly magazine and create an international, peer-reviewed magazine with open access and the possibility to subscribe.

Our plan is to publish it three times a year; its first regular issue was released on 20 February 2022.

The **September 2021 edition** of e-mostly was also a “zero” edition of e-BrIM.

We believe that with the current development of BIM, there will be plenty of interesting and useful content to share.

Let us introduce and welcome our **Editorial Board Members**. Thank you all for accepting our invitation.

We all will do our best to prepare technical, educational and informative content for our readers.

We would also like to invite you to contribute with your articles to this newly established magazine e-BrIM:

CALL FOR PAPERS

20 October 2022 Edition:

Deadline for first drafts: 20 May 2022

Deadline for review: 20 August 2022

Deadline for final check: 5 October 2022

The text shall be in MS Word, 3 – 5 pages plus relevant images, drawings, 3D models, links and videos and shall be sent to our email address.

You may also send an abstract before starting work on the article or contact us to discuss other options.

All abstracts and articles will be peer-reviewed and also subject to approval by the Editorial Board.

READ OUR FIRST REGULAR ISSUE:



EDITORIAL BOARD

Antonio Caballero, MSc PhD

Chief Technology Officer,
Screening Eagle
Technologies, Switzerland



Vanja Samec, MSc PhD

Independent Bridge & BIM
Consultant
Chair of IABSE Task Group
5.6 “BIM in Structure
Management”



**Marek Salamak, PhD DSc
CEng**

Associate Professor,
Faculty of Civil Engineering,
Silesian University of
Technology, Poland



**심창수 Chang-Su Shim,
Prof. Dr.**

Professor, School of Civil
and Environmental
Engineering, Chung-Ang
University, South Korea
Vice Chair of IABSE Task
Group 5.6 “BIM in
Structure Management”



e-BrIM



SUBSCRIBE

The magazine **e-BrIM** is an international, interactive, peer-reviewed magazine about bridge information modelling.

It is published at www.e-brim.com and can be read free of charge (open access) with the possibility to subscribe.

It is typically published three times a year:
20 February, 20 May and 20 October.

The magazines stay **available online**
on our website as pdf.

The magazine brings **original articles** about **bridge digital technology** from early planning till operation and maintenance, **theoretical and practical innovations**, **Case Studies** and much more from around the world. Its electronic form enables the publishing of high-quality photos, videos, drawings, 3D models, links, etc.

We aim to include **all important and technical information**, **to share theory and practice**, **knowledge and experience** and at the same time, to show the grace and beauty of the structures.

We are happy to provide media support for important BIM and bridge conferences, educational activities, charitable projects, books, etc.

Our **Editorial Board** comprises BIM and bridge experts and engineers from academic, research and business environments and the bridge industry.

The readers are mainly bridge leaders, project owners, bridge managers and inspectors, bridge engineers and designers, contractors, BIM experts and managers, university lecturers and students, or people who just love bridges.

OUR PARTNERS



We
build
technologies

**Pipenbaher
Consulting Engineers**
PIPENBAHER INŽENIRJI d.o.o., Slovenia



INTERNATIONAL ONLINE MAGAZINE

e-mosty

BRIDGE DESIGN, CONSTRUCTION,
OPERATION AND MAINTENANCE

Offer of partnership and promotion
of your company in our magazines

e-mosty

e-BrIM

We would like to offer you a partnership
with e-mosty and e-BrIM magazines.

Depending on the type of a partnership – Platinum, Gold or Silver -
the partnership scheme typically involves:

- Your logo on all pages of the magazine website.
- 1-page interactive presentation of your company in every issue which we can help you prepare (free of charge).
- Your logo and /or the name of your company on every publication and output we release.
- Continuous promotion of your company and projects on our social media.
- Publication of one technical article during the year (which we can help you prepare).

The Partnership can be arranged for either magazine separately,
or for both magazines – for a discounted price.

Both the price and the extent of cooperation are fully negotiable.

Please [contact us](#) for more details and partnership arrangement.

PARTNERSHIP OFFER - CONDITIONS

PELJEŠAC BRIDGE, CROATIA - DESIGN AND CONSTRUCTION

Marjan Pipenbaher

Pipenbaher Consulting Engineers, Slovenska Bistrica, Slovenia

Ponting Bridges, Maribor, Slovenia



Figure 1: View of the complete Bridge Credit: CRBC

The 2,404 m long Pelješac Bridge, Croatia ranks among the most demanding bridges in the world in terms of both the technological complexity of construction and the complexity of the design.

The bridge is located in an area of extremely high seismic activity, exposed to strong and gusty north and south winds.

It is designed as a multi-span cable-stayed bridge with a semi-integral hybrid structure with five 285 m long central spans.

The bridge ranks among largest and most attractive European bridges built in the early 21st century.

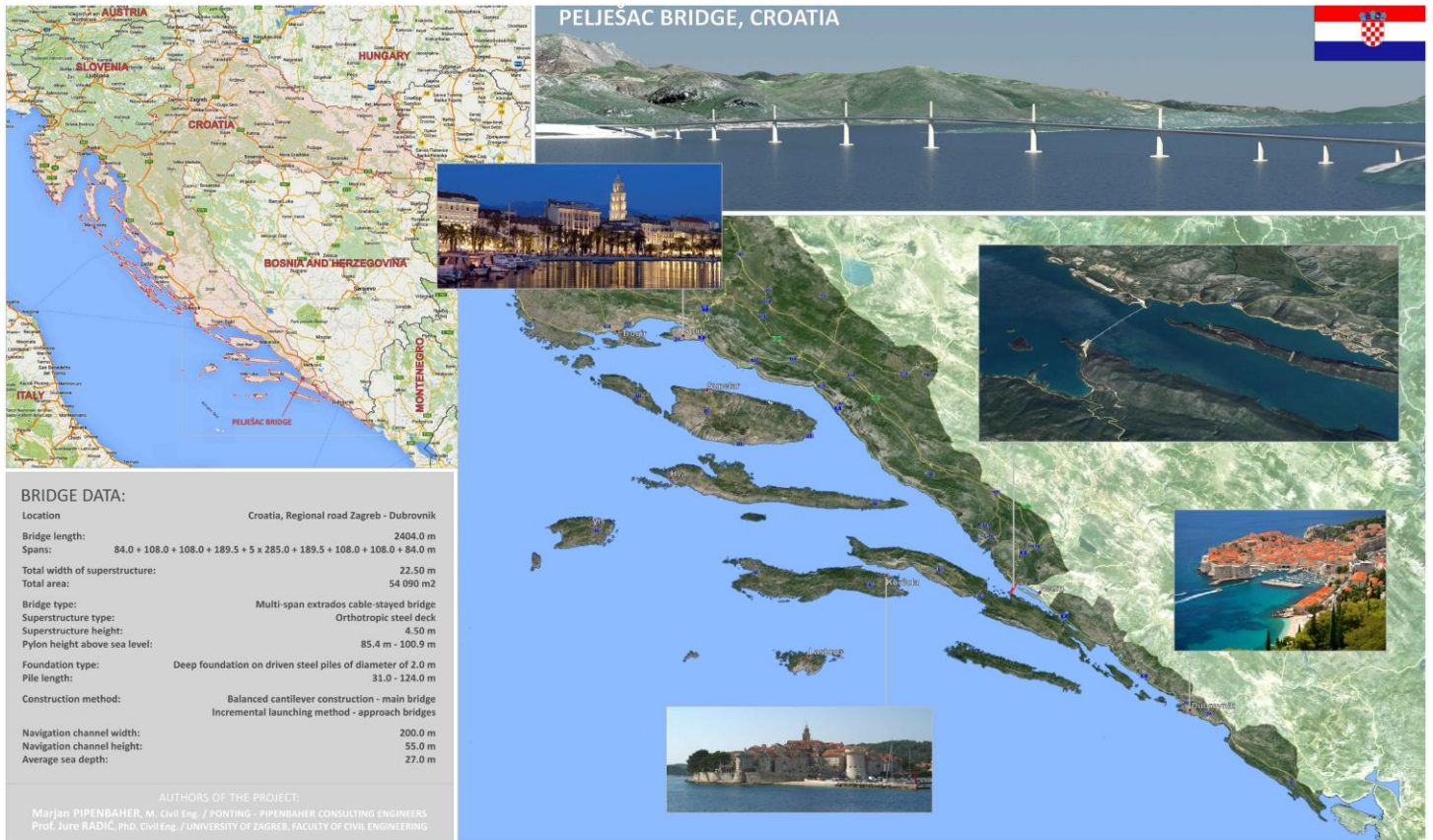


Figure 2: Location of the bridge

[Click on the image to open it in a higher resolution](#)

INTRODUCTION

A solid road link between all parts of Croatia has been established upon completion of the Pelješac-Mainland Bridge.

The Dubrovnik-Neretva County is now linked with the Croatian territory, which will greatly contribute to the development of Dubrovnik, Pelješac Peninsula, and the entire Southern-most County of Croatia.

The bridge is located in a highly sensitive and Natura 2000 protected area of Mali Ston Bay which hosts the largest oyster cultivation facilities in the Adriatic Sea.

The distance over the bay amounts to approximately 2,140 m at sea level. The total length of the bridge between the abutment axes is 2,404 m, while the overall bridge length is 2,440 m. The sea depth varies between 7.0 and 28.0 m, Figure 2.

The minimum required navigation clearance, harmonized with Bosnia and Herzegovina, is 200 m wide x 55 m high.

GENERAL BRIDGE DATA:

<u>Client:</u>	HRVATSKE CESTE d.o.o., Zagreb, Croatia
<u>Designer:</u>	Design Joint venture: Pipenbaher Consulting Engineers, Slovenia / www.pipenbaher- consulting.com Ponting Bridges, Slovenia / www.ponting.si Faculty of Civil Engineering, Zagreb, Croatia
<u>Author - Main designer:</u>	Marjan PIPENBAHER, MSCE
<u>Contractor:</u>	CRBC - China Road and Bridge Corporation, China
<u>Construction supervision:</u>	IGH Institute, Zagreb, Croatia
<u>Investment value:</u>	278.000,000.00 EUR 85% of the costs co-financed from EU funds

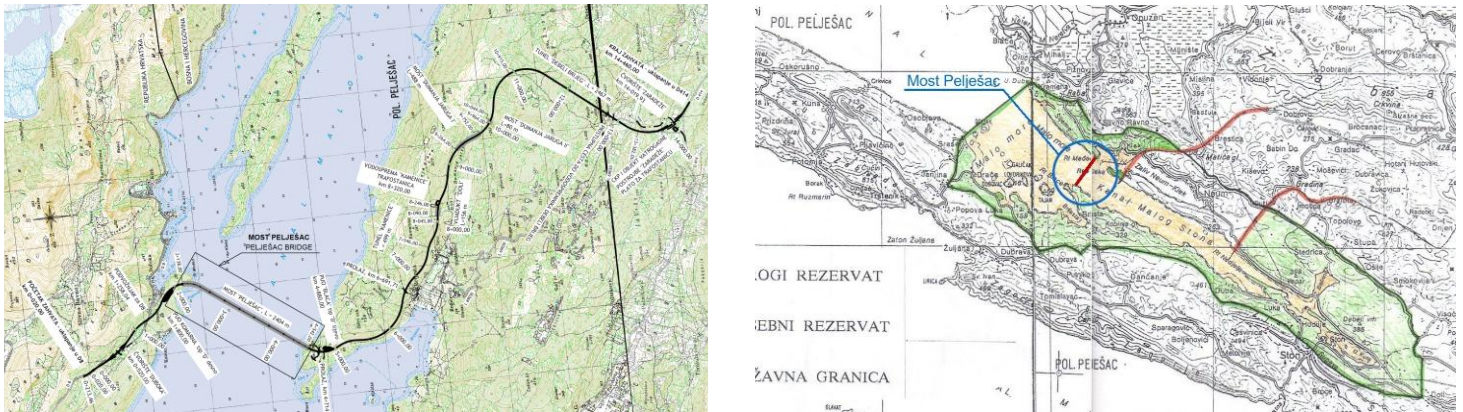


Figure 3: Location of the bridge with area protected by Natura 2000

[Click on the image to open it in a higher resolution](#)

MAIN CHARACTERISTICS OF BRIDGE LOCATION

The bridge is located in a highly sensitive and protected area of Mali Ston Bay. It is a bay enclosed by the Pelješac peninsula and the mainland.

The bay is 21 km long and has a maximum breadth of 2.2 km and the depth is between 7 and 28 m. On account of its clean waters, it was declared a Special Natural Reserve in 1983, Figure 3.

The entire area is also protected by Natura 2000 - a comprehensive ecological network of areas

designated by the European Union member states. The main objective of the network is to conserve valuable biodiversity for future generations.

The bridge is located in a zone of a very high seismic activity, with the design acceleration of soil at the bedrock level of $a_g = 0.34g$ and importance factor for no-collapse requirement $\gamma_I = 1.60$ according to Croatian national standard HRN EN 1998-1:2011/NA, Figure 4.

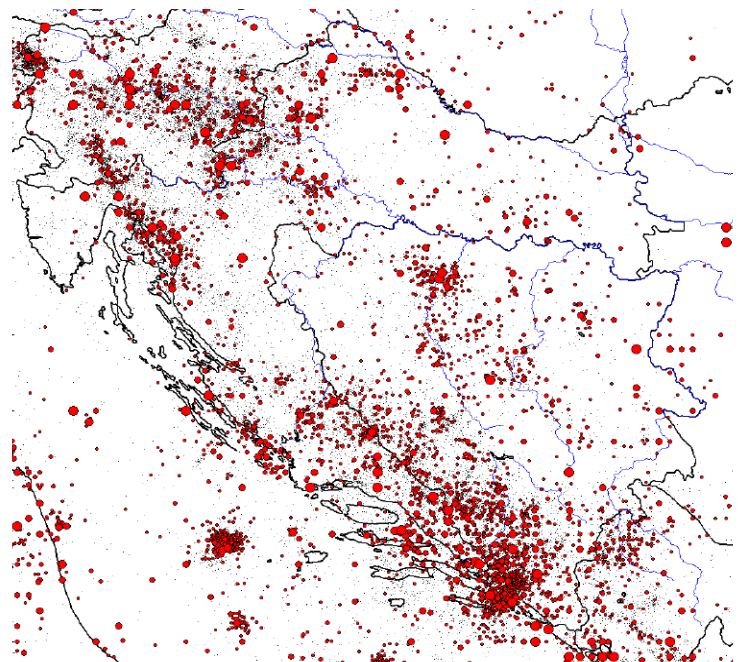
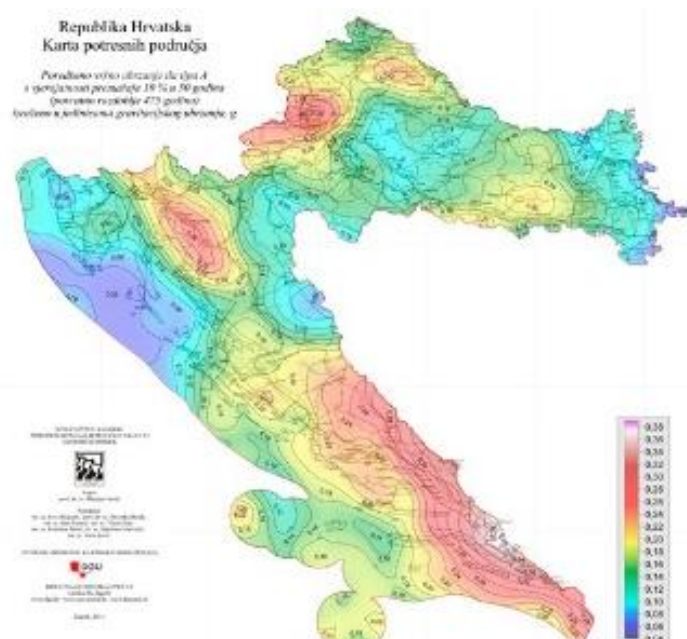
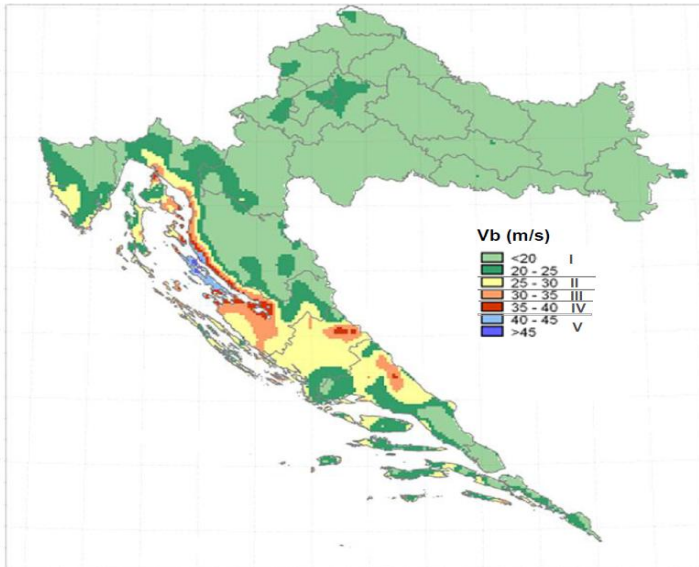


Figure 4: Map of seismic areas and earthquake epicentres (Croatian Earthquake Catalogue, 2011)

[Click on the image to open it in a higher resolution](#)



T (god)	PLOČE					KOMARNA				
	5	10	20	50	100	5	10	20	50	100
P (%)	80	90	95	98	99	80	90	95	98	99
N	13,3	14,6	15,8	17,3	18,6	15,2	19,0	22,6	27,3	31,1
NNE	14,2	15,3	16,3	17,7	18,8	15,7	18,9	22,0	26,1	29,3
NE	11,7	13,6	15,3	17,6	19,5	16,3	20,7	24,9	30,4	34,7
ENE	8,9	10,1	11,3	12,9	14,2	13,8	16,6	19,3	22,8	25,6
E	8,5	9,3	10,1	11,1	11,9	14,0	18,0	21,9	27,0	31,0
ESE	12,2	13,7	15,2	17,2	18,8	17,0	22,3	27,3	33,7	38,9
SE	14,5	16,0	17,4	19,3	20,8	17,4	22,4	27,1	33,3	38,2
SSE	12,4	14,5	16,5	19,1	21,2	12,7	16,3	19,8	24,4	28,0
S	10,8	13,9	16,8	20,7	23,7	13,1	16,5	19,7	23,9	27,3
SSW	11,2	13,6	15,9	18,9	21,3	10,1	13,1	16,0	19,7	22,6
SW	9,9	12,7	15,5	19,0	21,8	11,6	14,9	18,0	22,0	25,2
WSW	10,1	13,1	16,0	19,7	22,7	11,7	14,9	18,1	22,1	25,3
W	11,2	14,7	18,1	22,5	26,1	13,3	16,9	20,3	24,7	28,3
WNW	9,0	11,8	14,6	18,1	21,0	15,7	19,5	23,1	27,8	31,6
NW	7,8	10,4	12,9	16,1	18,7	11,6	14,9	18,0	22,0	25,2
NNW	9,3	12,6	15,7	19,8	23,0	12,5	15,5	18,4	22,1	25,1

Figure 5: Map of reference wind velocities and expected 10-minute speeds with associated probabilities (P%) for return periods T – measurements 2005 – 2014, meteorological stations Ploče and Komarna

The bridge location is also influenced by strong winds with reference wind velocities up to 40 m/s, Figure 5.

Geological - geotechnical properties of the foundation soils in the area of the bridge were determined on the basis of geological and geotechnical investigations carried out in 2004 and 2011 (60 research boreholes, length up to 130 m below the seabed).

In 2018, the contractor, China Road and Bridge Corporation carried out an additional 17 exploration boreholes.

The thickness of soil formations above the limestone rock varies along the bridge from 30 to 100 m. These formations are mostly made of silty clay with an occasional higher proportion of silty or gravelly fractions.

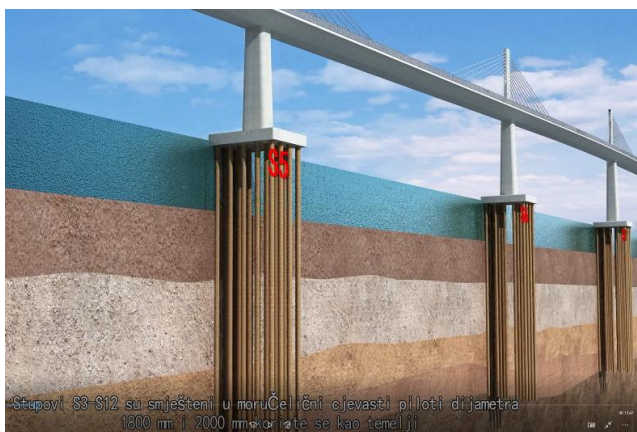


Figure 6: General presentation of the foundations and characteristics of foundation soils

Clay layers up to the depth of 40 - 50 m from the seabed are soft to very firm in consistency. Clay layers in a depth greater than 50 m are older formations. They are stiff to very stiff in consistency, locally cemented or with limestone concretions, slightly over-consolidated, and with porosity of less than 50%.

The weathered rock zone at the west side is situated at the depth of about 38 m under the seabed while toward the mainland the rock was found at the depths of about 75 -102 m, Figure 6.

BRIDGE ALIGNMENT AND CROSS-SECTION

The traffic surface on the bridge is formed of two carriageways.

Each carriageway consists of a 3.5 m wide traffic lane, 2.5 m wide stopping lane, and two marginal strips of 0.50 m. The carriageways are separated with a median strip bounded with safety barriers.

Wind barriers are also foreseen on the bridge, which will enable the use of the bridge in severe weather conditions, and traffic restrictions in case of strong and gusty winds will be reduced to a minimum.

The width of the carriageways with the median strip is 18.50 m and the total bridge width, together with inspection paths and wind barriers amounts to 22.50 m, see Figure 7.

Horizontally the bridge starts and ends with a radius of 450 m followed by a transition curve of length 75 m.

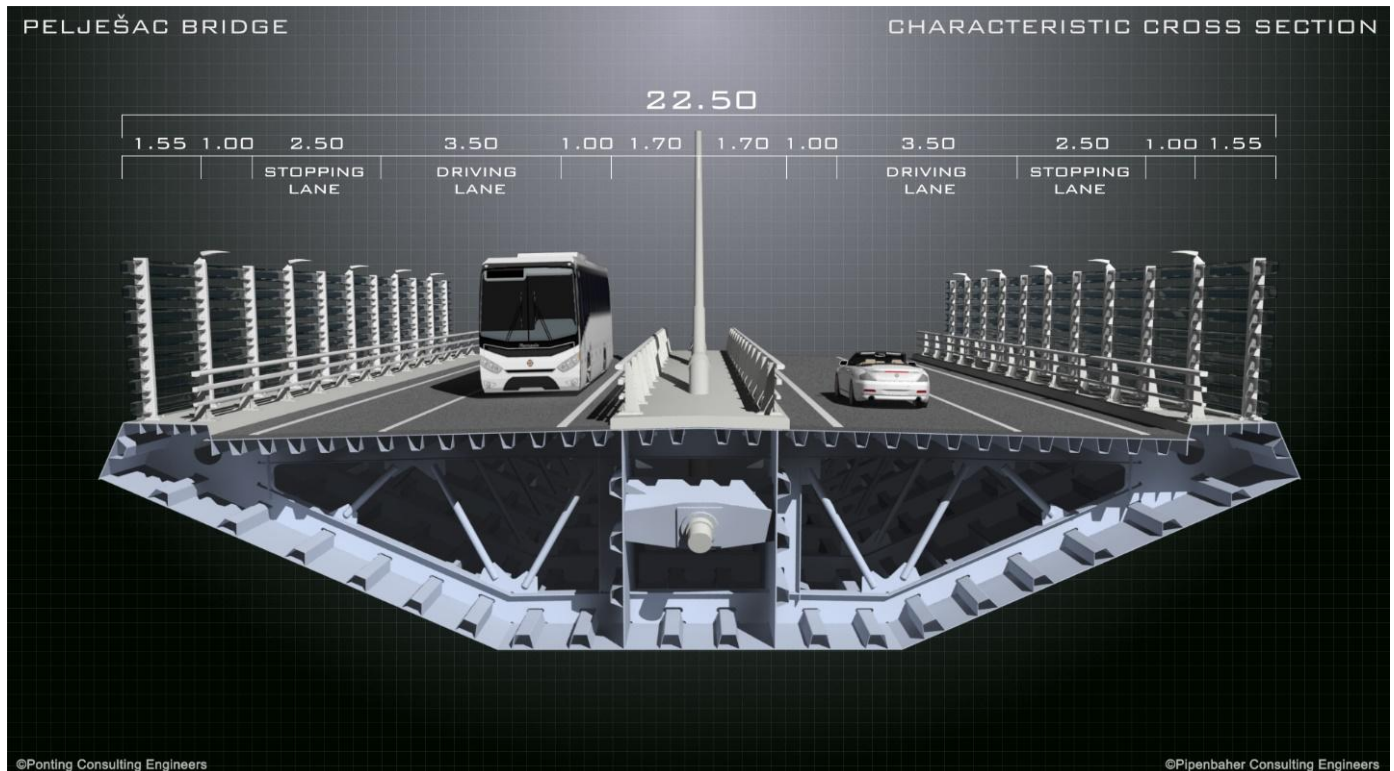


Figure 7: Bridge superstructure with traffic lanes

The main part of the bridge is in a straight line. Vertical alignment starts and ends with a sag curve of radius 8,000 m while the central part of the bridge is summit curve of radius 11,000 m.

In between the structure is practically on a constant slope of 2.98%. For the superstructure, a two-way crossfall of 2.5% was adopted on the straight part of the bridge and at the parts in horizontal curvature the crossfall changes to one-way of maximum 5.8% at the abutment U1.

The crossfall on the inspection paths and the median strip is 2.5%. Outer steel safety barrier of class H3W3 and inner steel safety barrier of class H2W1 according to European standard EN-1317 are provided on the bridge.

The bridge will be illuminated with ambient, road, navigation and signal lighting.

ARCHITECTURAL AND STRUCTURAL CONCEPT OF THE BRIDGE

A comprehensive optimization method was used in the development of structural and architectural concepts for this bridge.

It was necessary to find the optimal ratio between the number of supports, the lengths of the spans and the choice of materials.

The bridge has been designed as a single plane cable-stayed bridge with six 40.0 m high centrally placed pylons and five 285 m main spans.

The integral hybrid superstructure ensures the seismic stability of the bridge without the installation of large bearings and seismic dampers. Bearings are planned only at the approach spans of the bridge – at abutments and piers 2 - 4 and 11 - 13.

Bridge piers, situated in the sea are founded on driven steel piles of 1,800 and 2,000 mm diameter. The piles are 36 – 128.4 m long.

At sea level, the piles are integral with reinforced concrete pile caps. Pile caps of piers S3, S4, S11 and S12 are 4.5 m thick with dimensions of 17.0 x 17.0 m and pile caps of the pylon piers S5 – S10 are 5.0 m thick with dimensions of 23.0 x 29.0 m.

The foundation of the piers on the approach spans of the bridge is provided by a group of 9 piles.

Due to high seismic loads, the piles are designed as composite (steel pipes 1,800 – 2,000 mm in diameter, 40 mm thick, filled with concrete) with an additional 5.0 - 7.0 m long concrete socket under the steel tubes, made in a compact rock.



Figure 8: Pelješac peninsula with countless hills

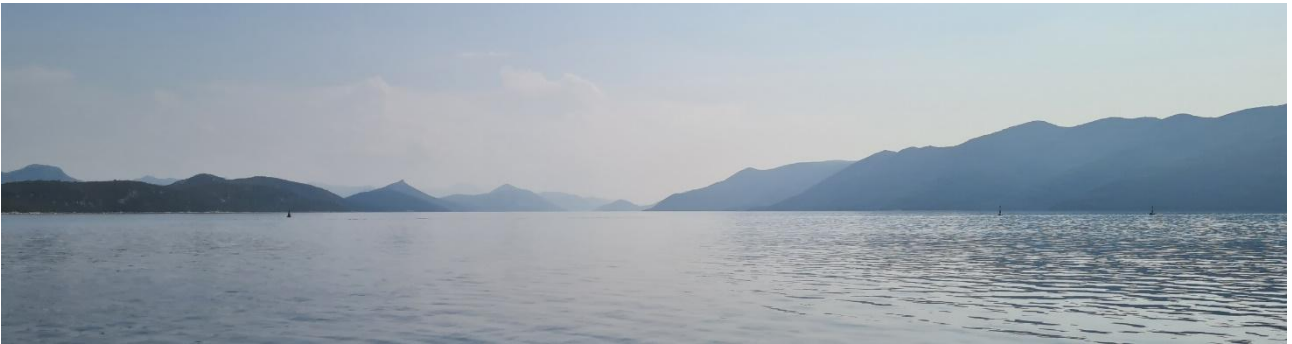


Figure 9: Genius Loci - landscape motif – flat sea area with countless number of hills in background

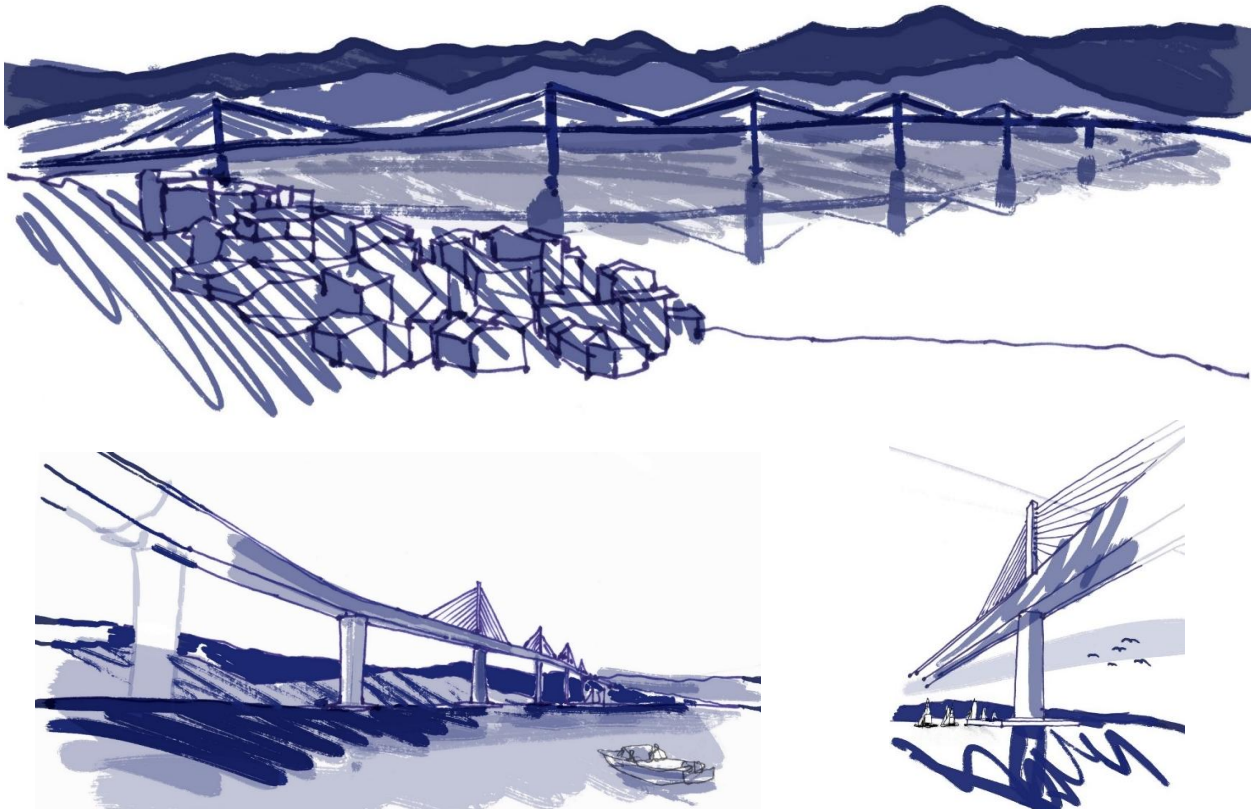


Figure 10: Development of architectural and structural bridge concept with several (“countless”) low pylons

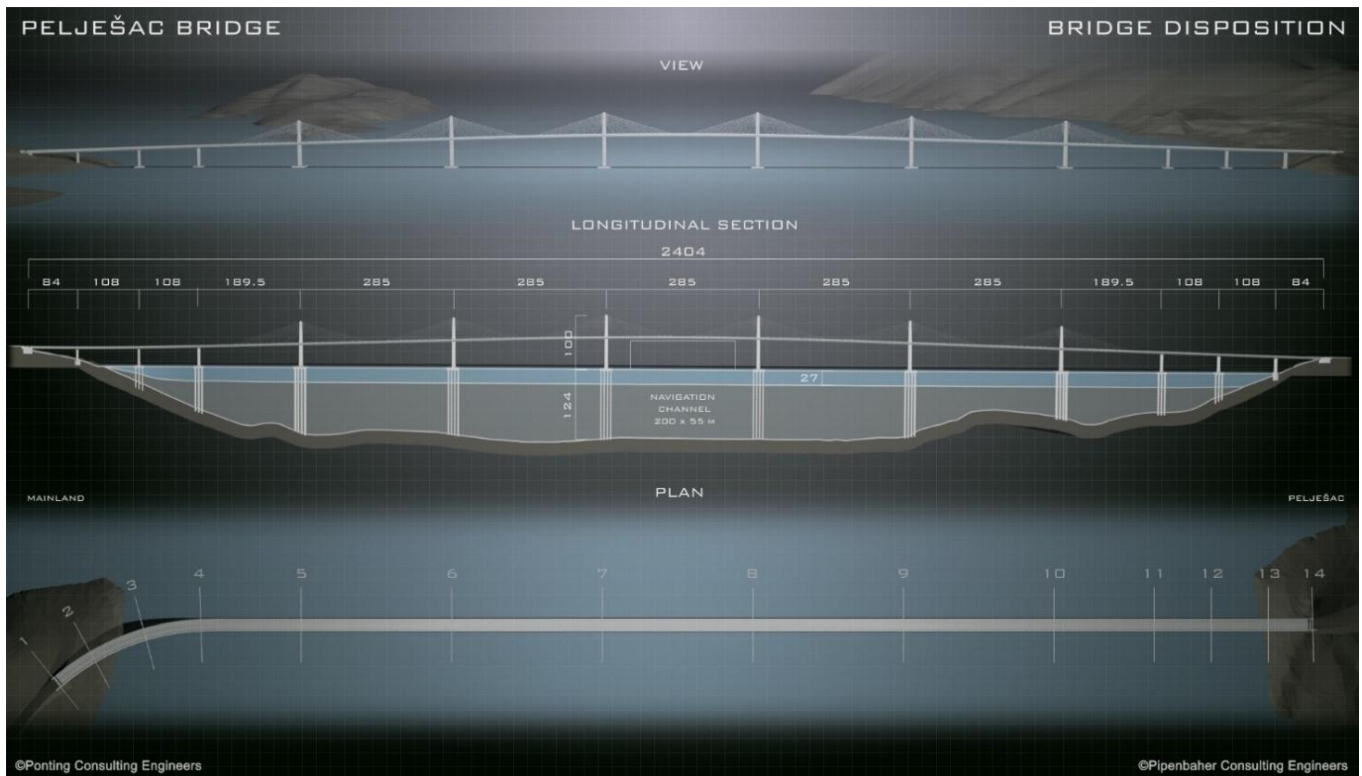


Figure 11: Bridge views, longitudinal section and plan view

The foundation of supports S5 - S10 comprise 18 (20) driven steel piles with a diameter of 2000 mm, a wall thickness of 40 mm and filled with reinforced concrete in the upper 40 m.

The superstructure comprises a three-cell steel box girder of depth 4.5 m with an orthotropic deck and span arrangement: $84.0 + 2 \times 108.0 + 189.5 + 5 \times 285.0 + 189.5 + 2 \times 108.0 + 84.0 = 2,404$ m, see Figure 11 and drawings after this Chapter.

The superstructure is supported with stay cables, arranged in a single plane at 12 m distances. Stay cables are connected to the pylons with passive ("dead end") anchorages, anchored to specially designed steel pylon links. Stays were stressed at the deck. These dead end anchorages are (internal & external) corrosion protected, they will be monitored and can be replaced in case of replacing of stay cable.

VSL stay cables with parallel, galvanized, waxed and HDPE-sheathed 7-wire strands, steel grade 1,660/1,860 are installed. The number of strands varies from 55 to 109 strands. Strands are additionally protected with high-density polyethylene (HDPE) pipes with helical ribs.

The bridge was designed according to the Eurocode Standards.

Nonlinear static and dynamic analyses of the bridge

The Pelješac Bridge, due to the demanding characteristics of its location, ranks amongst the most demanding bridges, not only in terms of technological complexity of construction but also in terms of complexity of the design.

In the phase of searching for the optimal structural design of the bridge, numerous and extensive preliminary static and dynamic analyses were performed.

The main loads that significantly affected the structural design of the bridge were earthquake and wind.

Since the bridge is located in a highly sensitive and protected area of Mali Ston Bay which hosts the largest oyster cultivation facilities in the Adriatic Sea, the Croatian marine authorities defined special navigation conditions and restrictions for ship traffic in the Mali Ston Bay.

After the completion of the preliminary analyses and the optimization phase, detailed analyses were performed.

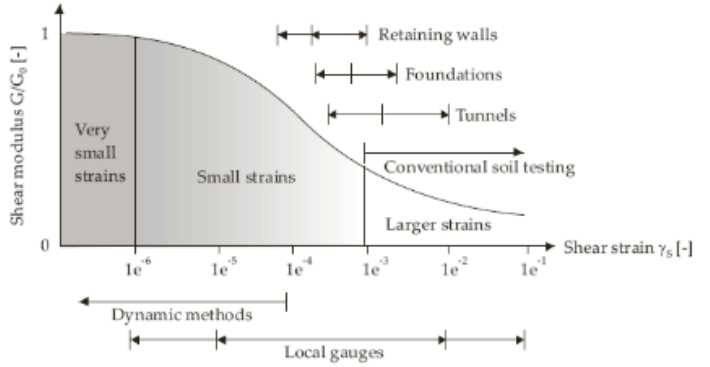
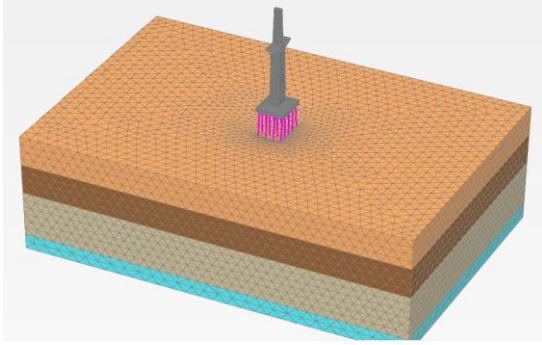
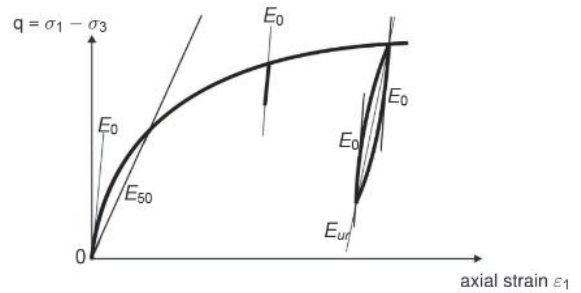


Figure 12: 3D FE-Model of typical support with surrounding soil

Due to the fact that the bridge is founded on very long and slender piles penetrating through the layers of soft soil, it was not sufficient to use a simple linear stiffness-impedance matrix to represent the foundation characteristics.

It was necessary to develop a fully coupled analytical model of the entire system - including the superstructure, pylons, stay cables, piers, pile caps and piles with non-linear soil springs.

To be able to reliably derive non-linear inelastic soil springs and to validate the soil foundation model



used in the coupled bridge response analysis, a 3D soil structure analysis was created.

The analysis was performed on the HSS-Hardening Soil with small-strain stiffness geotechnical model, Figures 12 and 13.

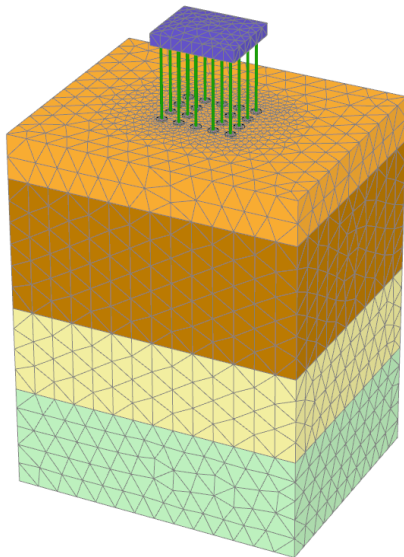


Figure 13: Analysis of vertical displacement and bearing capacity

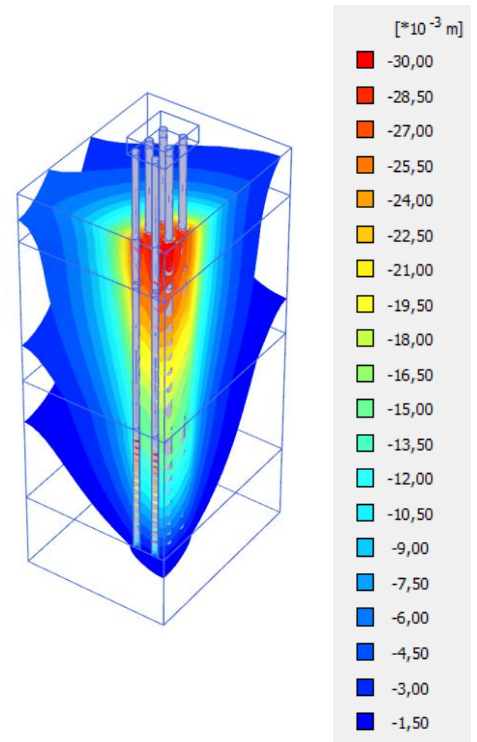
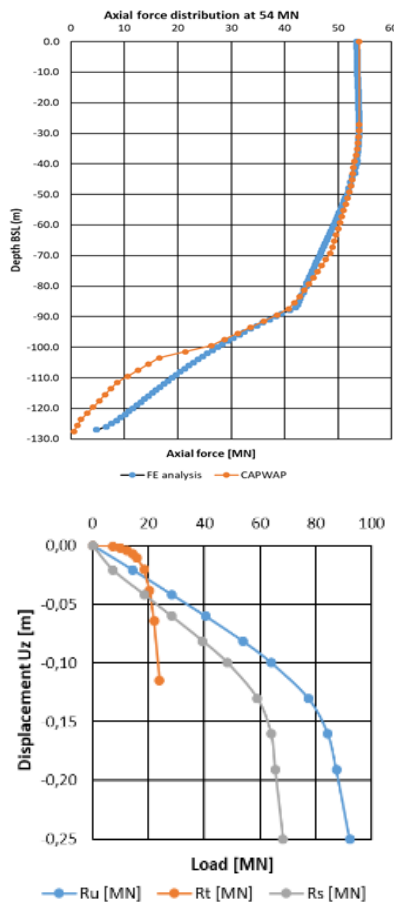




Figure 14: RM Bridge/Bentley computer model with beam elements



Figure 15: SOFiSTiK computer model with beam/shell elements

Complete global analyses of the bridge were performed parallel with two different software packages, RM-BRIDGE/Bentley and SOFiSTiK Figures 14 and 15.

Both models were modelled with the same accuracy, considering soil-structure interaction. All the in-service loads and construction stages were considered.

Comprehensive time history analyses were performed based on the results of a site-specific seismological study made by the Geology department of the Faculty of Science, University of Zagreb (72 numerically generated accelerograms for magnitudes 6.0 - 7.5 and epicenter distances of 5.0, 10.0, 25.0, 50.0, 100.0, 150.0 km in the depth of 10 km), which comprised altogether 24 different EQ load sets.

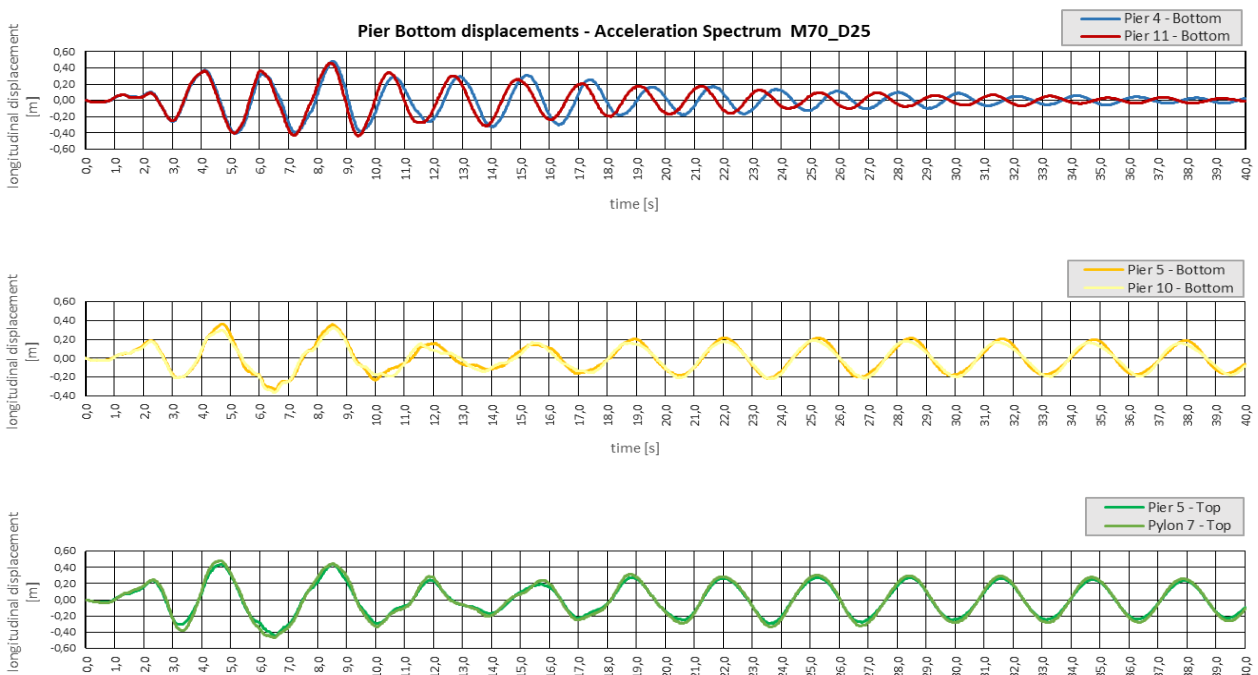


Figure 16: Results of Time history analysis (time dependent displacements of piers and pylons in bridge axis direction)

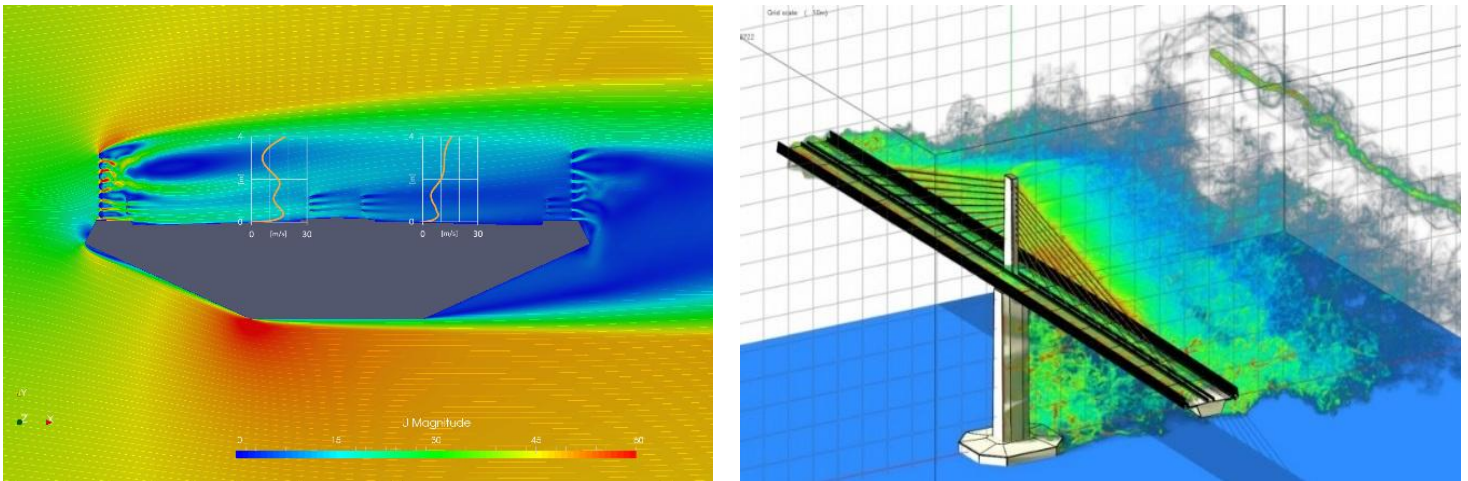


Figure 17: CFD Analyses

Nonlinear time history analysis was performed on a computer model with nonlinear springs.

For horizontal direction nonlinear (p-y) springs were defined, and for vertical direction nonlinear springs for skin friction were considered in the analysis, Figure 16.

With CFD (Computational Fluid Dynamic) analyses, the optimization of the cross-section of the superstructure and the wind fence was performed, Figure 17.

The aerodynamic characteristics of the bridge were tested also in the wind tunnel by Force Technology, Copenhagen, Denmark.

In the first stage, section model tests were performed but later also full aeroelastic bridge model tests were performed, Figure 18.

Detailed analysis of bridge elements was performed for all relevant loads and load combinations, Figures 19 and 20.

Maximum/minimum normal, shear and principal stresses in individual elements in the construction phases and in service were checked.

Global analysis of steel superstructure was followed by plate buckling resistance analysis and dimensioning of the welds.

The thickness of the superstructure steel plates was limited to 40 mm, so in the areas where stresses were exceeded for S355 quality steel, higher quality steel (S460) was used.

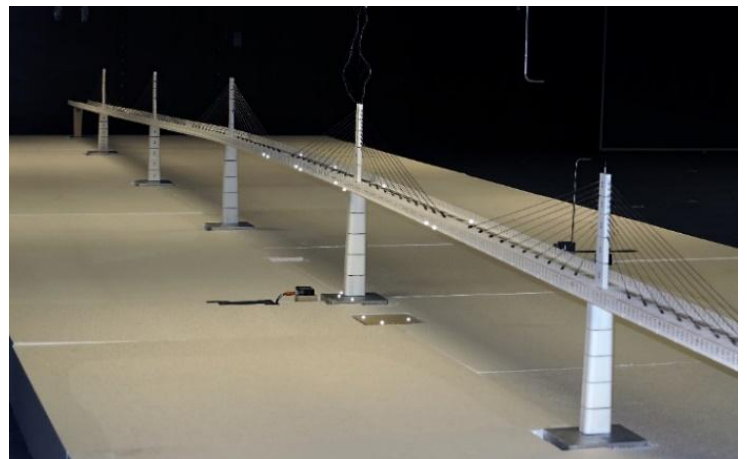


Figure 18: Concept of wind barrier and Full bridge model test, scale 1:150

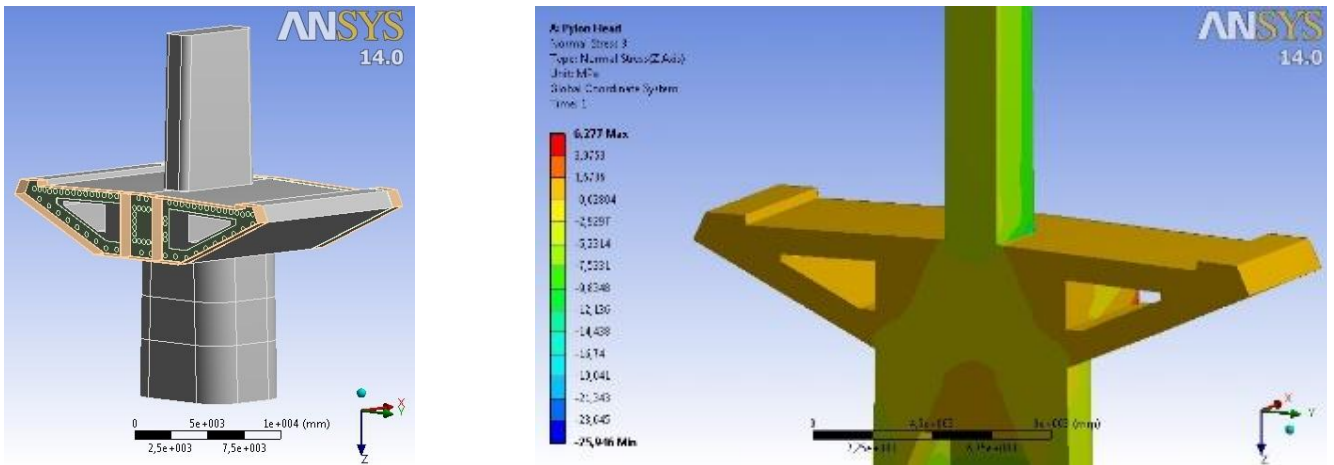


Figure 19: Detailed analysis of the connection between the pier, pylon and superstructure with solid elements

[Click on the image to open it in a higher resolution](#)

Monitoring during construction and in service

During construction and in service the following structural behavior of the bridge, weather conditions, seismic activity and durability was and will be monitored in real time from one central position, Figure 21:

- Parameters describing the current state of the structure (temperature of the superstructure, stay cables and concrete elements, stresses, deformations, vibrations, forces in the stay cables, ...),
- The weather station with built-in ultra-sonic anemometer will monitor the air

temperature and humidity, wind direction and speed (average 10 minutes speed and the speed of 3s wind gusts), which are crucial data for traffic safety,

- Seismic activity in the near surrounding of the bridge,
- Special attention will be paid to the monitoring of the durability of the structure (depth of concrete carbonization, corrosion of reinforcement, anti-corrosion protection and corrosion of steel superstructure, condition of steel wires of stay cables, ...).

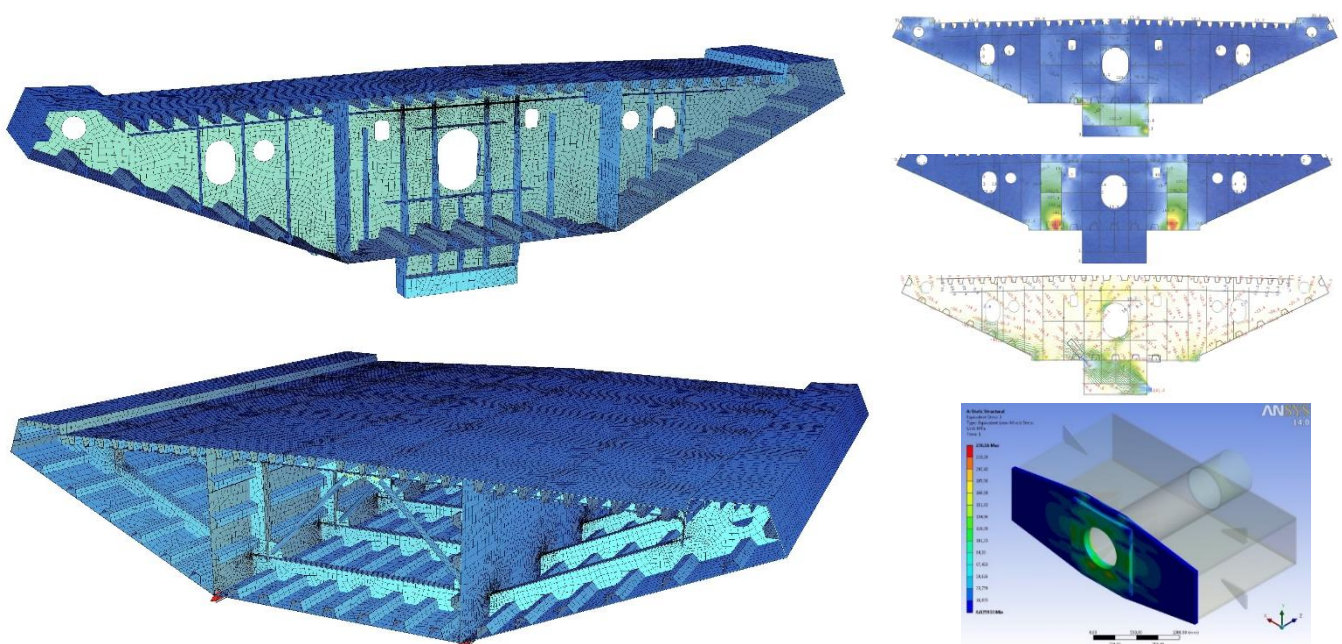
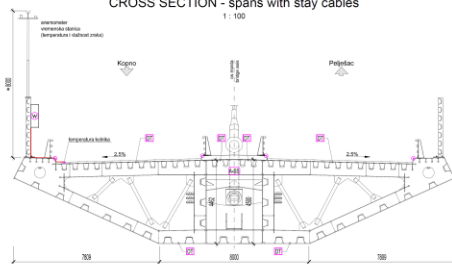


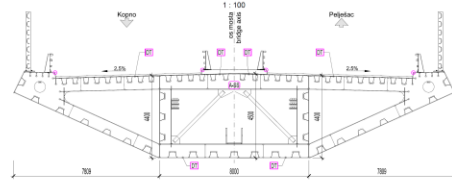
Figure 20: Detailed analysis of superstructure with shell and solid elements

KONCEPT MONITORINGA MOSTA / BRIDGE MONITORING CONCEPT

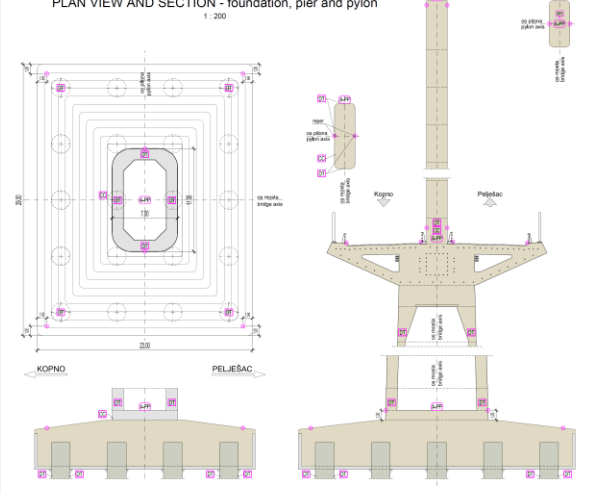
POPREČNI PRESJEK - područje kosih zatega CROSS SECTION - spans with stay cables



POPREČNI PRESJEK - područje kontinuirane grede CROSS SECTION - continuous girder spans



TLOCRT I PRESJEK - temelj, stup i pilon PLAN VIEW AND SECTION - foundation, pier and pylon



TLOCRT I PODOŽNI PRESJEK PLAN VIEW AND LONGITUDINAL SECTION

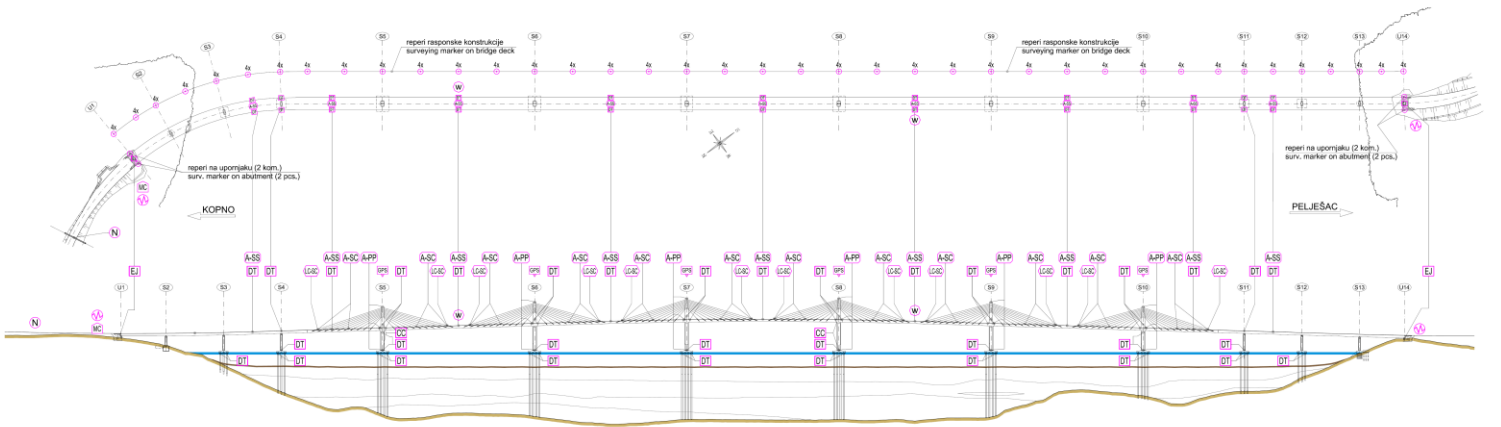


Figure 21: Bridge monitoring concept during construction and service

[Click on the image to open it in a higher resolution](#)

LEGENDA / LEGEND:

MC - monitoring centar
- monitoring center

N - brojanje, struktura i težina prometa
- traffic volume, composition and load measurement

W - seizmograf
- seismograph

W - anemometer
- anemometer

DT - senzor deformacija i temperatura
- strain and temperature sensor

CC - senzor korozije betona i armature
- concrete and reinforcement corrosion sensor

EJ - mjerilac pomaka prijelazne naprave
- expansion joint displacement meter

A-SS - akcelerator - rasponska konstrukcija
- accelerometer - superstructure girder

A-SC - akcelerator - kose zatege
- accelerometer - stay cables

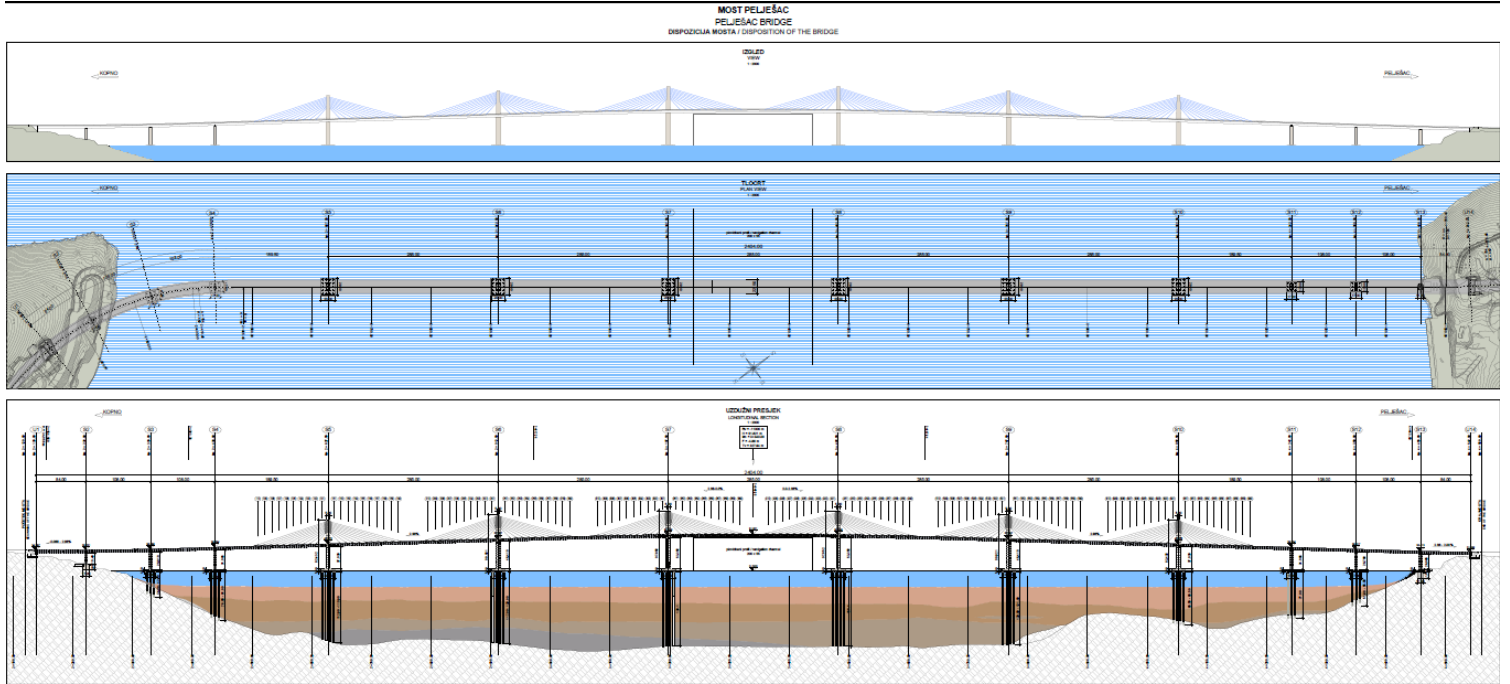
A-PP - akcelerator - stup i pilon
- accelerometer - pier and pylon

LC-SC - load cell - kose zatege
- load cell - stay cables

GPS - GPS senzor
- GPS sensor

○ - reper
- surveying marker

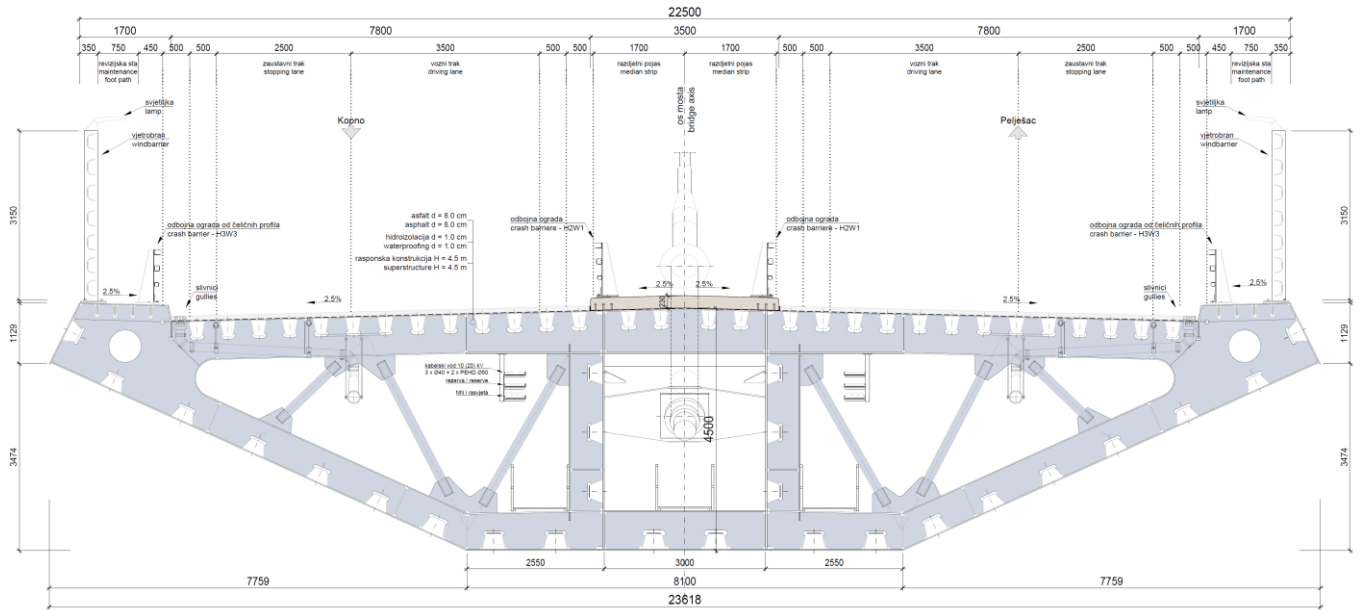
DRAWINGS



Plan View and Elevation of the Bridge

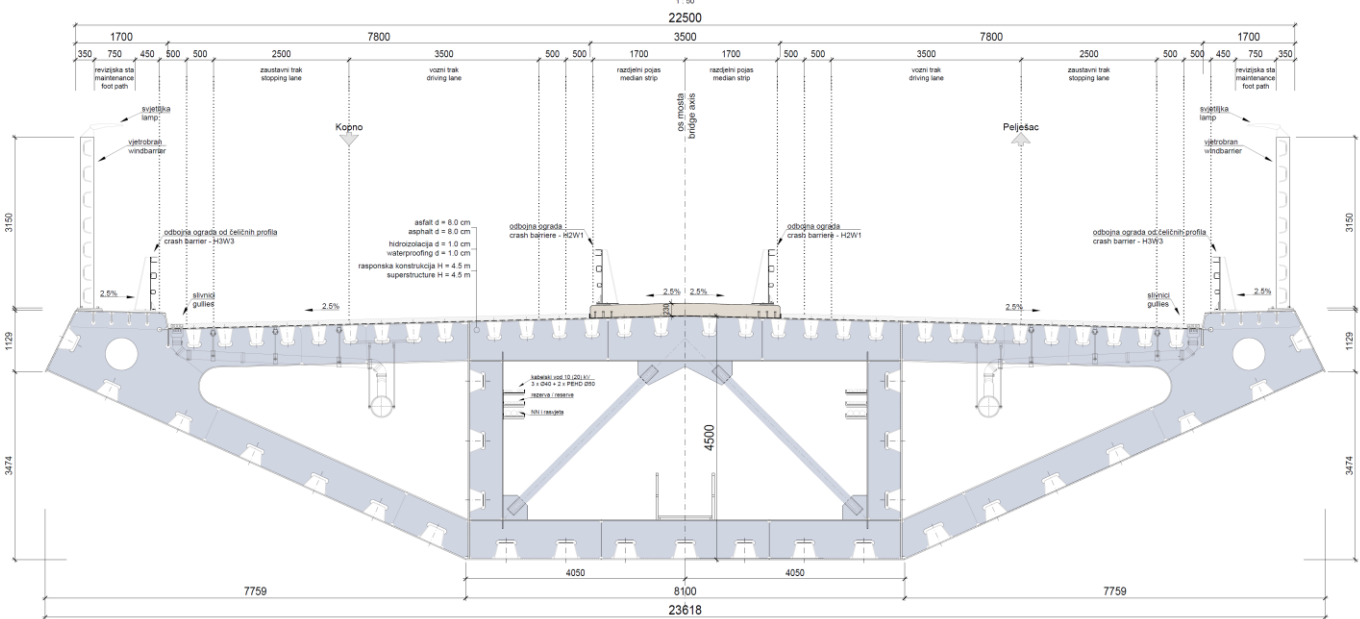
Click on an image to open it in a full resolution

KARAKTERISTIČKI POPREČNI PRESJEK - područje kosih zatega CHARACTERISTIC CROSS SECTION - main spans



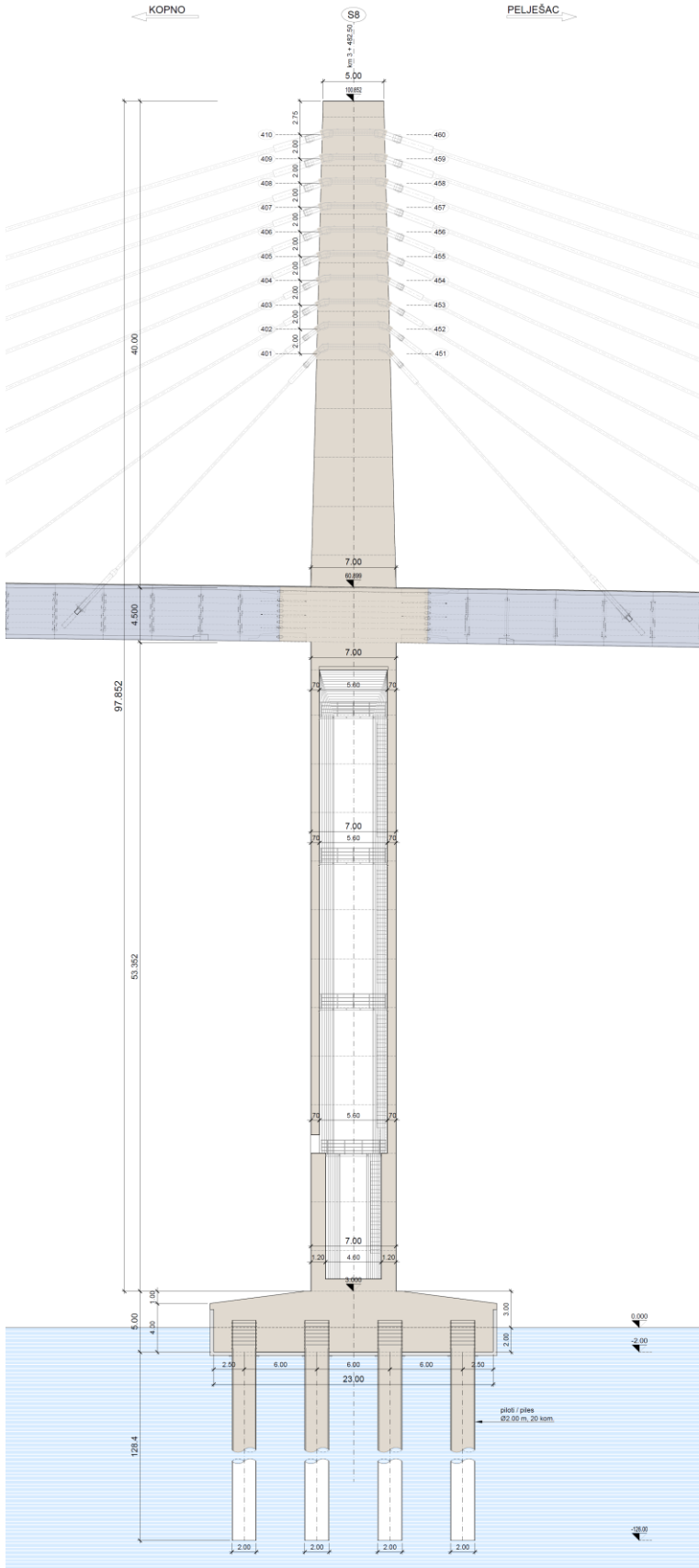
Cross-Section: Main Span

KARAKTERISTIČKI POPREČNI PRESJEK - područje kontinuirane grede CHARACTERISTIC CROSS SECTION - side spans

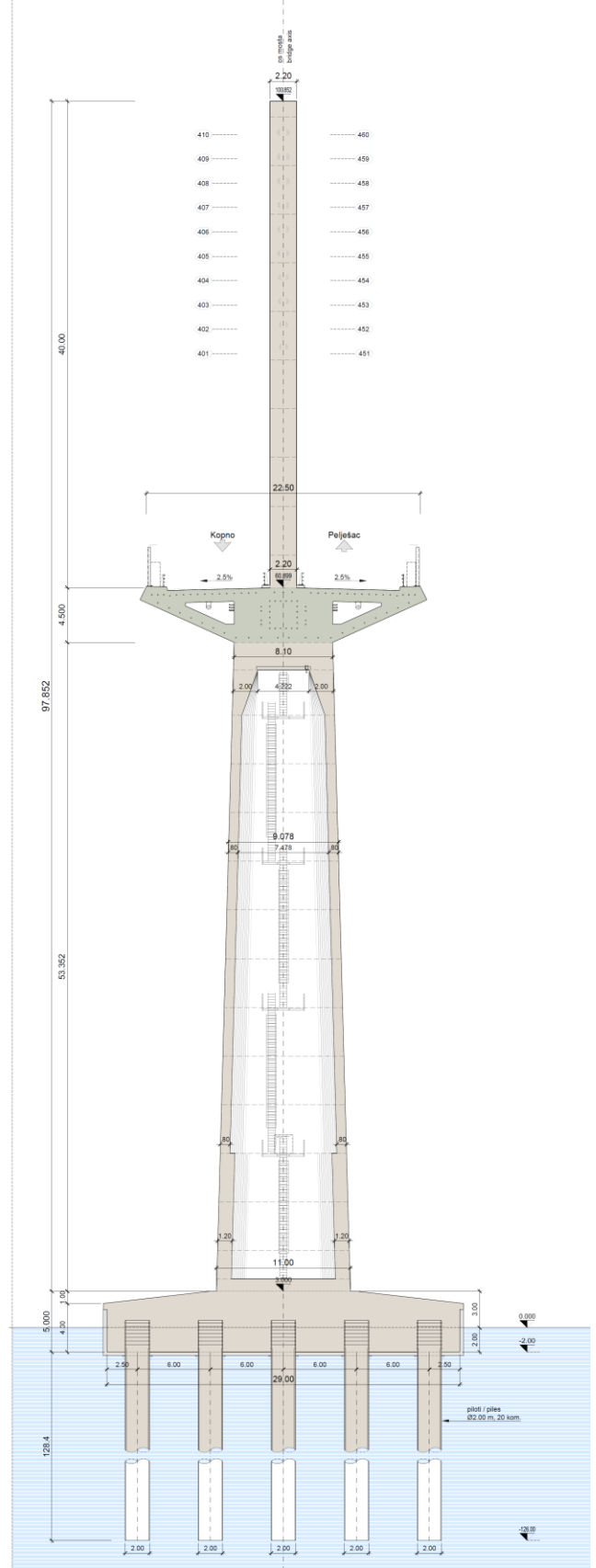


Cross-Section: Side Span

UZDUŽNI PRESJEK
LONGITUDINAL SECTION
1:200



POPREČNI PRESJEK
CROSS SECTION
1:200



Pier and Pylon

CONSTRUCTION OF THE BRIDGE

Construction site organization

In the detail design phase, the contractor prepared an outline of the construction site requirements, which precisely defined the organization of the construction site for the entire construction period, including all necessary technical equipment, machinery on the construction site and all materials used.

The contractor had to erect buildings and structures both for his own needs and for the needs of the investor.

It was also necessary to take into account all the required measures to protect the sensitive environment of the bridge location.

Manufacture, transport, driving and testing of steel piles

The driven steel piles provide the necessary foundation support, and at the same time, they were the optimal solution both from the ecological and from the execution point of view.

For the bridge foundation, 146 piles were driven on 10 supports positioned in the sea.

All 31,000 tonnes of steel piles were fabricated in China and transported to the site by boats. The length of the piles with a wall thickness of 40 – 60 mm ranged from 36 m to 130.6 m and the share of the piles longer than 100 m exceeded 70% of all piles.

The 130.6 m long test pile set a record as the longest prefabricated steel pile in the world, Figures 22 and 23.

According to the load transfer, there are two different types of the piles. The piles under the pylons S5 – S9 transfer the load by shaft friction and toe bearing capacity.

These piles are only partially filled with soil, with the upper 40 m filled with reinforced concrete.



Figure 22: Manufacturing of the piles



Figure 23: Transportation of the piles



Figure 24: Driving of up to 130.6 m long piles

The second group of piles transmits loads (both compressive and tensile forces) through reinforced concrete sockets in rock at the base of the piles and are completely filled with reinforced concrete.

This method is used for shorter piles on the approach parts of the bridge where the layers of compact clay are not thick enough to ensure resistance to tensile loads.

Driving of the piles was performed with a hydraulic hammer IHC 800 with a kinetic energy of 800 kJ, Figure 24.

Dynamic monitoring of the driving was performed according to ASTM D4 945-08 (Standard Test Method for High Strain Dynamic Testing of Deep Foundation). For each pile, at the end of driving and after re-driving, a shaft and tip bearing capacity analysis was performed with the CAPWAP - Case Pile Wave Analysis Program, Figure 25.

POVIJEST DINAMIČKOG ISPITIVANJA PILOTA - MOST PELJEŠAC HRVATSKA / PILE DYNAMIC TESTING HISTORY - PELJEŠAC BRIDGE-CROATIA					
Dinamička pilota / Pile name (PW)	S5.4-5				
	CELIK / HAMMER	IHC 800	IHC 800	IHC 800	IF50
Deblina telesa / Testing stake (L [m])	15.2.2019	16.2.2019	16.2.2019	15.2.2019	
Deblina vode / Water depth (m)	20.00				
PW & HW (m)	70.00				
LP1 - početak / start PDA (m)	70.40	69.50	69.67	69.67	
LP2 - kraj / end PDA (m)	69.52	69.67	69.67	69.67	
ZAVRŠETAK TESTANJA / END OF TESTING	0.30	0.15	0.15	0.15	
Max. udar / Max. blow (m)	80.0	80.0	80.0	80.0	
Max. brzina / Max. velocity (m/s)	467	506	506	506	
Br. udaraca / B.C.T. (B/T 20mm)	41	40.00	40	40	
PDA početak / PDA Start (m)	12.33	11.30	14.49	12.6	
PDA kraj / PDA Stop (m)	13.17	11.35	14.59	12.18	
Br. udaraca / Blow No.	1004	11	10	2	
POBUNA / SEF	0	3	0.1	1	
Pravak posrednik / Set per blow (mm)	17	23	24	30	
ENERGIJA / ENERGY	EMJ (kJ/m)	481	627	604	626
EF (%)	67%	67%	76%	100	
NAPON / STRESSES	CSX (MPa)	153	175	166	184
CSB (MPa)	131	156	156	143	
CASE	R01 (kN)	38.0	46.0	51.3	53.0
R02 (kN)	23.0	31.0	30.0	41.0	
CAPWAP	R0 (kN)	20.7	29.8	41.3	51.8
R1 (kN)	9.9	16.2	11.2	11.0	
R2 (kN)	10.8	3.6	0.1	0.8	
Br. udaraca / Blows					
max R0 (kN)	26.3	51.2	51.2	51.2	
R0_max (kN)	10.0	10.0	10.0	10.0	
R0_max (kN)	27.1	62.0	62.0	62.0	
max R1 (kN)	18.0	43.4	43.4	51.8	
max R2 (kN)	11.6	11.6	2.8	1.3	
Br. udaraca / Blows					
max R0 (kN)	18.0	43.4	43.4	51.8	
R0_max (kN)	10.0	10.0	10.0	10.0	
R0_max (kN)	27.1	62.0	62.0	62.0	
max R1 (kN)	18.0	43.4	43.4	51.8	
max R2 (kN)	11.6	11.6	2.8	1.3	
Br. udaraca / Blows					
max R0 (kN)	18.0	43.4	43.4	51.8	
R0_max (kN)	10.0	10.0	10.0	10.0	
R0_max (kN)	27.1	62.0	62.0	62.0	
max R1 (kN)	18.0	43.4	43.4	51.8	
max R2 (kN)	11.6	11.6	2.8	1.3	
Br. udaraca / Blows					
max R0 (kN)	18.0	43.4	43.4	51.8	
R0_max (kN)	10.0	10.0	10.0	10.0	
R0_max (kN)	27.1	62.0	62.0	62.0	
max R1 (kN)	18.0	43.4	43.4	51.8	
max R2 (kN)	11.6	11.6	2.8	1.3	
Br. udaraca / Blows					
max R0 (kN)	18.0	43.4	43.4	51.8	
R0_max (kN)	10.0	10.0	10.0	10.0	
R0_max (kN)	27.1	62.0	62.0	62.0	
max R1 (kN)	18.0	43.4	43.4	51.8	
max R2 (kN)	11.6	11.6	2.8	1.3	
Br. udaraca / Blows					
max R0 (kN)	18.0	43.4	43.4	51.8	
R0_max (kN)	10.0	10.0	10.0	10.0	
R0_max (kN)	27.1	62.0	62.0	62.0	
max R1 (kN)	18.0	43.4	43.4	51.8	
max R2 (kN)	11.6	11.6	2.8	1.3	
Br. udaraca / Blows					
max R0 (kN)	18.0	43.4	43.4	51.8	
R0_max (kN)	10.0	10.0	10.0	10.0	
R0_max (kN)	27.1	62.0	62.0	62.0	
max R1 (kN)	18.0	43.4	43.4	51.8	
max R2 (kN)	11.6	11.6	2.8	1.3	
Br. udaraca / Blows					
max R0 (kN)	18.0	43.4	43.4	51.8	
R0_max (kN)	10.0	10.0	10.0	10.0	
R0_max (kN)	27.1	62.0	62.0	62.0	
max R1 (kN)	18.0	43.4	43.4	51.8	
max R2 (kN)	11.6	11.6	2.8	1.3	
Br. udaraca / Blows					
max R0 (kN)	18.0	43.4	43.4	51.8	
R0_max (kN)	10.0	10.0	10.0	10.0	
R0_max (kN)	27.1	62.0	62.0	62.0	
max R1 (kN)	18.0	43.4	43.4	51.8	
max R2 (kN)	11.6	11.6	2.8	1.3	
Br. udaraca / Blows					
max R0 (kN)	18.0	43.4	43.4	51.8	
R0_max (kN)	10.0	10.0	10.0	10.0	
R0_max (kN)	27.1	62.0	62.0	62.0	
max R1 (kN)	18.0	43.4	43.4	51.8	
max R2 (kN)	11.6	11.6	2.8	1.3	
Br. udaraca / Blows					
max R0 (kN)	18.0	43.4	43.4	51.8	
R0_max (kN)	10.0	10.0	10.0	10.0	
R0_max (kN)	27.1	62.0	62.0	62.0	
max R1 (kN)	18.0	43.4	43.4	51.8	
max R2 (kN)	11.6	11.6	2.8	1.3	
Br. udaraca / Blows					
max R0 (kN)	18.0	43.4	43.4	51.8	
R0_max (kN)	10.0	10.0	10.0	10.0	
R0_max (kN)	27.1	62.0	62.0	62.0	
max R1 (kN)	18.0	43.4	43.4	51.8	
max R2 (kN)	11.6	11.6	2.8	1.3	
Br. udaraca / Blows					
max R0 (kN)	18.0	43.4	43.4	51.8	
R0_max (kN)	10.0	10.0	10.0	10.0	
R0_max (kN)	27.1	62.0	62.0	62.0	
max R1 (kN)	18.0	43.4	43.4	51.8	
max R2 (kN)	11.6	11.6	2.8	1.3	
Br. udaraca / Blows					
max R0 (kN)	18.0	43.4	43.4	51.8	
R0_max (kN)	10.0	10.0	10.0	10.0	
R0_max (kN)	27.1	62.0	62.0	62.0	
max R1 (kN)	18.0	43.4	43.4	51.8	
max R2 (kN)	11.6	11.6	2.8	1.3	
Br. udaraca / Blows					
max R0 (kN)	18.0	43.4	43.4	51.8	
R0_max (kN)	10.0	10.0	10.0	10.0	
R0_max (kN)	27.1	62.0	62.0	62.0	
max R1 (kN)	18.0	43.4	43.4	51.8	
max R2 (kN)	11.6	11.6	2.8	1.3	
Br. udaraca / Blows					
max R0 (kN)	18.0	43.4	43.4	51.8	
R0_max (kN)	10.0	10.0	10.0	10.0	
R0_max (kN)	27.1	62.0	62.0	62.0	
max R1 (kN)	18.0	43.4	43.4	51.8	
max R2 (kN)	11.6	11.6	2.8	1.3	
Br. udaraca / Blows					
max R0 (kN)	18.0	43.4	43.4	51.8	
R0_max (kN)	10.0	10.0	10.0	10.0	
R0_max (kN)	27.1	62.0	62.0	62.0	
max R1 (kN)	18.0	43.4	43.4	51.8	
max R2 (kN)	11.6	11.6	2.8	1.3	
Br. udaraca / Blows					
max R0 (kN)	18.0	43.4	43.4	51.8	
R0_max (kN)	10.0	10.0	10.0	10.0	
R0_max (kN)	27.1	62.0	62.0	62.0	
max R1 (kN)	18.0	43.4	43.4	51.8	
max R2 (kN)	11.6	11.6	2.8	1.3	
Br. udaraca / Blows					
max R0 (kN)	18.0	43.4	43.4	51.8	
R0_max (kN)	10.0	10.0	10.0	10.0	
R0_max (kN)	27.1	62.0	62.0	62.0	
max R1 (kN)	18.0	43.4	43.4	51.8	
max R2 (kN)	11.6	11.6	2.8	1.3	
Br. udaraca / Blows					
max R0 (kN)	18.0	43.4	43.4	51.8	
R0_max (kN)	10.0	10.0	10.0	10.0	
R0_max (kN)	27.1	62.0	62.0	62.0	
max R1 (kN)	18.0	43.4	43.4	51.8	
max R2 (kN)	11.6	11.6	2.8	1.3	
Br. udaraca / Blows					
max R0 (kN)	18.0	43.4	43.4	51.8	
R0_max (kN)	10.0	10.0	10.0	10.0	
R0_max (kN)	27.1	62.0	62.0	62.0	
max R1 (kN)	18.0	43.4	43.4	51.8	
max R2 (kN)	11.6	11.6	2.8	1.3	
Br. udaraca / Blows					
max R0 (kN)	18.0	43.4	43.4	51.8	
R0_max (kN)	10.0	10.0	10.0	10.0	
R0_max (kN)	27.1	62.0	62.0	62.0	
max R1 (kN)	18.0	43.4	43.4	51.8	
max R2 (kN)	11.6	11.6	2.8	1.3	
Br. udaraca / Blows					
max R0 (kN)	18.0	43.4	43.4	51.8	
R0_max (kN)	10.0	10.0	10.0	10.0	
R0_max (kN)	27.1	62.0	62.0	62.0	
max R1 (kN)	18.0	43.4	43.4	51.8	
max R2 (kN)	11.6	11.6	2.8	1.3	
Br. udaraca / Blows					
max R0 (kN)	18.0	43.4	43.4	51.8	
R0_max (kN)	10.0	10.0	10.0	10.0	
R0_max (kN)	27.1	62.0	62.0	62.0	
max R1 (kN)	18.0	43.4	43.4	51.8	
max R2 (kN)	11.6	11.6	2.8	1.3	
Br. udaraca / Blows					
max R0 (kN)	18.0	43.4	43.4	51.8	
R0_max (kN)	10.0	10.0	10.0	10.0	
R0_max (kN)	27.1	62.0	62.0	62.0	
max R1 (kN)	18.0	43.4	43.4	51.8	
max R2 (kN)	11.6	11.6	2.8	1.3	
Br. udaraca / Blows					
max R0 (kN)	18.0	43.4	43.4	51.8	
R0_max (kN)	10.0	10.0	10.0	10.0	
R0_max (kN)	27.1	62.0	62.0	62.0	
max R1 (kN)	18.0	43.4	43.4	51.8	
max R2 (kN)	11.6	11.6	2.8	1.3	
Br. udaraca / Blows					
max R0 (kN)	18.0	43.4	43.4	51.8	
R0_max (kN)	10.0	10.0	10.0	10.0	
R0_max (kN)	27.1	62.0	62.0	62.0	
max R1 (kN)	18.0	43.4	43.4	51.8	
max R2 (kN)	11.6	11.6	2.8	1.3	
Br. udaraca / Blows					
max R0 (kN)	18.0	43.4	43.4	51.8	
R0_max (kN)	10.0	10.0	10.0	10.0	
R0_max (kN)	27.1	62.0	62.0	62.0	
max R1 (kN)	18.0	43.4	43.4	51.8	
max R2 (kN)	11.6	11.6	2.8	1.3	
Br. udaraca / Blows					
max R0 (kN)	18.0	43.4	43.4	51.8	
R0_max (kN)	10.0	10.0	10.0	10.0	
R0_max (kN)	27.1	62.0	62.0	62.0	
max R1 (kN)	18.0	43.4	43.4	51.8	
max R2 (kN)	11.6	11.6	2.8	1.3	
Br. udaraca / Blows					
max R0 (kN)	18.0	43.4	43.4	51.8	
R0_max (kN)	10.0	10.0	10.0	10.0	
R0_max (kN)	27.1	62.0	62.0	62.0	
max R1 (kN)	18.0	43.4	43.4	51.8	
max R2 (kN)	11.6	11.6	2.8	1.3	
Br. udaraca / Blows					
max R0 (kN)	18.0	43.4	43.4	51.8	
R0_max (kN)	10.0	10.0	10.0	10.0	
R0_max (kN)	27.1	62.0	62.0	62.0	
max R1 (kN)	18.0	43.4	43.4	51.8	
max R2 (kN)	11.				

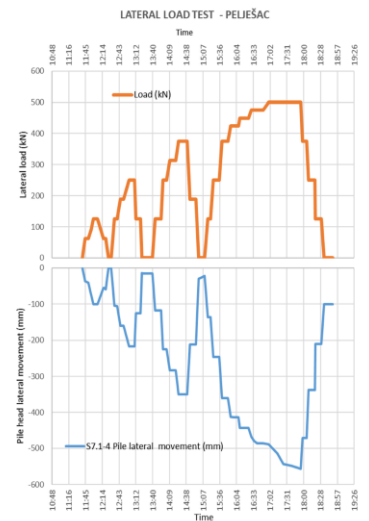


Figure 26: Load test of lateral resistance of the piles

Click on the image to open it in a higher resolution

Load testing of lateral resistance of the piles was also performed and compared with values considered in the nonlinear analyses, Figure 26.

Construction of pile caps

Pile caps in the sea were constructed in several phases, Figure 27.

The first phase was the preparation and assembly of the formwork. The formwork consisted of prefabricated concrete formwork panels on which side steel formwork panels were mounted.

The assembled formwork was hydraulically lowered to the designed height, and the space between the piles and the bottom formwork slab was cast under water with sealing concrete.

Water was then pumped out of the formwork.

The concrete casting was carried out in three layers, each approximately 1.5 m thick.

The piles and the reinforcement of the pile caps are additionally protected against corrosion by cathodic protection, Figure 28.

The cathodic protection system of steel reinforcement in concrete pile caps consists of electrical sources of direct, automatically regulated current, MMO mesh anodes, MnO₂ reference electrodes, cables and steel reinforcement as cathodes.



Figure 27: Construction of pile caps

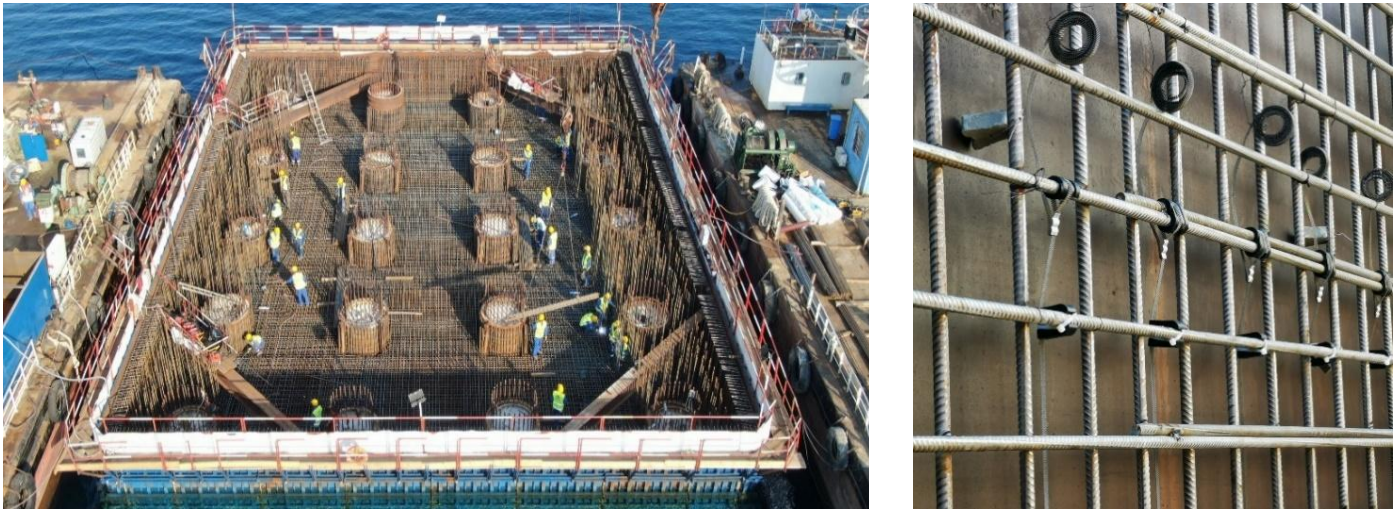


Figure 28: Construction of pile caps with cathodic protection

Construction of superstructure initial segments, piers and pylons

Piers of supports S5 - S10 represent the bottom part of the pylons. They are constructed integrally with the massive pile caps at the bottom and to the superstructure and pylons at the top. Heights of the intermediate piers are between 37.9 m and 53.4 m.

The piers have a hollow box cross-section with rounded corners. The outer dimensions at the bottom of the tallest piers are 7.0 m x 11.0 m and at the top 7.0 m x 8.1 m.

The wall thickness of piers is 0.70 m perpendicular to the bridge axis and 0.80 m in the direction of the bridge axis.

The piers of the pylons and the piers of the approach parts of the bridge were constructed

using self-compacting concrete SCC C50/60, and the pylons of the main spans were constructed using SCC C70/85 concrete which in addition to providing higher strength provides additional durability to the highly loaded structural elements exposed to the aggressive marine environment.

Piers and pylons were constructed using self-climbing formwork of approximately 4.0 long segments, Figure 29. Vertical reinforcement with bars up to 40 mm in diameter was spliced using mechanical couplers.

At the connection between the piers and the pylons, part of the superstructure is constructed in concrete (C50/60) and made integral with the piers and pylons.



Figure 29: Execution of the piers

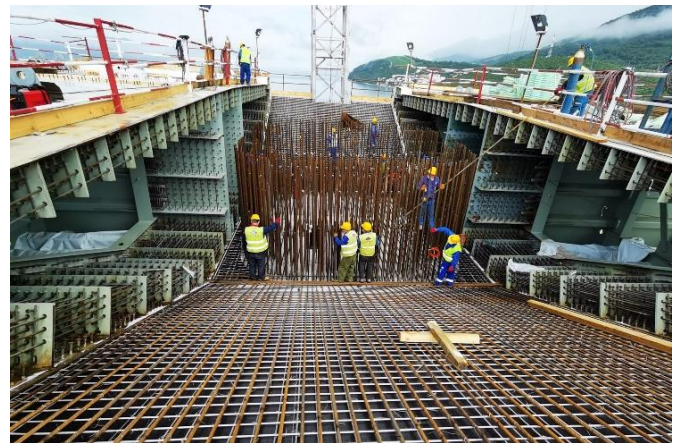
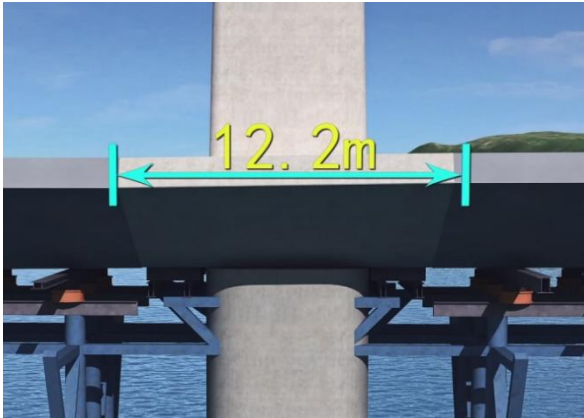


Figure 30: Construction of the base segment

The initial superstructure segments are prestressed with tendons, providing additional load-bearing capacity and providing a compression state in the contact area of the steel and concrete part of the superstructure, Figure 30.

Centrally positioned vertical pylons of supports S5 – S10 are 40 m high. They are constructed of solid reinforced concrete.

At the top, they measure 2.20 m x 5.0 m and at the superstructure level 2.20 m x 7.0 m. Reinforced concrete pylons are cast integral with the initial concrete superstructure segments.

On each pylon 10 steel anchors – pylon links were cast into the pylon for the subsequent installation of stay cables, Figure 31.



Figure 31: Steel anchorages – pylon links for stay cables in the pylons

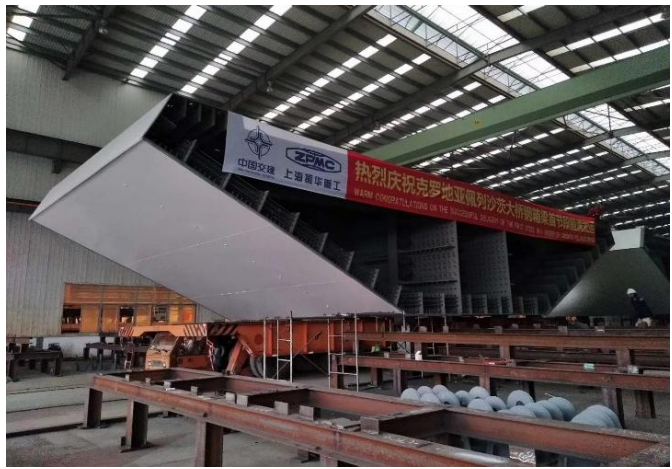
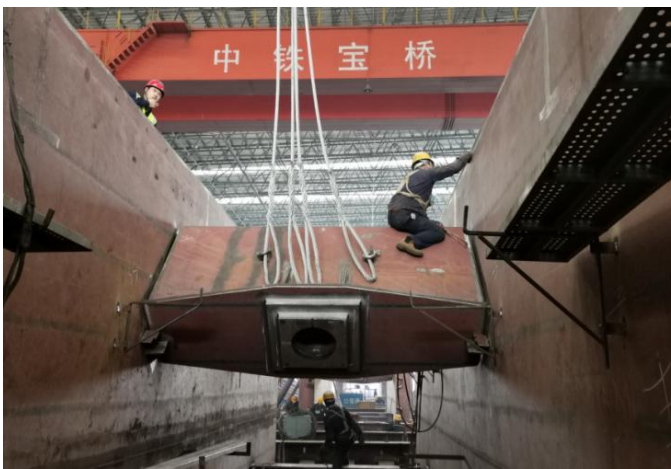


Figure 32: Production of steel segments in production plants in China

Manufacture of steel superstructure segments

34,700 tonnes of steel and more than 450 km of butt and fillet welds were required for the construction of the 2,404 m long steel superstructure.

All 165 segments with a length of 12 to 56 m were fabricated in two production plants in China,

namely ZPMC in Nantong and CRBBG in Shaanx, Figure 32.

Each of the subcontractors produced half of the segments and was also in charge of the assembly and execution of all welds on the construction site.

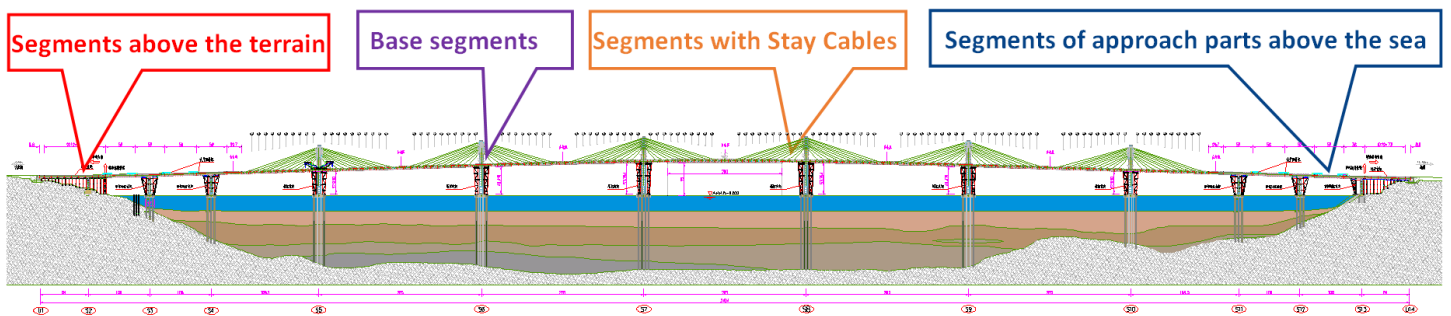


Figure 33: Segments of the steel superstructure



Figure 34: Installation of segments of the approach parts of the bridge above the terrain

Installation of steel segments and stay cables

The segments of the steel superstructure are divided into several sections; the base segments, which are partly connected to the initial concrete segments, the segments of the approach parts of the bridge over the terrain and above the sea, the segments with stay cables and connecting segments.

A different installation method was required for each type of segments, Figure 33.

Segments of the approach spans above the terrain were lifted to a fixed steel scaffolding by a floating crane with a capacity of 1,000 t.

Each segment was then launched towards the abutment to the final position by 3-directional jacks and welded to the previous segment, Figure 34.

The segments of the approach parts above the sea are 36 to 56 m long and were installed by a floating crane.

Segments SS3, SS4, SS11, and SS12, positioned above the piers were installed directly on top of the piers and the auxiliary scaffolding on both sides of the piers.

The segments R203, R3, R11 and R12, which are positioned in the middle of the spans, were temporarily supported by the segments above the piers by means of temporary suspension beams, Figure 35.

Segments with stay cables in the main spans of the bridge were installed using the balanced cantilever construction method, Figure 36.



Figure 35: Installation of large segments of the approach parts of the bridge



Figure 36: Installation of segments with stay cables



The length of the first pair of cantilevered segments was 11.4 m (mass 220 t), and the other nine pairs of segments were 12 m long with a maximum mass of 192 t.

The segments were floated by barge directly to the assembly position.

This was followed by simultaneous lifting of the segments with formwork travellers mounted on the previously installed segments and precise positioning of the new segments before welding. After the welding was completed, the installation and tensioning of the stay cables followed, Figures 37 - 39.

At the end of the assembly of the cantilevered sections of the superstructure, the installation of connecting segments followed.

↑ Figure 37: Balanced cantilever construction and installation of stay cables

↓ Figure 38: Balanced cantilever construction





Figure 39: Balanced cantilever construction

There are seven connecting segments on the bridge, five of them (CR5 - CR9), connecting individual cantilevers in the main part of the bridge are 18.6 m long and two of them (CR4, CR10), connecting approach parts of the bridge with the main part are 29.7 m long, Figures 40 and 41.

All connecting segments were fabricated 10 cm longer on both sides.

Cutting to the final measure was performed on the barge immediately before assembly, depending on the temperature of the structure and the geometry of already assembled parts of the superstructure.



Figure 40: Connecting segments of the bridge



Figure 41: Connected bridge

Specifics of execution – welding and geometry control

Welding of the superstructure was one of the most demanding production processes in the construction of the bridge, Figure 42.

The highest quality of welds (execution class EXC4 according to EN 1090-2) was required.

All necessary NDT testing (visual, magnetic, ultrasonic and radiographic) of performed welds were carried out on a regular basis, Figure 43.



↑ Figure 42: Welding of the steel superstructure

← Figure 43: NDT testing (VT, MT, UT, RT)

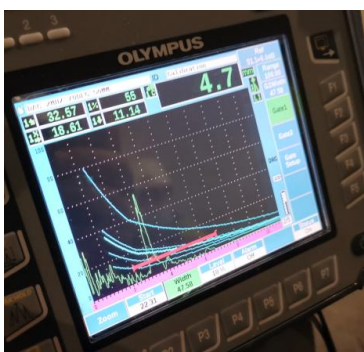




Figure 44: Pelješac Bridge, November 2021

In order for the superstructure to have the necessary final geometry, the segments had to be fabricated in the production plants considering the required camber values.

The camber values for individual segments were determined based on the complex computational analyses in which all construction stages were taken into account, Figure 45.

During the complete period of steel superstructure assembly, geodetic control and monitoring of the actual positions of installed segments were carried out and compared with the calculated positions. Final deviations from the target bridge alignment were local and did not exceed 30 mm.

The construction of the bridge was completed in January 2022 and the Bridge will be opened to traffic after the completion of works on the access roads in the summer 2022.

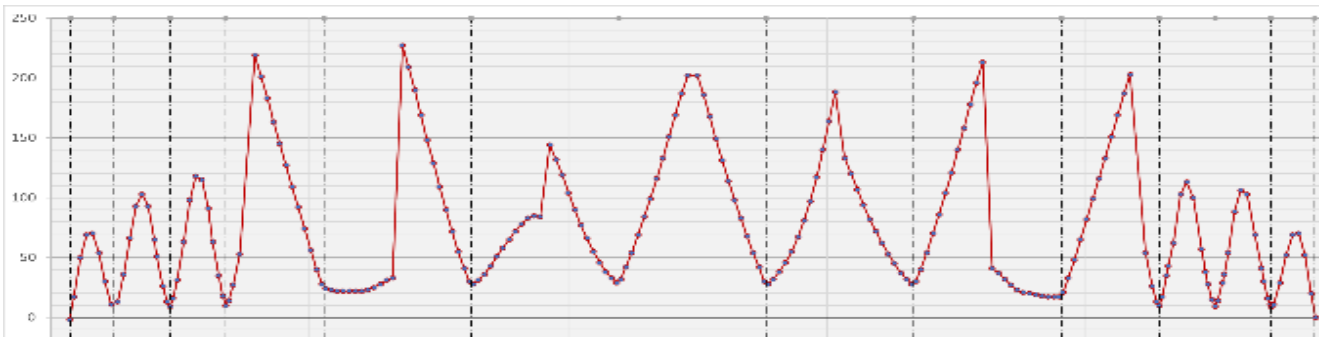
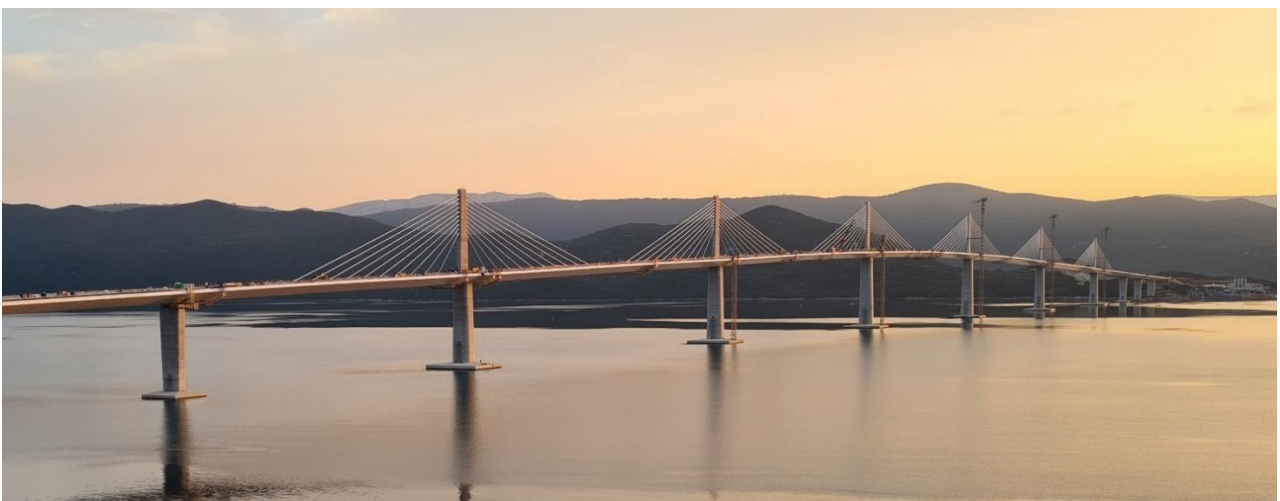


Figure 45: Required camber values of the steel superstructure

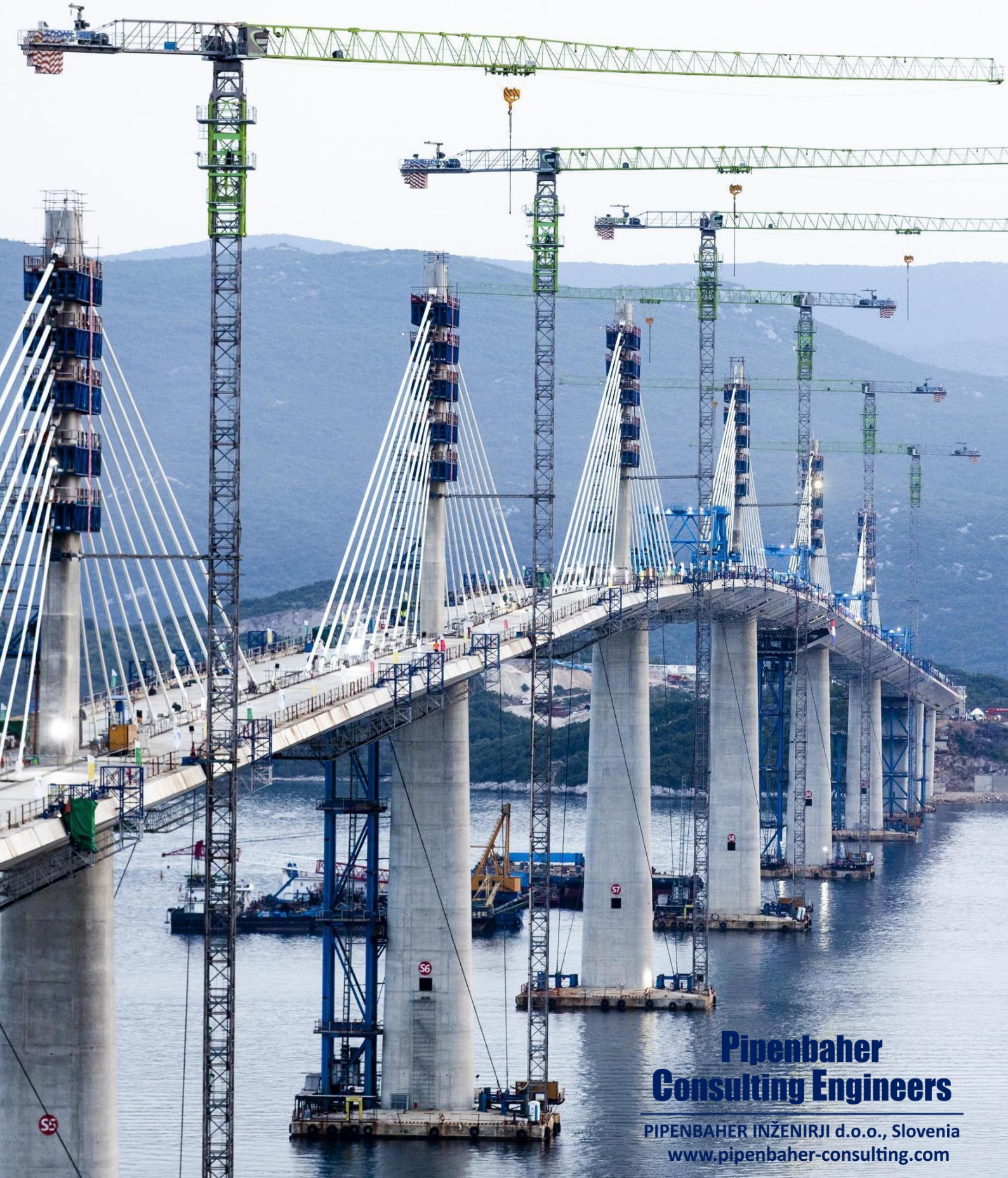


↑ Figure 46: Pelješac Bridge, December 2021

↓ Figure 47: Bridge load testing, January 2022



PELJEŠAC BRIDGE, CROATIA



**Pipenbahr
Consulting Engineers**

PIPENBAHER INŽENIRJI d.o.o., Slovenia
www.pipenbahr-consulting.com

Pipenbahr Consulting Engineers / PIPENBAHER INŽENIRJI d. o. o.

Žolgarjeva ulica 4a, 2310 Slovenska Bistrica, Slovenia



SPHERICAL BEARINGS

FOR THE PELJEŠAC BRIDGE IN CROATIA

Luca Paroli, MAURER



Figure 1: Aerial View of the Bridge towards Pelješac Peninsula in September 2020

The Pelješac Bridge connects northern Croatia with the country's south, in particular the region of Dubrovnik.

Before that, the southern of Croatia could only be accessed overland via the city of Neum that, however, belongs to Bosnia-Herzegovina.

The opening of the new bridge thus offers a complete overland route from the north to the south of Croatia. The bridge is designed as an express highway with two traffic lanes in each direction.

The construction works at the current Pelješac Bridge – the first project was discontinued ten years ago – started in 2018 and the bridge is scheduled to be completed in 2022.

The remarkable length of the bridge of 2,404 m is subdivided into 13 different areas. The main bridge across the so-called Pelješac Canal is a cable-stayed bridge with twelve pylons.

The five central span widths each amount to 285 m. The maximum vertical clearance is 55 m.

Seismic faults are of big importance: the region is an earthquake zone; thus, the bearings must be capable of accommodating large movements and high horizontal forces. For this reason, half of the bearings have been installed vertically.

To this end, MAURER developed a special solution to ensure that no gaps can arise between the sliding surfaces.

In this way, wear is reduced and service life of at least 50 years can be achieved.

SPHERICAL BEARINGS INSTEAD OF POT BEARINGS

Since the entire region is earthquake-prone, the bridge bearings must meet special requirements in terms of movability, durability, and load capacity.

The planners envisaged two spherical bearings and two pot bearings each for the abutments and six of twelve pylons in total.

We succeeded in convincing the customer that spherical bearings are the only way to meet the technical requirements.

Spherical bearings are sliding bearings capable of accommodating arbitrary rotations in all directions without noticeable resistance via an internal spherical calotte joint and thus the bearings can transfer remarkably high forces restraint-free from the bridge deck into the substructure.

16 VERTICALLY INSTALLED SPHERICAL BEARINGS

In autumn 2020, MAURER installed 32 spherical bearings in the bridge, see Figure 2.

The 16 bearings for bridge guidance in longitudinal direction presented a particularly technical challenge.

They must accommodate high horizontal loads of up to 19 MN and have to be installed vertically. In the process, it must be ensured that the sliding surfaces stay in close contact at any time.

Wherever a gap arises, dust can ingress and compromise the sliding properties such as low friction.

Moreover, this would result in wear that reduces the service life to five to ten years instead of at least 50 years as required.

To this end, MAURER developed special bearings featuring disc springs in the core. The springs keep the sliding surfaces in close contact at any time with a force of approx. 500 kN in center position.

In addition, they have been designed fatigue-resistant – due to often occurring wind forces.

This would not have worked out with pot bearings. In case of rotations, there would have been the risk of a gaping joint, resulting in significant wear and shortened service life due to a too rigid elastomeric element.

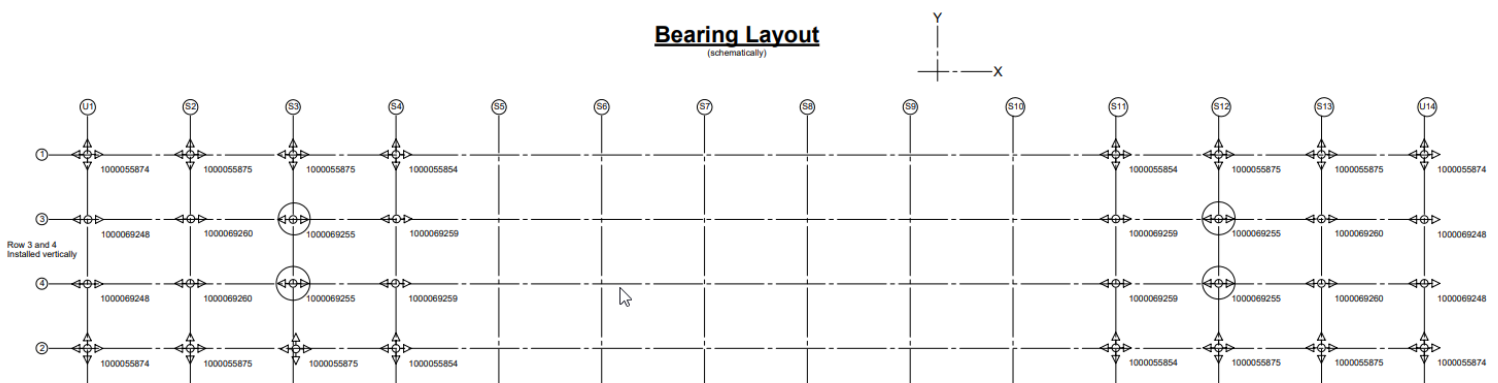


Figure 2: Layout of the bearings

[Click on the image to open it in higher resolution](#)



Figure 3: Spherical bearing with a length of 3m on the concrete base, the white steel deck has still to be lowered.

The bearings accommodate vertical forces of up to 33 MN.

Clearly visible: the cramp shape of the upper sliding plate that prevents the bridge from uplifting for forces up to 2 MN.

As a basic principle, MAURER uses MSM® (MAURER Sliding Material) as high-performance material on all sliding surfaces.

Compared to customary Teflon (PTFE), it can stand at least twice the structural load, in other words: the bearings can be built smaller by approx. 30% and more economical. In addition, MSM® can bear at least five times the movements without wear.

This is particularly important with bridges like the Pelješac Bridge in combination with the forces of nature acting on them.

According to their technical approval, MSM® Spherical Bearings achieve a service life of 50 years.

Additional 16 MSM® Spherical Bearings, two for each pylon, were installed to accommodate vertical forces up to 33 MN.

Since wind and earthquakes can result in uplift forces of up to 2 MN, the upper sections of the bearings are equipped with a cramp to prevent them from uplifting.

Furthermore, all bearings have to accommodate large, fast movements of up to ± 1.3 m in case of an earthquake. That requires a bearing length of up to 3 m.

The largest bearings feature a width of 1.2 m and a height of approx. 330 mm.



*Figure 4: A mirror image:
The bearing (lower half) is reflected in the mirror-bright sliding plate made of stainless steel (top).*

This is why the cramps preventing uplift forces appear double at the top and bottom.

AN IMPORTANT ISSUE FOR BEARINGS AND JOINTS: CORROSION PROTECTION

For reasons of corrosion protection (aggressive sea air), the steel components of the spherical bearings are treated with a suitable C5-m coating and the important inner calotte joint is completely manufactured from one single material: MSA® – MAURER Sliding Alloy.

Compared to a chrome-plated surface, this mirror-bright, extremely smooth and highly corrosion-resistant material allows for a reduction of tolerances by at least 5% while featuring better accuracy of fit in the joint and three to four times longer service life.

The required corrosion protection also affects the design of the expansion joints. These flexible structural elements balance the temperature and seismic movements of the bridge deck of up to 1,400 mm versus the mainland.

Concurrently, it is ensured that traffic can pass these expansion joints without restriction, irrespective of their displacement condition. The expansion joints are installed right-angled in the direction of traffic.

The two joints, type swivel joint expansion joint DS1400 with 14 profiles, were built by MAURER in a hybrid design.

In this case, hybrid means that the upper section of the steel profiles consists of stainless steel whereas the bottom section is made of structural steel, which provides high corrosion protection.

The expansion joint was delivered to Croatia in one piece since no welding work on the joint was allowed at the job site.

This means the expansion joint must only be lifted in position as one component by means of a crane and fastened to the structure, which took no more than one to two days per joint.

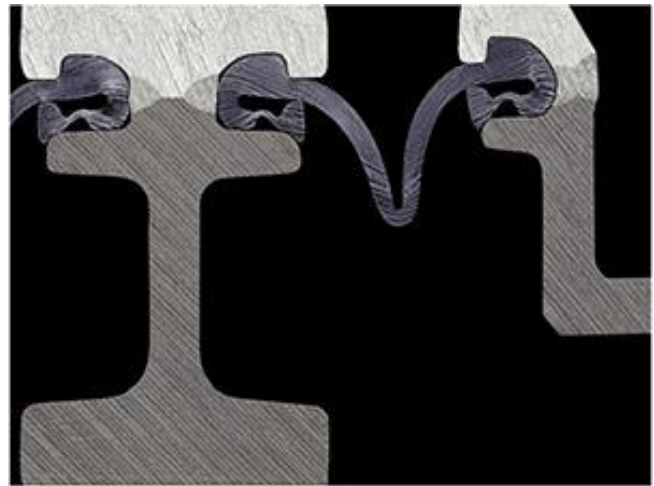


Figure 5: Cross-section of a hybrid profile: the upper part made of stainless steel features outstanding corrosion resistance, exactly in the area of highest impact by traffic and weather conditions



Figure 6: One of the two expansion joints with a length of 23.6 m, type swivel-joint expansion joint DS1400 with 14 profiles; picture taken in the production hall in Munich prior to delivery to Croatia

MAURER MSM[®] Swivel Joist Expansion Joint

OSMAN GAZI BRIDGE, IZMIT, TURKEY | WORLD NO. 4 SUSPENSION BRIDGE WITH HIGH SEISMIC LOAD



Scope of application:

The installation of the MAURER Swivel Joist Expansion Joint shall allow access to and protect the bridge deck from horizontal over load during a seismic event.

Features:

- Unrestrained absorption of specified movements and simultaneous transmission of traffic loads
- Serviceability of the structure after the earthquake
- Protection of the bridge deck from horizontal overload caused by extreme closing movements during the earthquake
- High life time expectation through use of high performance components
- Longitudinal seismic displacement of ca. 4 m
- Service velocity up to 20 mm/sec (10 times higher than for a regular bridge)
- Watertight across the bridge width
- Maintenance free

References:

- Bahia de Cadiz, Spain
- Hochmoselübergang, Germany
- Osman Gazi Bridge, Izmit, Turkey
- Mainbrücke Randersacker, Germany
- Millau Viaduct, France
- Rheinbrücke Schierstein, Germany
- Rion Antirion, Greece
- Russky Island Bridge, Vladivostok, Russia
- Tsing Ma, China

AUTOMATIC CLIMBING FORMWORK XCLIMB 60 FOR PIERS AND PYLONS OF THE PELJEŠAC BRIDGE, CROATIA

František Madleňák, Global Expertise Center Infrastructure, DOKA



Figure 1: General overview of the lower pylon parts

The total length of the Pelješac Bridge is 2,404 meters with a maximum span of 285 meters. The superstructure is designed as a cable-stayed bridge and is connected to the pylons by ten tensioned cables. The highest pylon is 98 meters tall and the construction period was 24 months.

For the realization of piers and pylons, Doka supplied the necessary formwork, especially Automatic climbing formwork Xclimb 60.

Automatic climbing formwork Xclimb 60 is a hydraulically climbing system that can also be quickly raised by a crane if sufficient craneage is available. Because it is guided on the structure at all times, the system can still be climbed even in windy conditions.



To find out more go to
www.doka.com/Xclimb-60

Additionally to the Automatic climbing formwork Xclimb 60 Short track, Doka supplied Large-area formwork Top50 for all shapes and the easy-to-operate Climbing formwork MF240 for the piers in the approach spans.

On site, the Doka Formwork Instructor was present to train and support the site crew during assembling and setting-up the formwork in order to provide the licences for the operation of the system.

All components used in this bridge project are also in use in a large number of construction projects worldwide.

Technical Details

of Automatic climbing formwork Xclimb 60

- Lifting capacity: 6 metric tons/lifting unit; Load capacity: 6 metric tons/lifting unit
- Guided climbing – by crane or hydraulics
- Weight-optimised guiding shoes (19 kg) and hydraulic cylinders (24 kg)
- Formwork positioning by travelling units or roller suspension and spindles
- Wall inclinations +/- 7°
- Double-acting, mobile hydraulic system with optional wireless remote control for simultaneous repositioning of up to 4 climbing units (8 lifting units)
- Modular system components allow for use as a protection screen



See more in
our video:

www.doka.com/xclimb60shorttrack-video

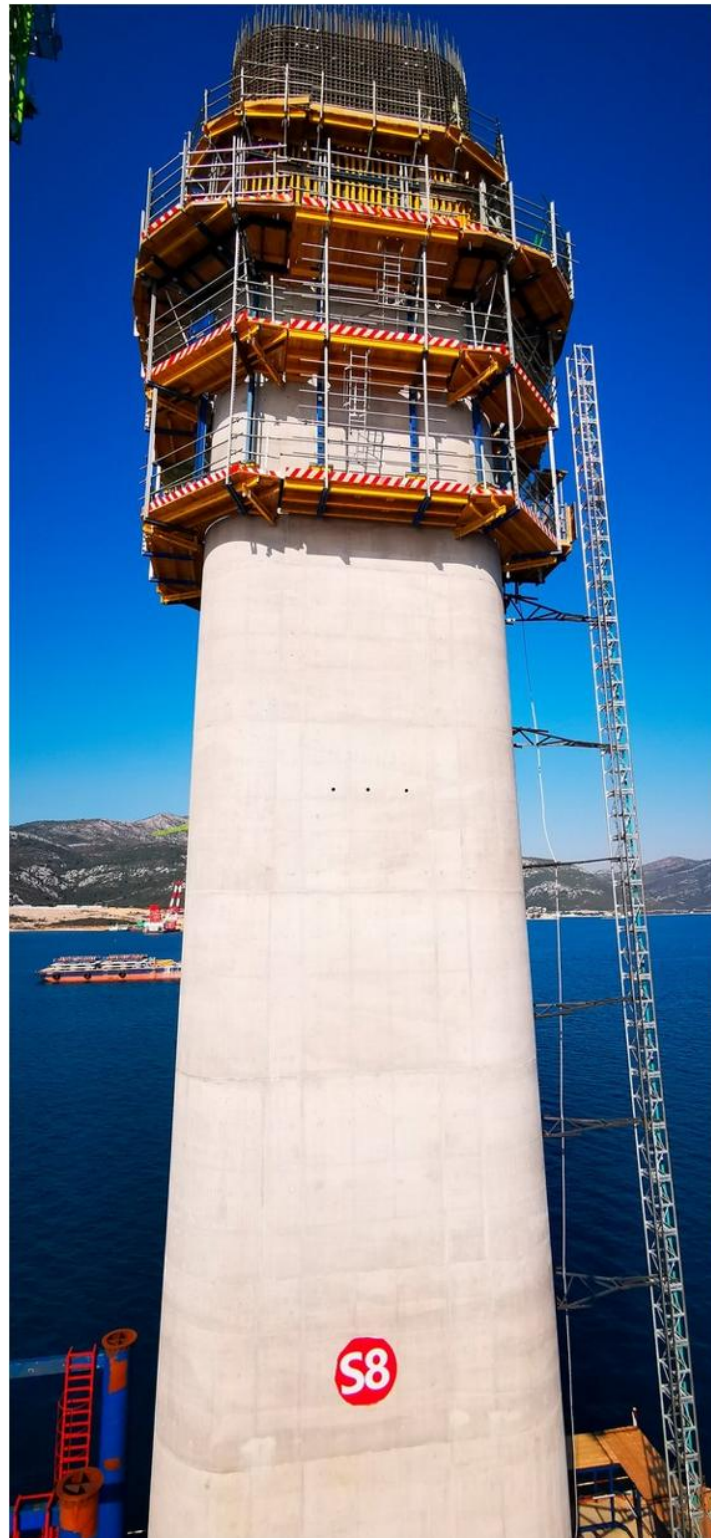


Figure 2: Lower part of Pylon S8
with Automatic climbing formwork Xclimb 60
in regular casting step

In Figure 3 below, you can see typical section and cross-sections of the pylon, pier and formwork.

The works on the pylon can be described as follows:

- 1) Vertical profiles of the climbing units are connected to the structure at all times by guiding shoes;
- 2) Positioning by crane or mobile hydraulic system, depending on the version;
- 3) Main working platform for formwork and reinforcement operations;
- 4) A suspended platform for the removal of the guiding shoes and free access to the wall.

Section C-C

The material used in the lower pylon (Section A-A / B-B) had to be reused for the upper pylon (Section C-C) despite the differences in geometry. Here, too, the Automatic climbing formwork Xclimb 60 delivered the desired results due to its high degree of modularity.

Section B-B

A special solution was used for the last construction section in the lower pylon, where the Doka team was confronted with another challenge: In this part, the structure has a massive increase in wall thickness and load, which has to be transferred into the structure.

Thanks to special formwork with shaped timber boxes and a special platform consisting of WS10 brackets. Due to the use of these components, this task could be solved in the best possible way. The sequence of dismantling in predefined assembly units was already taken into account in the planning.

Section A-A

The reusability of the formwork material used was an issue to which great importance was attached throughout the entire process. The changing geometry as well as the inclination in the lower part of the pylon posed major challenges.

In addition, the curves were a challenge that had to be mastered: because here, the brackets of the Automatic climbing formwork Xclimb 60 had to be anchored. Without having to be detached from the structure, fitting areas and components could be adapted to the existing geometry.

During the construction works, particular attention was paid to high safety requirements which was also important because of the size of the construction site and the ocean passage. Thanks to the commitment of the entire team and the project solution, the construction process was fast and safe.

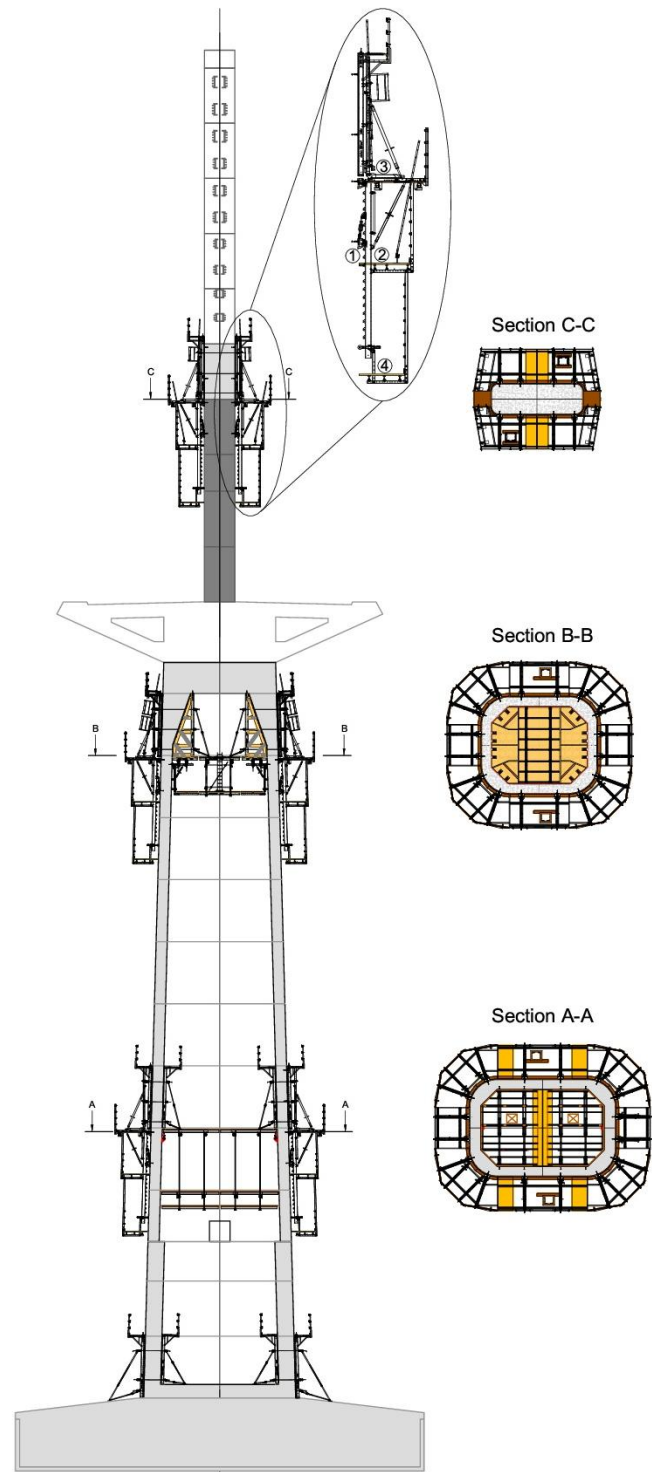


Figure 3: Typical section and cross-sections of the pylon, pier and formwork

THE MCKINLEY STREET STEEL TIED ARCH BRIDGE CITY OF CORONA, CALIFORNIA, USA

*José C Calisto da Silva, Engineering Manager, Director Complex Analyses;
Mahsa Farzad, Staff Engineer; Austin Emrich, Assistant Engineer;
Ben Chan, Assistant Engineer, Biggs Cardosa Associates*



Figure 1: Perspective View of the Bridge

Credit: BCA rendering, Google Earth

INTRODUCTION

The McKinley Street Steel Tied Arch Bridge (also referred to as McKinley Street Grade Separation) in the City of Corona, California, USA, is located at the intersection of McKinley Street and the BNSF Railway (largest freight railroad network in the

USA), south of State Route 91 and east of interstate I-15. This hazardous intersection will be grade-separated by elevating McKinley Street over the BNSF Railway, Sampson Avenue, and the Arlington Channel.

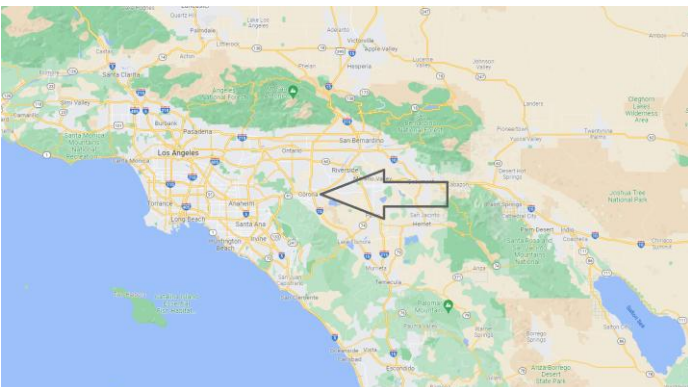


Figure 2: Location of the bridge on the map. Source: maps Google



Figure 3: Aerial View of the location

Credit: BCA rendering, Google Earth



Figure 4: View from the Roadway Credit: BCA rendering

The profile of McKinley Street will be raised just under 9,1 m (30 ft) high (at the highest point) in order to provide sufficient vertical clearance over the BNSF tracks, improve safety, provide unhindered access for emergency vehicles, reduce traffic congestion and reduce air pollution by grade-separating the crossing.

Due to right-of-way constraints and the desire to minimize impacts to adjacent businesses, elevating McKinley Street required that retaining walls be constructed along the approach's alignment.

The McKinley Street Bridge will be a steel network tied-arch bridge with a basket configuration.

An arch bridge was selected over conventional bridge types because of its ability to limit structure depth and to avoid relocating a portion of the Arlington Channel.

Through-arches feature the main load-carrying members (arch ribs) above the deck level, minimizing structure depth.

Arches tend to be less expensive and are better suited for median span lengths (75 m to 250 m) than other cable-supported bridge types (e. g. cable-stayed, extradosed, or suspension bridges).

The network arch type, which features inclined arches was selected because the inclined hangers tend to minimize the moments in the arches and deck allowing for increased cost efficiency when compared to vertical hangers.

While the basket configuration was chosen mainly for aesthetic reasons, during design other advantages were also found, such as a better stabilization of the arch ribs against buckling and lateral actions, such as wind or seismic events.

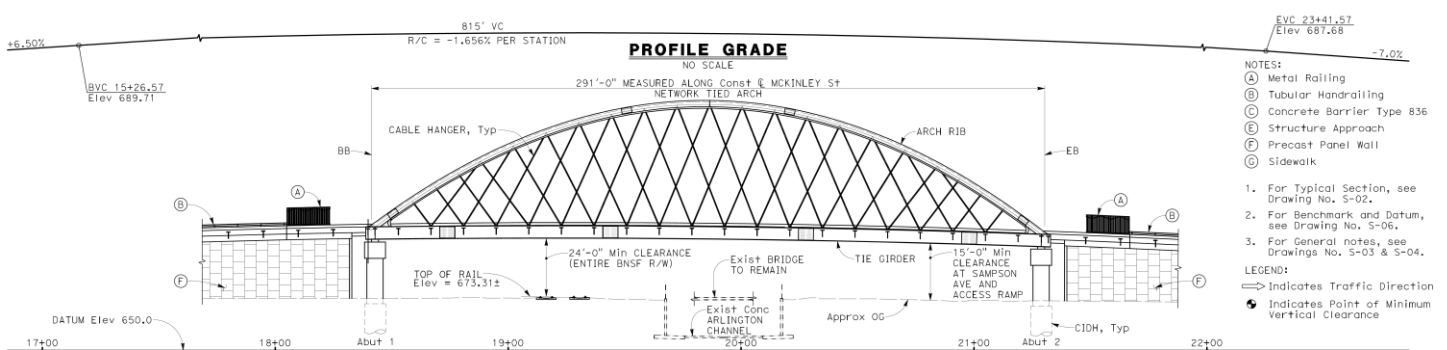


Figure 5: Elevation of the Bridge Click on the image to open it in higher resolution

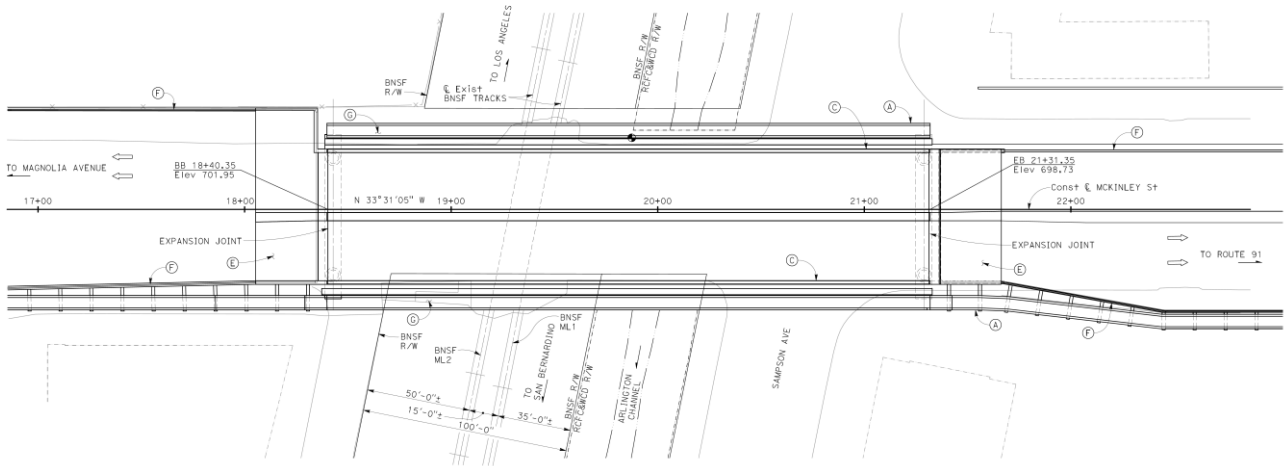


Figure 6: Plan of the Bridge [Click on the image to open it in higher resolution](#)

DESIGN

The structure comprises a single clear span of 87.2 m (286 ft) between bearings, with a space of 3.5 m (11.5 ft) between the bearings C/L and the abutment walls at both ends, thus spanning a total of 94.2 m (309 ft) from abutment retaining wall to retaining wall, over Sampson Avenue, the Arlington Channel, and the BNSF Railway.

The bridge will accommodate two 3.66 m (12 ft) lanes of vehicular traffic in each direction, with 1.52 m (5 ft) shoulders on both sides and 2.13 m (7 ft) cantilevering deck sidewalks provided on both sides.

The two arch ribs that will support the span will be inclined 16° towards the center of the bridge, the maximum possible in order to respect the road clearance at the start of the arch ribs while taking advantage of the inclination, from an aesthetical point of view to a better behavior under seismic excitation and buckling resistance.

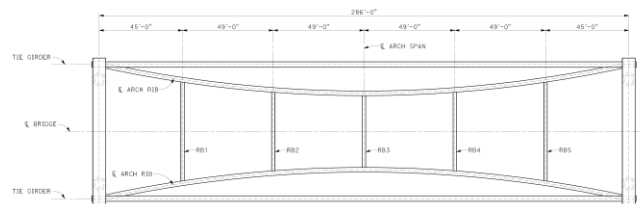
In spite of the inclination of the arch ribs, the Knuckles (i.e. the elements making the transition and connection between the Arch Ribs and the Tie Girders) were designed as vertical rectangles,

deviating from the normal procedure of inclining them in the same angle as the Arch Ribs.

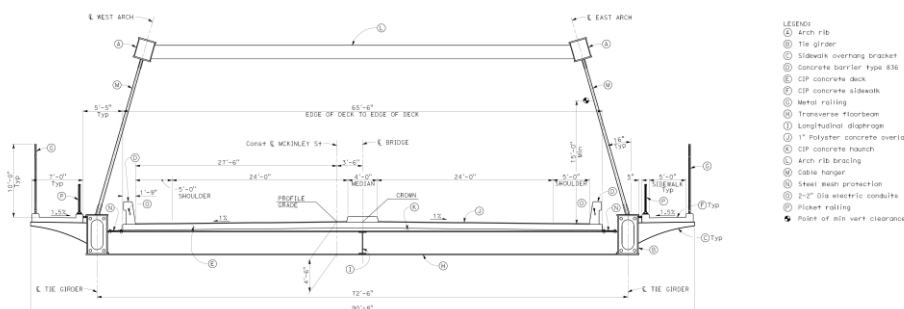
With this, not only was construction simplified but also, in the team's opinion, aesthetics improved. However, this required some extra effort in the analysis and detailing, using extra stiffeners inside the hollow steel box Tie Girders as well as some less common welding procedures.

This design was finalized in the third quarter of 2020, and construction of the project started at the beginning of the New Year 2022.

The project is funded by United States Senate Bill 132 and those funds need to be utilized by June 2023, leading to the use of innovations like Accelerated Bridge Construction to meet the demanding schedule.



↑ Figure 7: Plan of upper lateral bracing



← Figure 8: Typical cross-section

[Click on the image to open it in higher resolution](#)

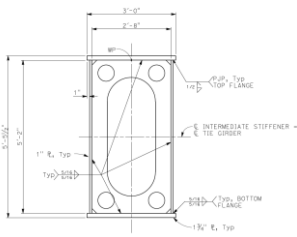


Figure 9: Tie Girder Standard Cross-Section

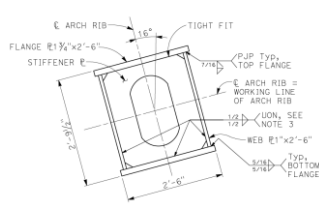


Figure 10: Arch Ribs Cross-Section

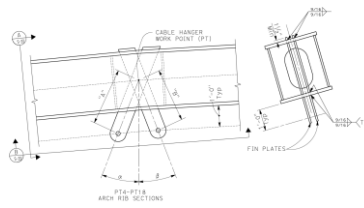


Figure 11: Connection Fins Hangers - Arch Ribs (top)

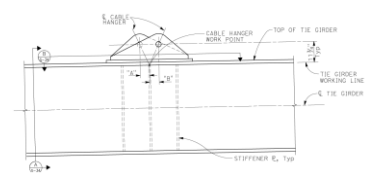
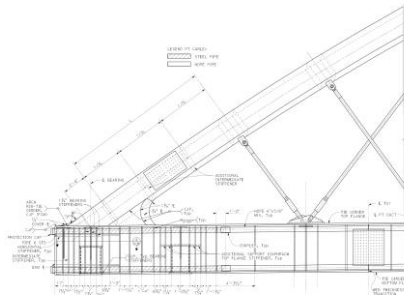
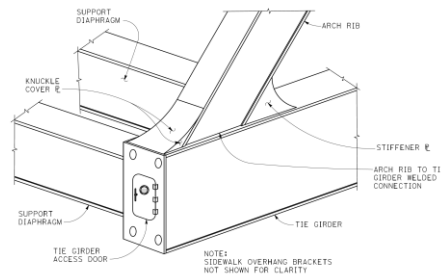


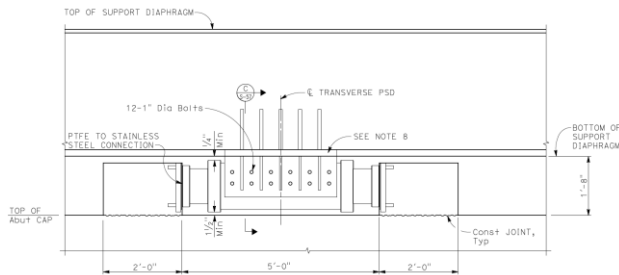
Figure 12: Connection Fins Hangers - Tie Girder (bottom)



←← Figure 13: Knuckle Elevation

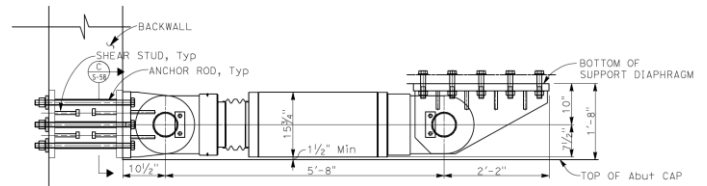


← Figure 14: Isometric View of Connection of Arch Ribs to Knuckle



↑ Figure 15: Seismic Units - PSDs Connection

↗ Figure 16: Seismic Units - VFDs Connection



Client: City of Corona

Design: Biggs Cardosa Associates

Computer models: CSiBridge, with an exhaustive definition of the construction phasing (95 stages for the permanent loads), using 2nd order non-linear analysis, including the effects of creep & shrinkage, and detailed modeling of all structural elements, both in geometry, in offsets, and in the connections to the rest of the structure.

Design of the Knuckles: SOFiSTiK

Design of the welded and bolted connections the software: Idea-Statica

The **analysis and design of piles** and their interaction with the surrounding soil layers: the softwares **LPile** from Ensoft Inc., in Austin, Texas, USA, and **FB-Multiplier** from BCI (Bridge Construction Institute) of the University of Florida, in Gainesville, Florida, USA.

Independent Check Engineering: DEA (David Evans Associates Inc.), using the software **MIDAS Civil** and **LUSAS** (Knuckle analysis).

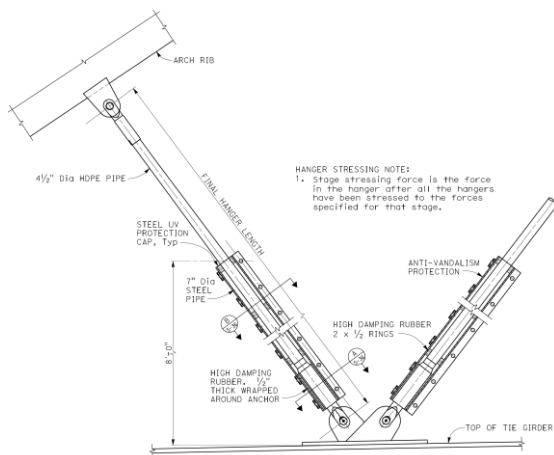
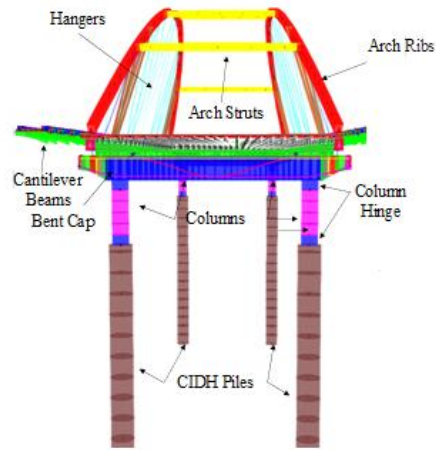
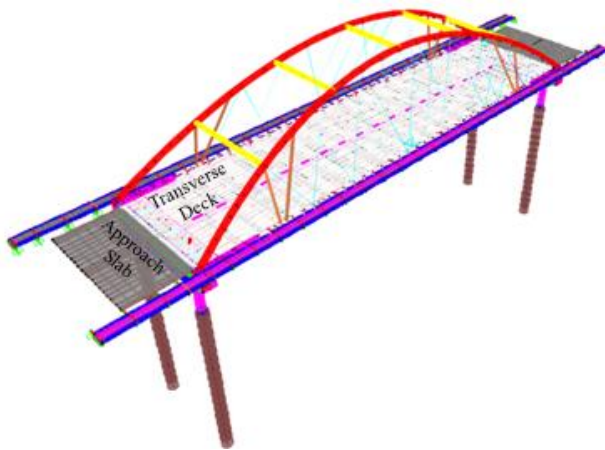


Figure 17: Hanger Assembly

Click on any image on this page to open it in higher resolution



Figures 18 and 19:
Two Extruded
Perspective Views
of the Computer
Model

INNOVATIVE ASPECTS OF THE BRIDGE DESIGN

In the design of this bridge, a few innovative concepts were used, especially in what concerns the seismic-resistant design and the philosophy behind it, which will be described further in the course of this article.

MSE retaining walls

Retaining walls are needed to support the raised portions of McKinley Street. Retaining walls consist of a combination of mechanically stabilized earth (MSE) walls and cast-in-place concrete walls at the ends of those, in order to facilitate concordance with the pavement and streets below.

MSE walls employ wires or geogrid straps which act as soil reinforcement and are attached to precast concrete facing panels. The reinforced soil zone provides stability against sliding and overturning.

Abutments as MSE (Mechanically Stabilized Earth) Walls Backfilled with LCC (Lightweight Cellular Concrete)

For alleviating the weight of the surcharge on the existing soil at the original level, and the utilities underneath, as well as reducing downdrag on the foundation piles for the support bents, some 2.3 m (7.5 ft) apart from the face of the wall to C/L of the pile, lightweight cellular concrete (LCC) backfill is used in lieu of conventional soil backfill.

As a brief introduction, LCC, also known as “Foam Concrete”, is a mixture of Portland cement and water that incorporates air-entraining agents producing significant amounts of entrained air bubbles.

This results in a sponge-like internal structure that is both lighter and stronger than the typical structural fill although it is more brittle and with a very low crushing strength – 80psi = 552kPa – for Class III, as used, with 40psi (276 kPa) used for design pressure.

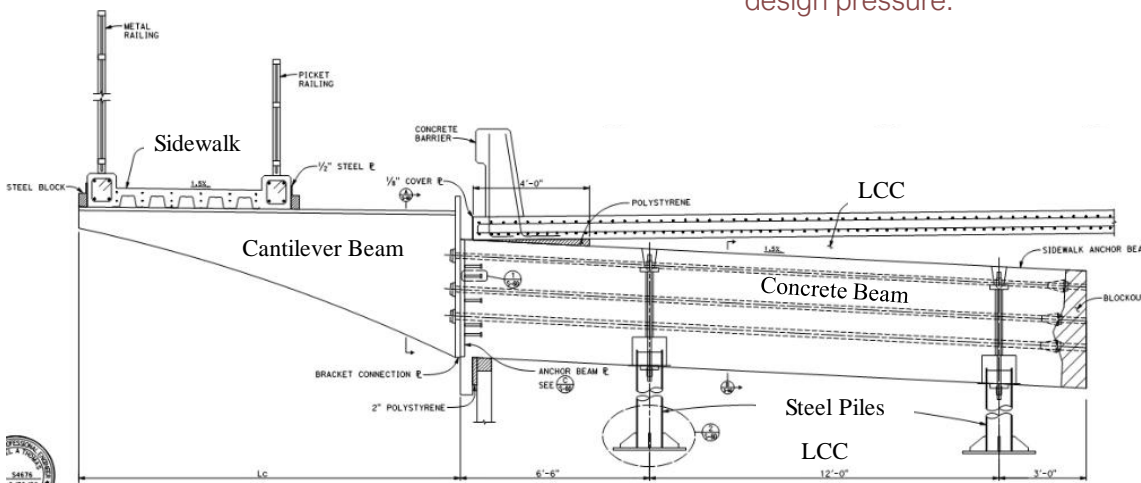


Figure 20: Concrete
Anchor Beams on the
LCC material for the
cantilevered sidewalk
along the MSE walls

The benefits of using LCC include:

- **Easy Placement:** With low density and flowability, LCC is easily pumped at low pressure over long distances without the need for additional compaction or vibration operations.
- **Its self-leveling ability** allows it to fill every void, so the material does not require mechanical compaction.
- **Lightweight Strength:** LCC is lightweight because it is made by replacing stone aggregate with air bubbles, but it is stronger than compacted fills or soil.
- **Cost-effective:** LCC is less expensive to produce and place, and also reduces costs associated with transportation and storage.
- **Permeable or Non-permeable:** Depending on the mix components, LCC can be designed to either prevent water from penetrating, or allow water to drain through.

To attend to the fact that the LCC is rather light ($\gamma = 576 \text{ kg/m}^3$) and has a low crushing strength ($f'_c = 552 \text{ Pa}$), a system had to be devised that could anchor the cantilevers supporting the sidewalk protruding out of the MSE walls, while distributing those highly eccentric loads in a way avoiding peaks of stresses and at the same time distributing them in quasi-uniform contact pressure on the LCC backfill.

This was achieved by designing a concrete beam actively anchored against the LCC, with vertical anchors, eccentrically placed towards the end of the beam, which extend deeper into the backfill through inclination (4%).

For the anchors, standard soil anchors could not be used because the anchoring bulb's high-

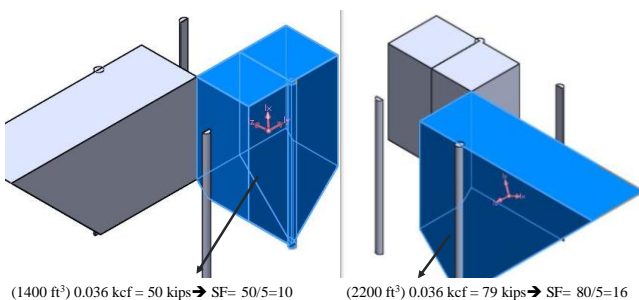


Figure 21: Pull-out cone volume modeled by Solid Works

pressure grout injection could break through the LCC material, weakening its integrity, with the possibility of causing loss of support at the road level and possible settlement issues.

Thus, the anchoring is done by steel tubes provided with circular anchor plates at the bottom, sufficiently deep so that the overburden weight of the pull-out cone would be larger than the active anchor force applied at the top of the concrete beam, with a safety factor of 10, while a safety factor of 4 is usually applied to soil anchors, due to all uncertainties with this new material.

Figure 21 shows the 3D sketch of the piles and LCC cones modeled in SOLIDWORKS with a limiting angle of 30 degrees to calculate the pull-out cone and minimize cracking inside the LCC.

The introduction of the active anchor force was made by tensioning, using a threaded high-strength steel rod (DYWIDAG bar) using a transition between the steel tubes and the threaded bars by means of a solid steel cylinder bolted to the steel pipes, and with the threaded bars fixed at the bottom of the cylinder using the system's anchor plates and nuts, see Figure 22.

Bridge supported on End-Bents, separated from the face of the MSE walls by a gap between them

As mentioned before, the gap between the face of the MSE walls and the backwalls is 1.1 m (3.5 ft) which facilitates construction and will allow the inspection and maintenance of the bearings from behind.

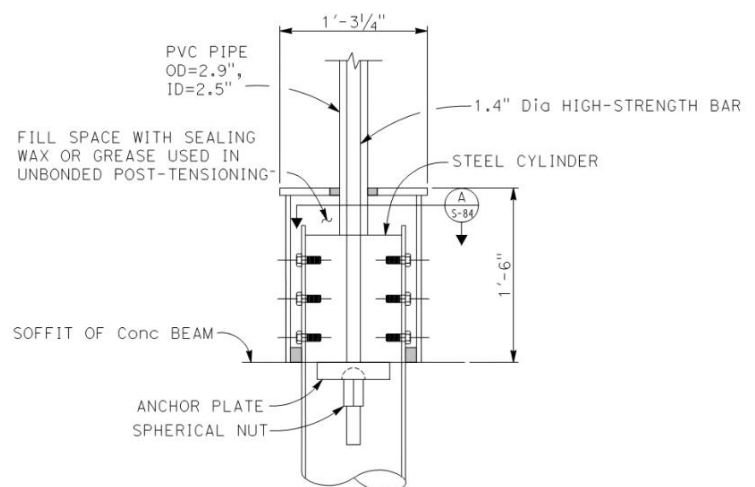


Figure 22: Pretensioned Threaded Bar with Steel Cylinder Connection to Pile

The Approach Slabs span over this 1.1 m gap and are elastically supported on the backfill on one side, while on top of the backwalls through elastomeric pads on the other side.

The Approach Slabs were modelled as part of the bridge model, using elastic linear springs to simulate the elastomeric pads and area distributed elastic vertical springs modelling the vertical subgrade reaction of the LCC.

To simulate the friction between the Approach Slabs and the LCC backfill, area distributed non-linear friction links, acting in the two horizontal directions were used, sliding for the friction force corresponding to the self-weight of the Approach Slab.

This arrangement also contributed to some extent in the dissipation of the energy imparted to the structure by the earthquakes.

Polyurethane injection

As the case with many steel bridges, corrosion of structural elements was a concern. The bridge has a multitude of hollow members including the arch ribs and support diaphragms.

In order to reduce the effects of corrosion, the voided, box-shaped members will be injected with polyurethane foam with a density of approximately 32 kg/m³ (2 lb/ft³). The foam will be able to conform to the geometric shape as needed and oppose the ingress of water or water vapor.

Although this type of foam is commonly used for application in marine environments, we see great potential for usage in corrosion protection for structural steel bridges and structures with internal inaccessible voids.

Knuckle

For tied-arch bridges, a knuckle is critical for transferring the Arch thrust. Because of the complexity in geometry and load transfer, a detailed finite element model was built, using SOFiSTiK, to investigate the stress demands on the different components and welds.

In the elements with voided cross-sections, such as the Arch Rib, Tie Girder, Support Diaphragms, and End Trusses, “spider-elements” (rigid links radiating from a point to all the points in the perimeter of the cross-section) were used, in order to create single nodes to apply concentrated loads (axial, shears and moments, extracted from the

results of the global analysis model), or fixities to the entire cross-section.

While loads were applied at the “spider nodes” of the Arch Ribs, Support Diaphragms, and End Trusses, together with distributed loads on the flanges of the cantilever beams and at the bearing location, the Tie Girder is fixed at the end, in order to provide stability to the model and compatibility of the continuity forces with the applied ones.

The bearing was modelled with a circular element located at the soffit of the Tie Girder, simulating the sole plate at the bearing position.

The following are the load cases considered:

- Strength Limit State - Strength 1 & 2*
- Extreme Limit State*
- Fatigue Limit State - Fatigue 1 & 2*

*According to AASHTO’s Load Combination Tables (Tables 3.4.1-1 to 3.4.1-4)

The applied loads input for the Extreme limit state correspond to the “Maximum Credible Earthquake” (MCE) results combined with the Permanent Loads.

The MCE results correspond to load sets relative to the Maximum and Minimum of each of the internal forces (axial load, shear in two directions, torsional moment, and bending moments about two directions), therefore totalling 2 x 12 cases, and corresponding to the concurrent loads during each one timestep, from which the envelope results were extracted.

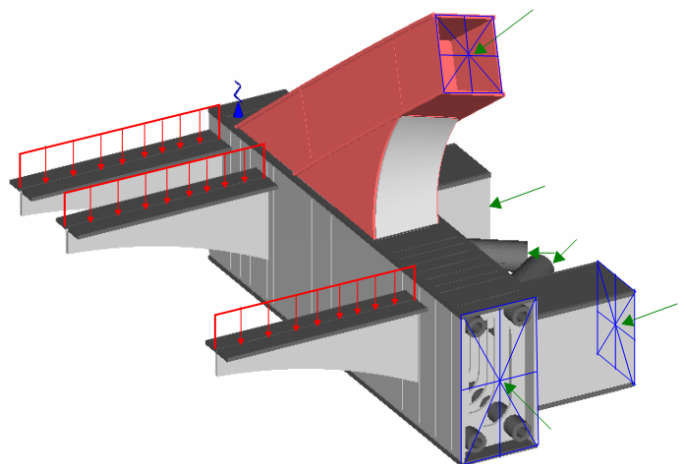


Figure 23: A knuckle with spider-like elements

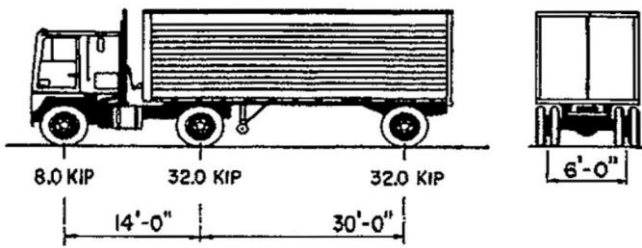


Figure 24: HL-93 Type Vehicle used for Fatigue 1

This was done in order to avoid being overly conservative, as done in common practice. The load input for the other elements, such as the Arch Ribs, Support Diaphragms, End Trusses, and Bearing, also refer to the same timestep as for the Tie Girder.

The load input for the Fatigue limit states is based on responses coming from the live load analysis using the fatigue HL-93-F (Fatigue 1) and P-9 (Fatigue 2) vehicles, see Figures 24 and 25, according to CALTRAN's (the Department of Transportation in California) Bridge Design Practice.

Analysis results are compared with the threshold limit specified in AASHTO LRFD BDS Table 6.6.1.2.3-1. It is noted that the load input on the different elements, for the Fatigue cases, almost certainly will not be concurrent for the same load case because of the limitation of the analysis software in reporting results of the global model, in what concerns envelopes relative to moving load vehicles.

The loads input for the Strength limit states (according to AASHTO's Load Combination Tables) are based on the calculations of the envelopes for the moving live load analysis both with the standard traffic vehicle HL-93 (Strength 1 combination) and permit vehicle P-15 (Strength 2 combination). The stresses resulting from the Strength Load Combinations of the analysis results are compared with the yield strength of the steel members. The analysis shows that all Knuckle components are passing both the Fatigue 1 and Fatigue 2 limit states.

For the Extreme limit states and Strength limit states, there were a few minor very concentrated and localized cases where the Demand/Capacity ratio was >1.0 ; however, it was justified that these localized stresses would be redistributed after an also very localized plasticization.

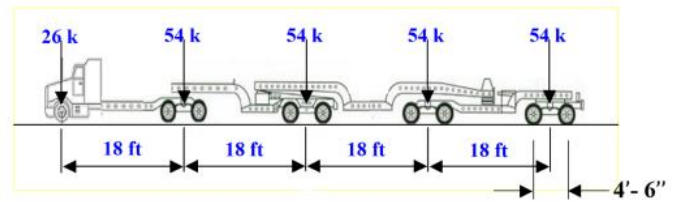


Figure 25: P-9 Permit Vehicle used for Fatigue 2

Some possible reasons behind these localized peak stresses, almost all of which occurred at the boundaries of the Knuckle model, would be the use of the spider connections for the loads application, since they still create concentrated loads application points. Please see more pictures [here](#).

Expansion joints

The design team also employed an innovative approach to the design of expansion.

As the bridge will experience significant longitudinal and transverse movements due to seismic forces, even for the more frequent earthquake motions, further compounded by the isolation approach to seismic design, this posed a problem for more traditional approaches to expansion joints.

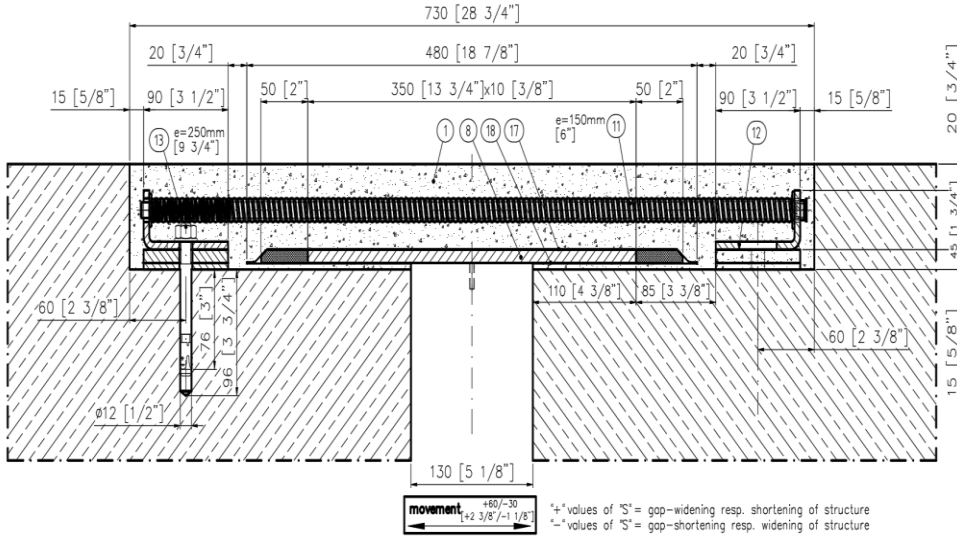
The design seismic movement was based on the response to the "Operational Basis Earthquake" (OBE), with a 50-year return period.

Although strip seals, a common approach to thermal movements in California, could still be used, the large seismic movement led to the consideration of modular joints, for which there would be no available depth in the concrete deck superstructure over the support diaphragms.

In order to address this issue, flexible plug joints were designed with the assistance of the Mageba Group, already the proposed supplier of the bridge bearings and seismic protection units. They suggested the adequacy of their product, Polyflex joints (TENZA® POLYFLEX® AdvancedPU), based on a flexible filling using a grout incorporating polyurethane polymers (PU) as a binder, together with silicious charges; resulting in an elastomeric grout.

Seismic Design Approach and Philosophy

One of the major challenges for arch design in California has been with the design of the Knuckles



1. Elastomeric grout;
2. Cover plate;
3. Stabilizer;
4. Perforated steel angle;
5. Anchor bolt;
6. Elastomeric stripe;
7. Elastomeric stripe.

Figure 26: Schematic Composition and Arrangement of a Flexible Joint

due to the high seismicity of this state which leads to the result of massive size Knuckles. Additionally, the Tie Girders are traditionally designed with an inclined geometry or shape, in order to follow the inclination of the arch ribs, as for the case of a “basket” type, such as the present one.

To reduce the Knuckle size and complexity, seismic isolation, i.e. decoupling the movements of the bridge from those of the substructure and foundation, was introduced by using four Spherical Multidirectional Sliding bearings on all four corners of the bridge, using as sliding material Ultra High Molecular Weight Polyethylene (UHMWPE) on top of a stainless steel sheet.

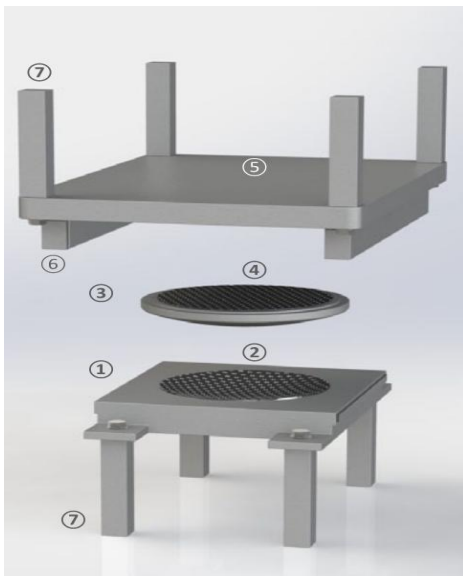
The bearings are placed on top of 2.44m x 2.13m (8 ft x 7 ft) concrete bent-caps, integral with two 1.52 m (5ft) diameter concrete columns, as extensions of 2.13 m (7ft) diameter cast-in-drilled-

hole (CIDH) concrete piles, as monopile foundations, under each column and at each bent near the abutment MSE walls.

An aspect limiting the possible “isolation” of the bridge was the connection between the approach slabs and the backwalls, traditionally materialized by using steel dowels.

In the present case, it was considered that this type of connection would introduce significant forces at the ends of the bridge, with the possibility of backwall failure with major damage, but more importantly, the stiffness of the connection would be a major hinderance to the desired “isolation” of the bridge.

Therefore, a support system of the approach slab on the backwalls was devised using elastomeric bearing pads placed along the top of the backwall, with the slab spanning over the 1.1 m (3.5 ft) gap



1. Concave part allowing rotation about any axis;
2. Sliding material (UHMWPE) of low friction;
3. Convex calotte with a polished hard-chromium surface;
4. Second sliding sheet, recessed into the upper surface of the calotte;
5. Sliding Plate covered on the lower surface by a polished stainless steel sheet;
6. Guide bars (for the case of “guided” bearings – not the present case, with multi-directional ones);
7. Anchor dowels, connecting the bearing to the superstructure and to the substructure (in the present case only exist dowels between the bearings and the substructure, since to the superstructure, in steel, the connection is made by welded and bolted steel plates).

Figure 27: Composition of a Spherical Bearing as used in McKinley Street Bridge

between the backwall and the abutment and spaced at 0.60m (2 ft).

The bearing pads are designed for displacements and not the vertical force. Therefore they have to accommodate the seismic displacements, since the vertical load on each pad was relatively small in relation to its capacity. These elastomeric pads, apart from allowing a flexible connection (movements and rotations) between the approach slabs and the backwalls, were also considered as part of the energy dissipation system and were modelled as horizontal non-linear elasto-plastic springs in the computer analysis model.

Since the spherical bearings can slide in all directions, no lateral stiffness was assigned to them, but the frictional forces relative to the dead loads were considered as applied forces. Similarly, as the elastomeric bearings allow rotations in all directions, no rotational stiffness was assigned to them.

Seismic Protection Units

The seismic units, included at the bents, were considered with the aim to decrease the overall demand on the bridge by seismic actions, especially in what concerns the site splice connections. This system consists of 12 units: two pairs placed in the transverse direction of the bridge (one pair at each abutment/bent) and four pairs placed longitudinally (two pairs per abutment/bent).

Initially, the seismic units were half of the final number, but space limitations at the chosen installation locations led to using smaller units but in twice the number.

Using a larger number of units also has the advantage of conferring to the system a higher

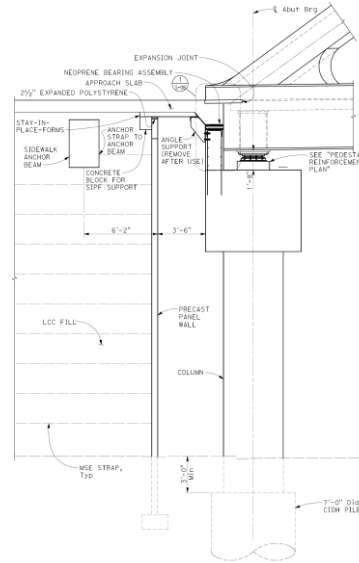


Figure 28: Sectional View of the Approach Slab and Elastomeric Support on the Backwall

[Click on the image to open it in higher resolution](#)

redundancy, being able to still operate with effectiveness after the loss of one or two of the same type units.

Four pairs of these units are Preloaded Spring Dampers (PSD), two pairs in the transverse direction, and two pairs in the longitudinal direction, while the remaining two pairs are Viscous Fluid Dampers (VFD), all in the longitudinal direction.

The two pairs of transverse PSDs are located in a centered disposition of the bent caps and act similarly in both abutments, while in the longitudinal direction there are two pairs of PSDs at the South abutment, and two pairs of VFDs at the North abutment, all of them also in a centred disposition to the bent cap.

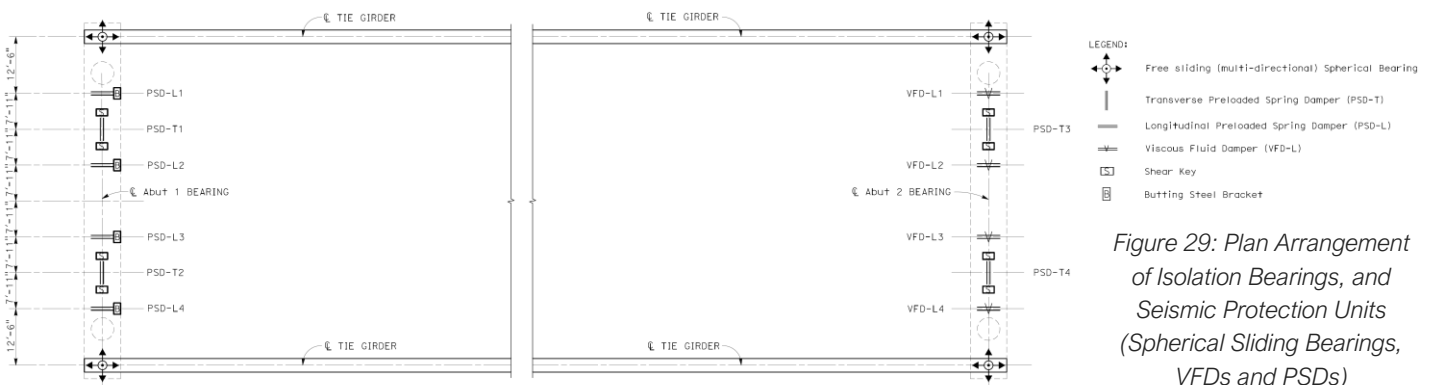


Figure 29: Plan Arrangement of Isolation Bearings, and Seismic Protection Units (Spherical Sliding Bearings, VFDs and PSDs)

[Click on the image to open it in higher resolution](#)

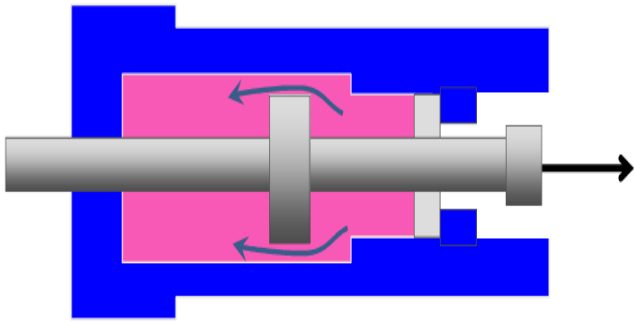


Figure 30: Damping is provided through the Annular Flow between Piston Head and Reservoir Walls

This disposition of the longitudinal units provides fixity on one side and allows translation on the other side for thermal actions and braking and traction of the traffic loads, and the participation of both abutments in about equal terms in the resistance to the seismic actions in the longitudinal direction.

For slow movements, VFDs virtually introduce no forces as they freely expand and contract. In opposition, for rapid movements, such as wind gusts and seismic actions, they act as viscous dissipaters, transferring forces proportional to a power of the relative velocity between ends (according to the Maxwell model, $F_V = C \times V^\alpha$).

Their main purpose is to dissipate energy, through the passage of a high viscosity fluid through tight valves. They only start having an effective action once the velocity of the movement reaches a certain minimum value of circa 1.0 mm/s (0.04 in/s).

On the other hand, PSDs act as shear keys up to a predetermined force value and as viscous

dissipaters above that force, meaning that they behave as fuses in relation to restraining horizontal actions.

These units are basically modified viscous fluid dampers, acting in parallel with a group of springs; which exhibit high stiffness up to a predetermined force value, and when that value is reached, they become soft springs, introducing a small elastic force; additionally, when the velocity of movement reaches the same minimal value of circa 1.0 mm/s (0.04 in/s), a viscous dissipation of energy also starts taking place.

Another important action introduced by the PSDs is that, after an earthquake action has occurred and the bridge, eventually, is out of place, the units will recenter bridge through the force accumulated in their springs.

The general force expression for these units is:

$$F_{TOTAL} = (F_0 + K_X \times d)_{STATIC} + (C \times V^\alpha)_{DYNAMIC}$$

In order to have both abutments contributing almost equally for the resistance to the seismic actions, the design parameters of the VFDs and the PSDs were calibrated for the total resulting forces, both the elastic and the ones from the viscous dissipation of energy, so that they would be approximately equal for the MCE.

Seismic Horizontal Load Paths

For the horizontal inertia loads generated by the seismic action in the transverse direction, it was considered that the deck would act as a stiff diaphragm and would channel those forces to the horizontal restraints – the transverse Preloaded Spring Damper units – at both extremities of the deck, through the very stiff support diaphragms in their longitudinal direction.



Figure 31: Elevation View of a Preloaded Spring Damper (PSD)



Figure 32: Viscous Fluid Damper (VFD)

The forces originated by the seismic movements of the Tie Girders and Arch Ribs, are also led to the deck slab, by the shear connections of the Floor Beams to the Tie Girders, also being rigidly connected to the deck slab by stud connectors. Certainly, the Tie Girders are also part of the transverse lateral resisting system, in conjunction with the deck slab, but since the slab is much more rigid, it will carry most of the seismic force, see Figure 35.

In the longitudinal direction the same inertial forces on the deck have to be carried to the restraints at the extremities – the longitudinal Preloaded Spring Dampers at one end and the Viscous Dampers at the opposite end. However, at those locations there would not be stiff enough elements to carry the loads to the restraints and such rigidity had to be created. This was materialized by a steel truss in the horizontal plane, utilizing the support diaphragms as chords and elements of the same type as uprights, and heavy steel tubes making up the diagonals.

Redundancy

Tie Girder PT

The AASHTO “Manual for Bridge Evaluation” defines bridge redundancy as “the capability of a bridge structural system to carry loads after damage to or the failure of one or more of its members.”

In order to fulfill this requirement, the Tie Girders needed to be detailed in such a way as to be classified as “redundant members”. Therefore, post-tensioning cables were designed to run along the inside of the tie girders and were optimized based on the redundancy requirements according

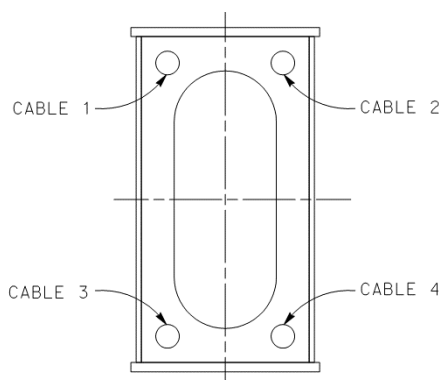


Figure 33: Cross-Section of the Tie-Girders showing Passages for the PT Cables

Each cable consisting of 14 x 0.6”, 270 ksi (1860 MPa) strands, introducing a total force of 2,400 Kip (10,700 kN)

to the two strength verifications as described in AASHTO’s “Guide Specifications for Analysis and Identification of Fracture Critical Members and System Redundant Members”:

- **Redundancy I** is intended to capture the effects of the dynamic amplification during free vibration immediately following the member failure in the presence of dead load and live load.
- **Redundancy II** is intended to characterize the loading scenario after the assumed fracture has occurred and the structure has reached a steady state.

Upon adherence to these guidelines, the Tie Girders were able to provide redundancy to the system, thus avoiding the costly requirements both for detailing, construction and inspection relative to FCMs.

CANTILEVER PEDESTRIAN SIDEWALKS

To allow the use of the bridge by pedestrians, while improving their safety, cantilevered sidewalks at both sides are provided along the bridge and extended along the MSE retaining walls that support the approaches. A 200 mm (7.75”) concrete sidewalk is cast on top of SIP corrugated metal forms supported on steel cantilevers. The cantilever beams are connected to the Tie Girders through steel plates as shown in Figure 36.

Vibration Control

According to AASHTO BDS, the vibration of the structure shall not cause discomfort or concern to pedestrians using the sidewalk which is investigated at the Service Limit State Service I combination in Table 3.4.1-1.

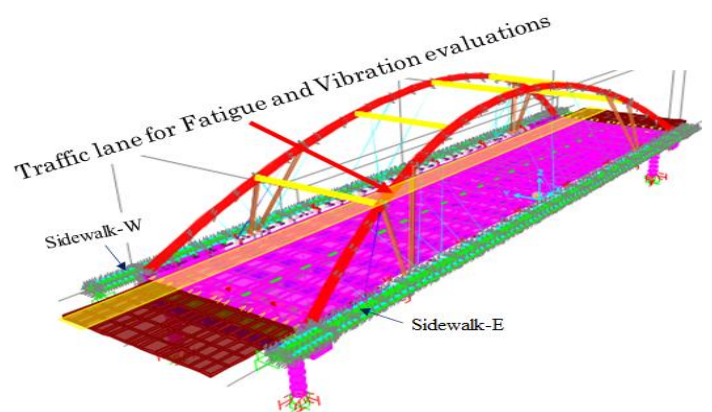


Figure 34: West and East Sidewalks & Traffic Lane for Evaluation of Fatigue and Vibrations

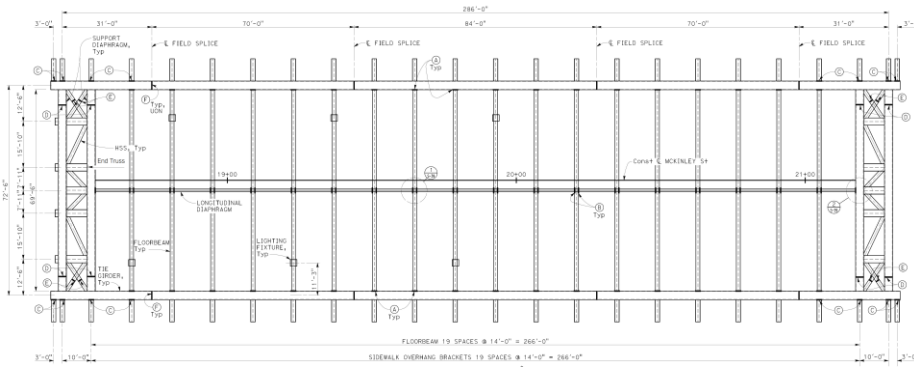


Figure 35: Framing Plan of the Bridge Deck Cantilevering Pedestrian Sidewalk
 Click on the image to open it in higher resolution

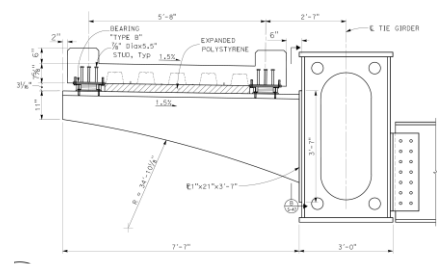


Figure 36: Cantilevering Pedestrian Sidewalk
 Click on the image to open it in higher resolution

The additional available recommendations in AASHTO's "Guide Specifications for the Design of Pedestrian Bridges" are used on a general basis. However, they are rudimentary guidelines and not wholly determinant in assuring pedestrian comfort involving a complex structure subjected to vehicular traffic and, proportionally with a much heavier mass.

Due to this insufficiency, additional criteria in SETRA (French) specifications, the ISO norms and the British norms were used to ensure pedestrian comfort, based on the maximum accelerations caused by heavy traffic.

In this present case, this condition, in order to not make it too demanding, was decided to respect the maximum accelerations for "Mean" comfort, i.e.: 1.0 m/s² (10.2%g) for vertical and 0.3 m/s² (3.1%g) for the horizontal directions.

To be consistent with the "Mean" comfort level according to SETRA, the ISO comfort should correspond to a degree between "a little uncomfortable" to "fairly uncomfortable", therefore,

Acceleration ranges	0	0.5	1	2.5
Range 1	Max			
Range 2		Mean		
Range 3			Min	
Range 4				

Figure 37: SETRA – Comfort Levels in Terms of VERTICAL Acceleration (m/s²)

Acceleration ranges	0	0.1	0.15	0.3	0.8
Range 1	Max				
Range 2		Mean			
Range 3			Min		
Range 4					

Figure 38: SETRA – Comfort Levels in Terms of HORIZONTAL Acceleration (m/s²)

Note: For the case of solely pedestrian bridges, the acceleration in both horizontal directions is limited to 0.1 m/s², in order to prevent "lock-in" effect (see brown line in figure above).

ISO 2631 - Acceleration Comfort Limits for Vertical Movement			
	a(v)	<	0.315 m/s ² = 1.033 ft/s ² => not uncomfortable
0.315 m/s ² = 1.033 ft/s ²	<	a(v)	< 0.630 m/s ² = 2.067 ft/s ² => a little uncomfortable
0.500 m/s ² = 1.640 ft/s ²	<	a(v)	< 1.000 m/s ² = 3.281 ft/s ² => fairly uncomfortable
0.800 m/s ² = 2.625 ft/s ²	<	a(v)	< 1.600 m/s ² = 5.249 ft/s ² => uncomfortable
1.250 m/s ² = 4.101 ft/s ²	<	a(v)	< 2.500 m/s ² = 8.202 ft/s ² => very uncomfortable
2.000 m/s ² = 6.562 ft/s ²	<	a(v)	=> extremely uncomfortable

Figure 39: ISO 2634 – Acceleration Ranges for Vertical Vibrations (horizontal limits approximately 30% of the vertical ones)

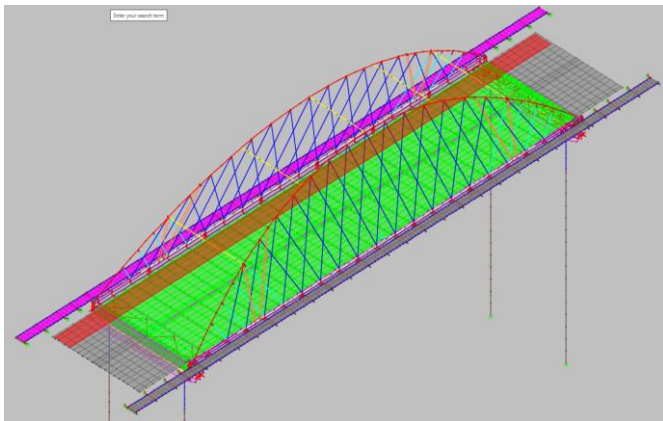


Figure 40: Lane on Bridge used for the Passage of the Fatigue Truck (West Side – East Side Symmetrical)

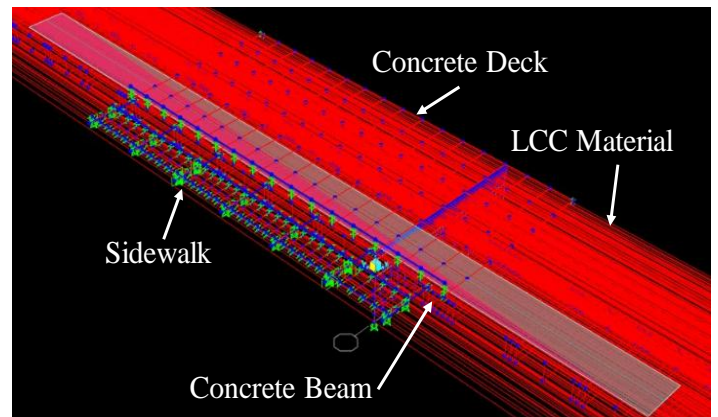


Figure 41: CSiBridge Model for analysis of accelerations Sidewalk along MSE Walls showing the Lane on backfill (brown strip) used for the passage of the Fatigue Truck

with accelerations falling between the limits of $0.315\text{m/s}^2 < 3.2\%g$ (1.033ft/s^2) and $1.000\text{m/s}^2 < 10.2\%g$ (3.281ft/s^2), which are consistent with the SETRA values for the vertical direction of vibration – acceleration smaller or equal than 1.0m/s^2 .

Dynamic analysis for the passage of the Fatigue design truck, as specified in AASHTO BDS Article 3.6.2, was done to determine the pedestrian comfort level accelerations.

The resulting accelerations along the sidewalk length were checked against the determined acceptance limits according to the above.

The model consists of the cantilever steel beam defined as a frame with a parabolically variable height, and the sidewalk slab either supported on top of the cantilever beam by concrete haunch with stud connectors, modelled with rigid links, or by elastomeric pads, modelled as elastic springs.

The walkway along the MSE walls was modelled in a separate model with the steel cantilevers rigidly connected to the concrete anchor beams.

The concrete anchor beams were defined as solid elements placed over the LCC material, modelled with frame elements, and the LCC itself was modelled with 3-D brick elements.

The depth and length of the LCC were taken as four times the length of the concrete beam, in order to neglect the effects of the boundary conditions.

The concrete roadway slab was defined as shell elements on top of the LCC, with the concrete barrier placed at the edge of the roadway slab, connected to it with rigid links.

The roadway lane was defined in the transverse direction as starting at the edge of the barrier. This gave us the conditions causing maximum accelerations on the sidewalk by the passage of heavy vehicles.

For this purpose, linear dynamic time-history analysis was performed considering the passage of the Fatigue design truck, both on the bridge and along the MSE walls, on the traffic lane closest to the sidewalk.

Truck speeds were considered to vary from 48 to 113 km/h (30 to 70 mph), in steps of 8 km/h (5 mph), in order to determine the value of the critical speed for this bridge.

With this value, a refined analysis was made for speeds varying from 8 km/h below the critical speed to 8 km/h above the critical speed in steps of 2 km/h (1.25 mph).

Accelerations were verified to conform to the following criteria:

- Vertical accelerations less than 1 m/s^2 (3.28 ft/s^2 - 10% g).
- Horizontal accelerations less than 0.3 m/s^2 (0.98 ft/s^2 - 3% g).

DESIGN VALIDATION

The practice trends of some key parameters of arch bridges, such as flatness (span-to-rise ratio), Arch depth, Tie Girder depth, bending stiffness, slenderness and shallowness, can be used for validating steel arch bridges designs as a means of evaluating feasibility, proportioning and assessing their efficiency.

Therefore, taking as reference the geometric information of 20 steel arch bridges, collected from existing provincial bridges in Ontario, Canada, and some other familiar steel arch bridges, the parameters of the McKinley Street Bridge were compared with those of the surveyed bridges, through graphs where those parameters were plotted against span length.

Below we present some of the results of the design check:

- The span-to-rise ratio comes as: $286/56.5 \approx 5.1$ (or inversely 19.8%) and this ratio falls well within the values relative to the surveyed bridges – around 6 (17%);
- The Tie Girders depth is $5'-5\frac{1}{2}'' = 5.458 \text{ ft}/1.664 \text{ m}$, and the Arch Ribs depth is $2'-9\frac{1}{2}'' = 2.792 \text{ ft}/0.851 \text{ m}$, thus, the system depth, being the sum of those two depths, is 2.515 m (8.25 ft).

All three represented depths fall within the dispersion of the values of the surveyed bridges, however, it can also be noted that the relative position between the Tie Girders and the Arch Ribs is inverted in relation to the shown tendency.

We believe that this is due to the fact that the Tie Girders were given the minimum depth for still being accessible from the interior, in order to facilitate inspections; additionally, it was intended that the Tie Girders would be stiff enough to be able to withstand some pretensioning of the hangers, as intended in the design, rather than keeping the cables slack to be tensioned by the dead loads, with tension accrued by the passing traffic, situation which would be more unfavourable for Fatigue.

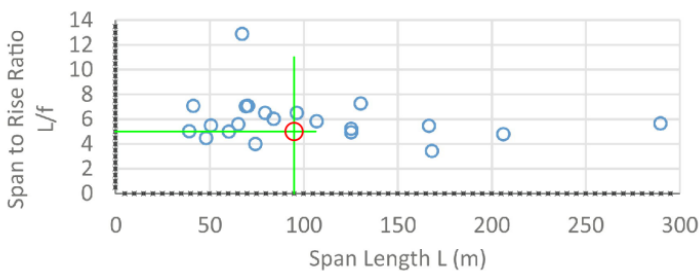


Figure 42: Span-to-Rise Ratio vs. Span Length¹

- Whether the cross-section of a member is built-up, hollow, or solid, makes a large difference in that member's moment of inertia.

Therefore, in order to take those differences into account, according to the authors of the survey, a parameter called “effective stiffness depth” – d_{eff} – was considered, calculated by assuming a rectangle with I_{Sys} , and is used to illustrate the total bending stiffness per meter width of the bridge.

The value of this parameter relative to the McKinley Bridge is seen to fit well within the range of the values of the surveyed bridges, and once again somewhat on the low side, denoting, as already mentioned, the slenderness of the bridge.

$$I_{Sys} = I_{Arch} + I_{TieGirder} \quad \text{and} \quad d_{eff} = \sqrt[3]{\frac{12I_{Sys}}{b_{deck}}}$$

- Another two parameters considered in the survey were the slenderness ratio – $\lambda = K \cdot S_{Arch}/r_{Sys}$ – and the system radius of gyration – $r_{Sys} = \sqrt{I_{Sys}/A_{Arch}}$.

Where “K” is an end fixity factor; S_{Arch} is the length of each Arch Rib, and A_{Arch} is the cross-sectional area of the Arch Ribs.

K = 0.35 for fixed ends (McKinley's case); 0.50 for pinned ends; and 0.54 for three-hinged arches

Looking at the Figure below, showing the representation of the values of those two parameters in relation to the values relative to the surveyed bridges, it can be seen that both values are well within the dispersion of values of the survey, with the Radius of Gyration – 0.88 m – above the average value of the majority for

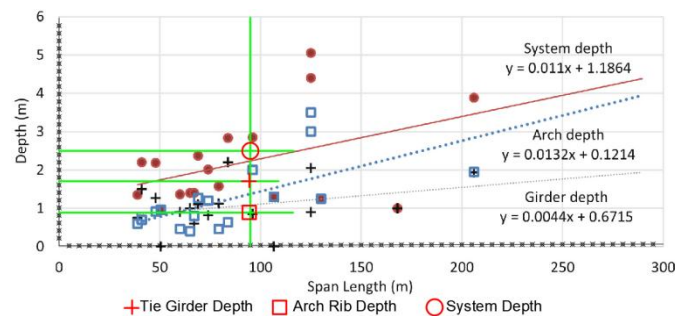


Figure 43: Arch Depth + Girder Depth + System Depth vs. Span Length¹

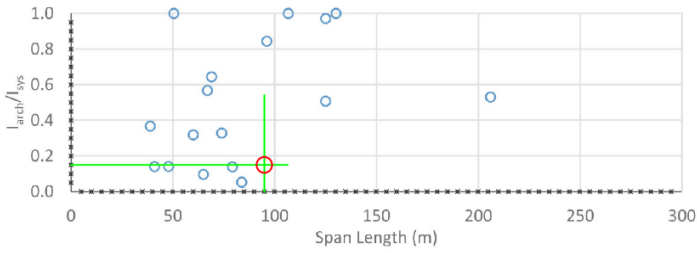


Figure 44: I_{Arch}/I_{Sys} vs. Span Length¹

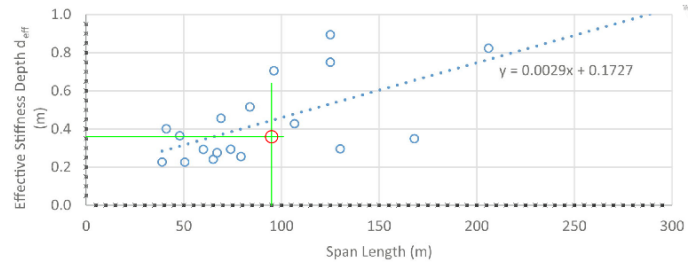


Figure 45: Effective Stiffness vs. Span Length¹

spans between 60 and 80 m – 0.40 m –, but right on top of the trendline, and the Slenderness Ratio – 38.2 – in line with the average of the minimum values of the surveyed bridges – ≈ 33.0 .

- The last parameter surveyed, and the most important from a cost point of view is the weight of structural steel per unit area. The weight of the structural steel was taken from the project cost estimate, including the Tie Girders, Knuckles, Arch Ribs, Arch Ribs Bracing Struts, Support Diaphragms, End Trusses, Floor Beams, Longitudinal Span Bracing, and the Sidewalks Cantilevers, as well as all gusset and cover plates, internal stiffeners, bolts and welds.

The value of this parameter for McKinley Bridge fits well with the dispersion of values of the surveyed bridges, but well below the trendline, and about the trend of values for the minimum values, which is a good indication of the weight optimization that was done.

It should be taken into consideration that this bridge is located in a zone of high seismicity, while many or most of the bridges in the survey were not.

This also attests that the isolation/dissipation created by the seismic units was quite effective since the increased demand due to the seismic action was not significant.

The fact that the weight of steel per unit area is of the order of the minimum values relative to the surveyed bridges, sitting well below the corresponding trendline, gave an indication that the desired optimization of the cost was met, with undeniable benefits to the Client (City of Corona), who ended up with a well-designed and economical bridge, satisfying both the tight operational and financial requisites.

The fact that the values of the reference parameters are well within the dispersion of the corresponding values for the surveyed bridges gave confidence that the design would not “suffer” from any kind of overlook or design shortcomings.

CONSTRUCTION

To minimize the temporary traffic detours and to avoid traffic disruptions during the construction of the bridge, the support bents at each end of the bridge will be constructed in their entirety, well in advance of placing the steel arches on top, and the steel arch will be constructed in a staging area and then moved into place.

Falsework within the railroad right-of-way is eliminated using this method, mitigating interference with the railways, such as reduced operating speed, work zone protection requirements, and railroad flagger.

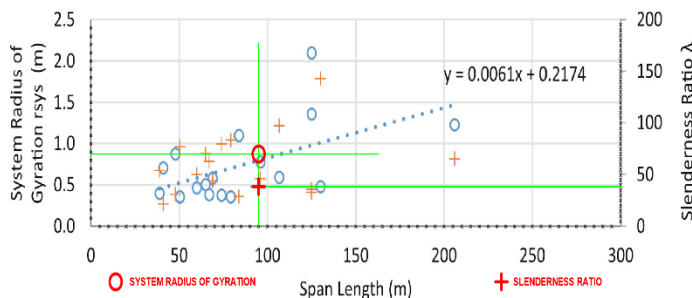


Figure 46: System Radius of Gyration + Slenderness Ratio vs. Span Length¹

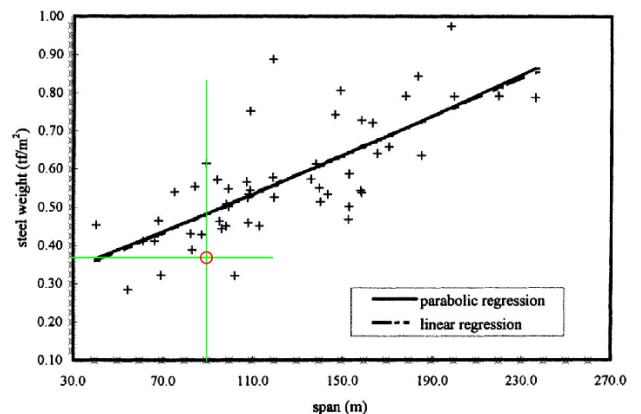


Figure 47: Steel Weight per Unit Area vs. Span Length²

Traffic will continue to flow between the columns. Near the grade crossing there is adequate space to flare traffic lanes back to their current configuration, allowing the existing grade crossing railway warning devices to be used without modification.

The arch bridge steel framing is lightweight, 900 tons (816 tf) in total, and will be constructed in its entirety concurrent with substructure construction at a nearby staging area. To save weight during transport, the concrete elements of the superstructure (i. e. road and sidewalks decks) will not be cast until after the steel skeleton has been placed in its final position.

Once the substructure has been completed, the steel skeleton of the bridge will be lifted and moved into place using the SPMTs. In order to still avoid interference with the railways during the construction of the concrete deck, it was decided to include the SIP corrugated metal forms with the steel structure to move from the assembly yard to the final position, despite the extra weight added for the move about 80 tons (73 tf), corresponding to circa 9% of the total.

The deck will be poured on top of the SIP corrugated metal formwork, and the barriers and median formed and poured. After appropriate curing time, two-way traffic will be shifted to the recently completed bridge and access embankments.

Equipment rental costs for the SPMTs are offset by savings in the overall construction schedule and reduced impacts to vehicles, pedestrians, and local businesses.

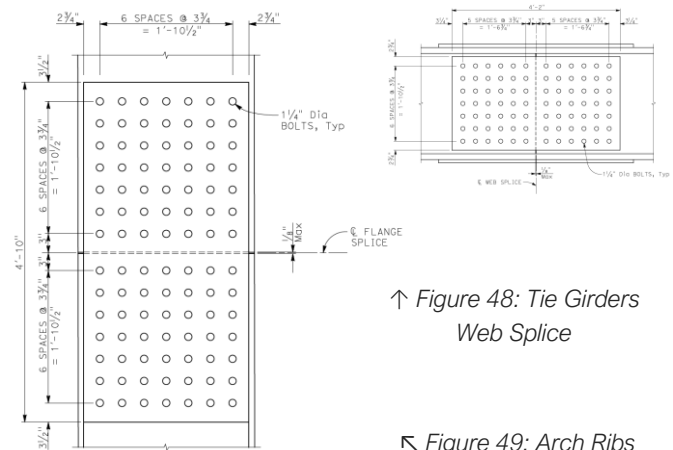
The two main components of the structure, the Arch Ribs and the Tie Girders, are both built-up steel box girders with welded steel plates, see Figures 11 and 12.

In order to allow transportation within the routine permit load dimensions in California (135 ft long and 15 ft wide), they will be built in segments that would not be longer than 100 ft (30.5 m), and 12 ft (3.7 m) wide.

Thus, the arch ribs will be built in 3 segments, and the Tie Girders also in three segments, all within those maximum dimensions.

The Knuckles, integrating part of the Arch Ribs, and part of the Tie Girders, will be built as independent units, smaller in length, but wider, given their more complex geometry. All these individual construction elements will be connected in the erection site by means of bolted cover plates on all four sides, each one integrating hundreds of large diameter (typically 1 1/4" = 32 mm) high-strength (120 ksi = 830 MPa) steel bolts.

As a general rule, all the connections made on-site were designed as bolted, based on shear-friction (slip critical) connections.



↑ Figure 48: Tie Girders Web Splice

↖ Figure 49: Arch Ribs Web Splice

Click on an image to open it in higher resolution

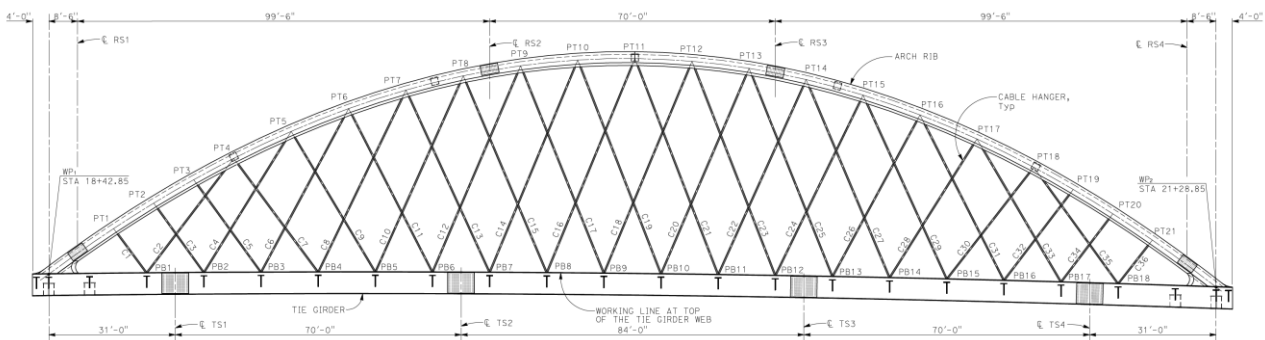


Figure 50: Bolted Splices Locations (Arch Ribs and Tie Girders)

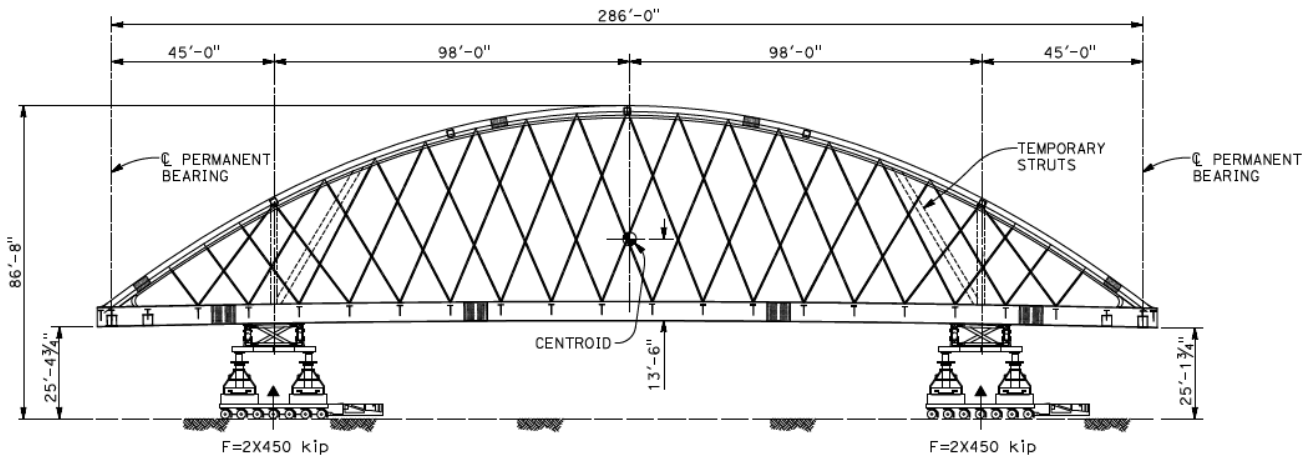


Figure 51: Elevation of the Steel Parts of the Bridge on Top of the SPMTs

The different units will be assembled, including the End Trusses and the Floor Beams, and later the Arch Bracing Ties, on top of temporary towers, which would allow the SPMT units to crawl under and make contact through hydraulic jacks on the predetermined support points.

The stressing of the hangers to circa 5% of their capacity (target force of 20kip = 89kN) will be made prior to moving the structure, in order to create extra stiffness and some additional stabilization for the arches.

Due to the complex fabrication and erection procedures used, a very elaborate pre-camber study had to be made, include all intermediate effects due to construction, and including the effects of the PT of the Tie Girders (pre-compressed without the arches being attached), which created a differential shortening of 1/2" (13mm) at each end.

Another unusual construction aspect was due to the fact that the structure has two quite strong and rigid trusses at each end, to which attaches the concrete slab.

Since the ends of the deck were immovable for the Shrinkage effects, this would create huge tensile stresses in the slab, and so several possible means to reduce shrinkage on the slab were used, such as additives, covering the concrete slab with a methacrylate membrane, with a final overlay of polyester concrete, and the concrete slab cast in four parts, with gaps in between to be filled after 30 days min.

CONCLUSION

- The design of The McKinley Street Steel Tied Arch Bridge has brought many challenges especially with regard to the fact, that the area is seismically active. Additionally a few innovations were introduced, which are summarized below:
- The bridge is entirely supported on four Spherical bearings which allow sliding in both horizontal direction, thus decoupling horizontal movements between the bridge and the substructure;
- The bridge was stabilized horizontally in place by means of shear keys attached to the bent caps, together with mechanical units acting as "fuses" (PSDs), preventing horizontal movements in both directions, or allowing them (VFDs), in the case of thermal movements, without introducing restraint forces in the structure;
- The mechanical stabilizing units also serve as energy dissipating units, for the occurrence of seismic events (seismic protection units);
- Other elements that were considered as part of the energy dissipation system were the elastomeric supports of the approach slabs on top of the backwalls, which were dimensioned in order to be able to accommodate the seismic displacements and the reaction to the weight of the approach slabs with traffic on top. Due to the high ratio between the generated horizontal forces and the permanent vertical reaction, the bearings were designed with steel shear keys at the support interfaces;
- The expansion joints are composed of "flexible joint fillers", according to new formulations, incorporating polyurethane as the gluing element, and silicious charges, being able to accommodate

without, or minor, damage the movements in all three directions due to the OBE earthquake, and with repairable damage for the MCE earthquake;

- Owing to their elastomeric behaviour, the joint fillers were also considered in the analysis model as part of the energy dissipation system;
- The hollow elements too small to be accessible from the inside, such as the arch ribs, the supports diaphragms and the transverse bracing struts, are injected with polyurethane foam, for corrosion protection;
- For keeping in place the nuts to be screwed and torqued of the bolted “blind connections” (i. e. not accessible from the inside) to be made on-site, and in order to avoid tack welding the nuts, as advised by AISC and AWS, two systems were suggested:
- Use of proprietary steel-to-steel acrylic glue, used in the automotive industry to replace riveting and tack welding;
- Or use of “structural nut keepers”, which are disposable wrenches that hold the nuts in place on the interior of inaccessible hollow members, allowing bolts to be installed and tightened from the exterior in the field, such as the “Shuriken”, recently released to the market by Atlas Tube.
- Tie Girders and Knuckles act as vertical steel boxes contrary to inclined arch ribs for a basket configuration;
- Redundancy was created for the Tie Girders by adding external PT cables, axial and straight, to the interior of the Tie Girders so that there would be no tension due to the combination of the permanent and traffic loads;
- Cantilevered pedestrian sidewalks along the Tie Girders, which extend along the face of the MSE walls, lining the access embankments with the bridge, and constituting a pedestrian bridge all by itself;
- Anchor beams for the pedestrian walkway along the MSE walls, pretensioned against the LCC backfill for a more uniform distribution of stress, when a full live load is on top of the walkway, given the low compressive strength of the LCC material – 80 lb/in², for the chosen Class III of the material;
- Anchors in the LCC for anchor beams designed according to the principles of helical anchors design;

- Vibration analysis was made for checking the comfort of pedestrians. This analysis was made both for the cantilevered sidewalks along the arch Tie Beams, and for the cantilevers along the MSE walls. As, in this case, the vibrations induced by the pedestrians were not significant, the vibrations were also investigated for the passage of a heavy truck, using the Fatigue truck defined in AASHTO. A time-step analysis for different speeds of the truck was made and the worst value of accelerations was taken and compared with the limits in the SETRA recommendations.

References:

1. Mermigas, K.K.; Wang, H., "Comparative Study of the Proportions and Efficiency of Steel Arch Bridges", Proceedings of ARCH 2019, 9th International Conference on Arch Bridges, 2019
2. Toma, S.: "Statistics of Steel Weight of Highway Bridges.", Bridge Engineering Handbook, CRC Press, 2000
3. "Design Guidelines for Arch and Cable-Supported Signature Bridges", The Federal Highway Administration, February 2012
4. Tveit, P., "An Introduction to the Network Arch", University of Agder, Norway, August 2006
5. Brunn, B ; Schanack, F., "Calculation of a double track railway network arch bridge applying the European standards", Grimstad, August 2003
6. Teich, S.; Wendelin, S., "Vergleichsrechnung einer Netzwerkbogenbrücke unter Einsatz des Europäischen Normenkonzeptes", Technische Universität Dresden, August 2001
7. "Footbridges - Assessment of Vibrational Behaviour of Footbridges under Pedestrian Loading", SETRA, October 2006
8. "Bases for Design of Structures - Serviceability of Buildings and Walkways against Vibrations", ISO 10137-2007.
9. Caetano, E.; Cunha, A.; Hoornaert, W.; and Raoul, J., "Footbridge Vibration Design", CRC Press, Taylor and Francis Group, International Footbridge Conference (3rd: July 2008: Porto, Portugal)
10. "Seismic Protection Devices, RESTON®PSD Preloaded Spring Damper", Mageba, 2019
11. "Hydrodynamic Devices based on the Compressibility of Highly Viscous Elastomer Fluids – Description of Technology", Mageba, February 2014
12. "AASHTO LRFD Bridge Design Specifications, 8th Edition", The American Association of State Highway and Transportation Officials, August 2019
13. "Seismic Design Specifications for Steel Bridges, 2nd Edition", The California Department of Transportation, May 2016
14. "Steel Construction Manual, 15th Edition", The American Institute of Steel Construction, Feb 2017
15. "AWS D1.5M/D1.5:2020 - Bridge Welding Code", The American Association of State Highway and Transportation Officials & The American Welding Society, 2020.
16. Naeim, F.; Kelly, J.M., "Design of Seismic Isolated Structures", John Wiley & Sons, Inc., March, 1999.
17. Patel, D.J., "Shock Transmission Units in Construction", ICE Publishing, 2013
18. Buckle, I.; Constantinou, M.; Dicleli, M.; and Ghasemi, H., "Seismic Isolation of Highway Bridges", MCEER - FWHA, Aug 2006

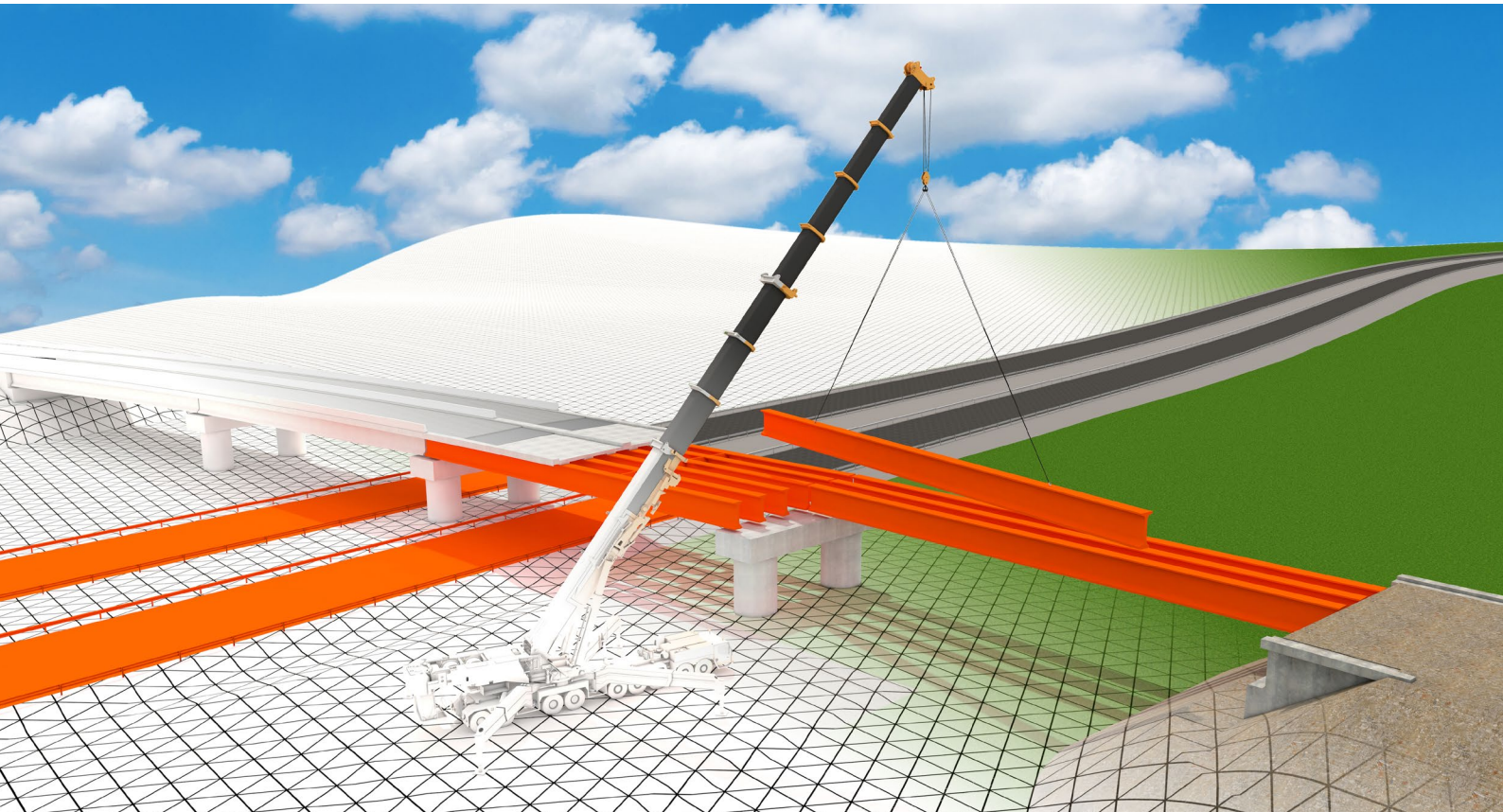
BIGGS CARDOSA
ASSOCIATES INC
STRUCTURAL ENGINEERS



BIGGS CARDOSA ASSOCIATES, INC.

Better Bridges through Advanced Design





THE PROFESSIONAL BIM SOLUTION FOR BRIDGE CONSTRUCTION

Allplan Bridge is the professional BIM solution for modeling, analysis, design, and detailing. Engineers work with a single solution from parametric model creation with high level of detail including prestressing to integration of the construction process, structural analysis, reinforcement design and detailing.

DESIGN YOUR BRIDGES MORE EFFICIENTLY:

- > The world's first complete solution for bridge engineers
- > OPEN BIM workflows with other disciplines and products
- > New in Allplan Bridge 2022:
Specialized Modeling Approach for Precast Girder Bridges

ARUP

Whether to span nations, make a statement or improve everyday links, Arup crafts better bridges

Arup works in active partnership with clients to understand their needs so that the solutions make their bridge aspirations possible —big and small. The Arup global specialist technical skills blended with essential local knowledge adds unexpected benefits.

www.arup.com

Naeem Hussain
naeem.hussain@arup.com

Global

Peter Burnton
peter.burnton@arup.com

Australasia

Richard Hornby
richard.hornby@arup.com

UK, Middle East & Africa

Marcos Sanchez
marcos.sanchez@arup.com

Europe

Steve Kite
steve.kite@arup.com

East Asia

Matt Carter
matt.carter@arup.com

Americas

Deepak Jayaram
deepak.jayaram@arup.com

UK, Middle East, India and Africa



Queensferry Crossing Scotland



We design and produce
formwork equipment
for **in-place casting of bridges**

RÚBRICA BRIDGES®

N25 New Ross Bypass (Ireland)

SOLUTIONS FOR BRIDGE CONSTRUCTION

INNOVATIVE | SAFE | SUSTAINABLE | FAST

BERD[®]
ONE BRIDGE, ONE SOLUTION



Photo Credits: D4R7

MSS M1-70-S @ BRATISLAVA BYPASS | **IN SITU CONSTRUCTION**



Photo Credits: Stephane Ciccolini

LG 36-S @ CAIRO METRO LINE 3 EXTENSION | **PRECAST SEGMENTAL**

FOLLOW US



WWW.BERD.EU



Bridges to Prosperity

We envision a world where poverty caused by rural isolation no longer exists.

Corporate Partners make this vision possible.

Join Bridges to Prosperity in helping isolated communities gain safe access to healthcare, education, jobs, and markets through simple, sustainable, trailbridges. Together, we can build more than a bridge; we can build a pathway out of poverty.



+60%

Women Entering
the Labor Force



+75%

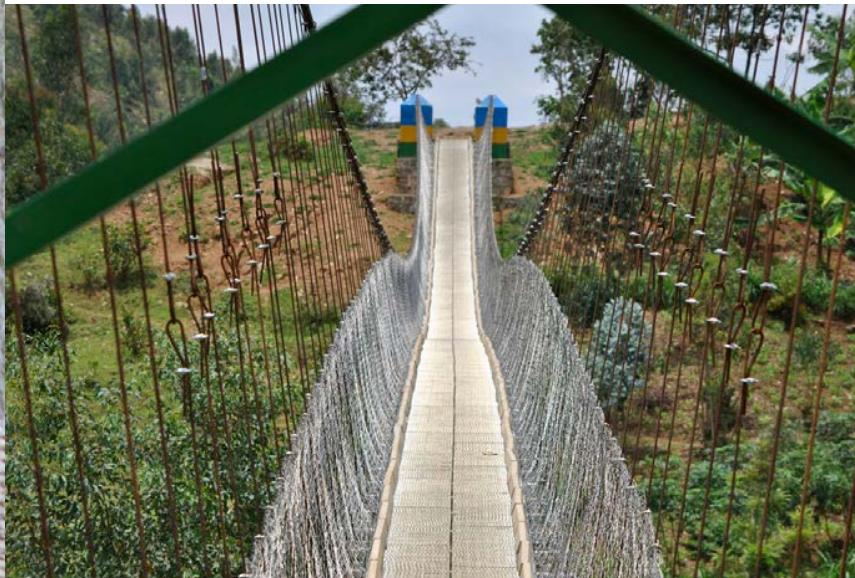
Farmer
Profitability



+35.8%

Labor Market
Income

*Wyatt Brooks and Kevin Donovan - "Eliminating Uncertainty in Market Access: The Impact of New Bridges in Rural Nicaragua," 2017.



info@bridgestoprosperty.org

 /bridgestoprosperty

 @bridgestoprosperty

 @b2p

bridgestoprosperty.org

BE A BRIDGE.

Together we can transform lives.



Everyone can be a bridge to a better world.

A BRIDGE THAT BRINGS SOCIAL CHANGE. A BRIDGE OF HOPE. A BRIDGE OF LOVE.

Bridging the Gap Africa believes everyone deserves access to the basic necessities of life: Better healthcare · Quality education · Robust commerce. We build bridges *with* the communities we serve. This approach enables Kenyan communities to be involved with the building process and empowers them to expand beyond geographies and borders to include corporate and private donors from around the globe.

BtGA is a 501(c)3 in the US that also has Charitable status in Canada. For more information, please visit the Bridging the Gap Africa website at bridgingthegapafrika.org.



Get involved. Be a bridge.



e-mosty

ISSUE 01/2022

MARCH

MCKINLEY STREET
BRIDGE

